UNIVERSITÀ DEGLI STUDI DI MILANO

DOTTORATO DI RICERCA
DBMC
IN BIOLOGIA MOLECOLARE E CELLULARE

Ph.D. School
in Molecular and Cellular Biology
XXXI cycle

Defining the GUN1-FtsH interactions in chloroplast biogenesis in *Arabidopsis thaliana*

Carlotta Peracchio
Ph.D. thesis

Supervisor:
Prof. Paolo Pesaresi
Tutor:
Post-doc Luca Tadini

Academic year 2017-2018

I declare

the work shown in this thesis has been done in the Department of Biosciences, University of Milan, Italy.

FSD BIO18

FSD BIO11

INDEX:

Abstract

The *GENOMES UNCOUPLED 1 (GUN1)* gene has been reported to encode a chloroplast-localized pentatricopeptide-repeat protein (PPR), which acts to integrate multiple indicators of plastid developmental stage and altered plastid function, as part of chloroplast-to-nucleus retrograde communication. However, the molecular mechanisms underlying the GUN1-dependent signal integration have remained elusive, until the recent identification of a set of GUN1-interacting proteins, by co-immunoprecipitation and mass-spectrometric analyses, as well as protein–protein interaction assays.

Within the list of GUN1 interactors the FtsH1, FtsH2, FtsH5 and FtsH8 subunits, that make up the thylakoid FTSH protease complex, were identified. The FtsH subunits are part of the ATP-dependent metalloprotease family and they play a fundamental role in the maintenance of the chloroplast protein homeostasis. In this thesis, I show that FtsH2 and FtsH5 subunits have a really important genetic interaction with GUN1 during the chloroplast biogenesis process in Arabidopsis cotyledons. In particular, I observed that GUN1 is important for the accumulation of the FtsH subunits in the thylakoid membranes, and for the import of several plastid precursor proteins that, in the absence of GUN1 protein, accumulate in the cytosol, with the consequent increase in total protein ubiquitination and cytosolic chaperone abundance.

In the attempt to give a molecular explanation to the observation reported above, I was able to demonstrate that in condition of plastid protein homeostasis alteration, GUN1 controls the accumulation of Nuclear encoded RNA polymerase (NEP)-dependent transcripts and, indirectly, affects the chloroplast protein import apparatus, since a major component of the 1MDa TIC complex

(Translocon at the Inner membrane of the Chloroplasts), i.e. Tic214, is encoded by the plastid genome. Such a defect in Tic214 accumulation appears to destabilize the entire plastid import machinery both in terms of protein amount and post-translation modification, as shown by the high ubiquitination levels of Toc34 subunit.

Strikingly, such chloroplast alterations are sensed by nuclear transcription factors, as shown by the negative effect on the accumulation of HY5, a main transcription factor involved in retrograde signaling and chloroplast biogenesis. Overall, during this three year as Ph.D. student I believed to have discovered the primary function of GUN1 protein, shining a new light on the intricate network of chloroplast-nucleus communication.

Sommario

Il gene *GENOMES UNCOUPLED 1 (GUN1)* è stato scoperto codificare una proteina PPR (pentatricopeptide repeat protein) localizzata nel cloroplasto, che agisce come integratore di segnali multipli riguardanti lo stadio di sviluppo del plastidio e l'alterata funzione plastidiale, come parte della comunicazione retrograda da cloroplasto a nucleo. Nonostante ciò, i meccanismi molecolari alla base dell'integrazione del segnale GUN1-dipendente sono ancora attualmente oscuri; almeno fino alla recente identificazione di una serie di proteine interagenti con GUN1, mediante analisi di co-immunoprecipitazione e spettrometria di massa, oltre a saggi di interazione proteina-proteina.
Nell'elenco degli interattori di GUN1 sono state identificate le subunità FtsH1, FtsH2, FtsH5 e FtsH8, che costituiscono il complesso FTSH tilacoidale. Le subunità FtsH fanno parte della famiglia di metalloproteasi dipendenti dall'ATP e svolgono un ruolo fondamentale nel mantenimento dell'omeostasi proteica nel cloroplasto. In questo lavoro di tesi, mostro che le subunità FtsH2 e FtsH5 hanno un'interazione genetica molto importante con GUN1 durante il processo di biogenesi dei cloroplasti nei cotiledoni di Arabidopsis. In particolare, ho osservato che GUN1 ricopre un ruolo importante nell'accumulo delle subunità FtsH nelle membrane tilacoidali e nell'import di numerosi precursori di proteine plastidiali che, in assenza della proteina GUN1, si accumulano nel citosol, con il conseguente aumento del livello totale di ubiquitinazione proteica e abbondanza delle chaperones citosoliche.
Nel tentativo di dare una spiegazione molecolare all'osservazione riportata sopra, sono stata in grado di dimostrare che, in condizioni di alterazione dell'omeostasi proteica nel cloroplasto, GUN1 controlla l'accumulo di mRNAs trascritti dalla RNA polimerasi codificata dal nucleo (NEP) e, indirettamente, condiziona il funzionamento dell'apparato di import di proteine del cloroplasto,

questo perché un componente principale del complesso 1MDa TIC (Translocon Inner Complex), cioè Tic214, è codificato dal genoma plastidiale. Un tale difetto nell'accumulo di Tic214 sembra destabilizzare l'intero macchinario per l'import di proteine del cloroplasto, sia in termini di quantità proteica che di modifiche post-traduzionali delle singole proteine, come dimostrato dagli alti livelli di ubiquitinizzazione della subunità Toc34.
Sorprendentemente, tali alterazioni che si verificano nel cloroplasto, vengono percepite a livello nucleare, rilevate da fattori di trascrizione, come dimostrato dall'effetto negativo sull'accumulo di HY5, uno dei principali fattori di trascrizione coinvolti nella segnalazione retrograda e nella biogenesi del cloroplasto. Complessivamente, durante questo triennio come dottoranda, ritengo di aver scoperto la funzione primaria della proteina GUN1, chiarendo un punto prima oscuro della complessa rete di comunicazione cloroplasto-nucleo.

1.Introduction

1.1 The origin of chloroplasts

Photosynthetic eukaryotes derived from an ancient endosymbiotic event that occurred approximately 1.5 billion years ago, a photosynthetic cyanobacterium was engulfed by an ancient eukaryotic cell through a primary acquisition (Jensen & Leister, 2014). During the transition from a free living organism to an organelle, most of the cyanobacteria genetic material was transferred to the eukaryotic nucleus and the chloroplast retained only a small part of its genome, together with the ability to perform independent division cycles. In *Arabidopsis thaliana*, the nuclear genome codes indeed about 2000-3000 plastid-located proteins, while the plastid genome codes 87 proteins and 41 among rRNAs and tRNAs only (Robles et al., 2012; Sato et al., 1999). As a consequence of this transfer of DNA in the nucleus, plastid protein complexes are composed of plastid- and nucleus-encoded proteins thus the coordination between the plastid genome and the nuclear genome expression is required for the proper development and functionality of plastids (Fig. 1.1) (Woodson and Chory, 2008). In this scenario, the nucleus-to-chloroplast communication, also known as anterograde signalling pathway, and the chloroplast-to-nucleus information flow, called the retrograde signalling pathway, are both essential to guarantee the optimal chloroplast development and its adaptation to environmental changes (Pogson et al., 2008).

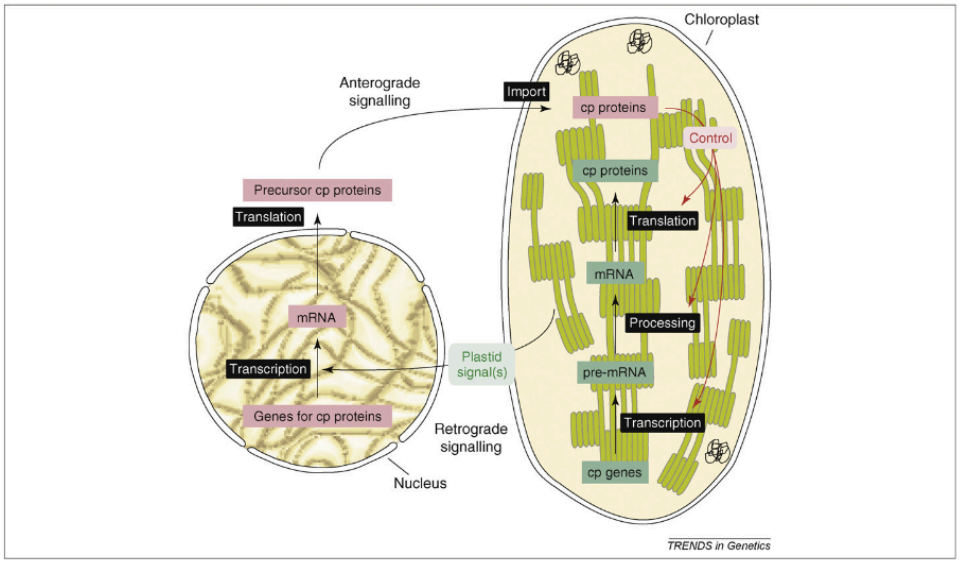

Figure 1.1. Plant intracellular communication networks: Anterograde signaling (nucleus-to-chloroplast) and retrograde signaling (chloroplast-to-nucleus); for details see the text (Kleine et al., 2009)

1.2 The retrograde signalling

The retrograde signalling pathways evolved for the necessity of communicating the plastid developmental and functional status to the nucleus, where most of the plastid-located proteins are coded. Retrograde signaling is, indeed, active during chloroplast biogenesis (called biogenic control) and to respond to environmental stimuli/stresses (operational control) (Pogson et al., 2008).

When the integrity of the plastid in wild type plants is disrupted by a treatment done with chemicals, such as norflurazon (NF), that inhibits β-carotene biosynthesis, the expression of the photosynthesis-associated nuclear genes (PhANGs), such as the *Light harvesting chlorophyll A/B binding protein 1.2 (Lhcb1.2)* and the *small subunit of ribulosebisphosphate carboxylase* (*RbcS*), is strongly repressed (Oelmuller et al., 1986), i.e. the retrograde signalling

pathway communicates to the nucleus the altered status of the chloroplast. Based on that, genetic screenings, using NF, led to the isolation of six Arabidopsis *genome uncoupled (gun)* mutants in which the retrograde communication pathway was defective and held the expression of PhANGs, in absence of functional chloroplasts (Susek et al., 1993). Among the six mutants so far identified, *gun2-to-gun6* are impaired in tetrapyrrole biosynthesis (TPB) (Fig. 1.2). More into details, the mutant *gun2* has a reduced activity of the Heme-oxygenase, a key enzyme active in the synthesis of the chromophores of the phytochromes while *gun3* mutant is defective in the phytochromobilin synthase involved in the conversion of the Heme molecule to Phytochromobilin; in the absence of these two enzymes, plastids accumulate Heme, that leads to negative feedback regulation of chlorophyll biosynthesis (Susek et al., 1993; Mochizuki et al., 2001). On the other hand, *gun4* mutant is defective in the regulatory subunit of the Mg-chelatase, that is the first enzyme of the tetrapyrrole biosynthesis pathway (TBP), while *gun5* is characterized by a mutated H-subunit (CHLH) of Mg-chelatase (Mochizuki et al., 2001; Larkin et al., 2003). Furthermore, Woodson et al. (2011) characterized the Arabidopisis gain-of-function mutant *gun6-1D* that overexpresses the enzyme Ferrochelatase 1 (FC1,) involved in the synthesis of Heme, suggesting Heme as positive regulator of the PhANGs expression.

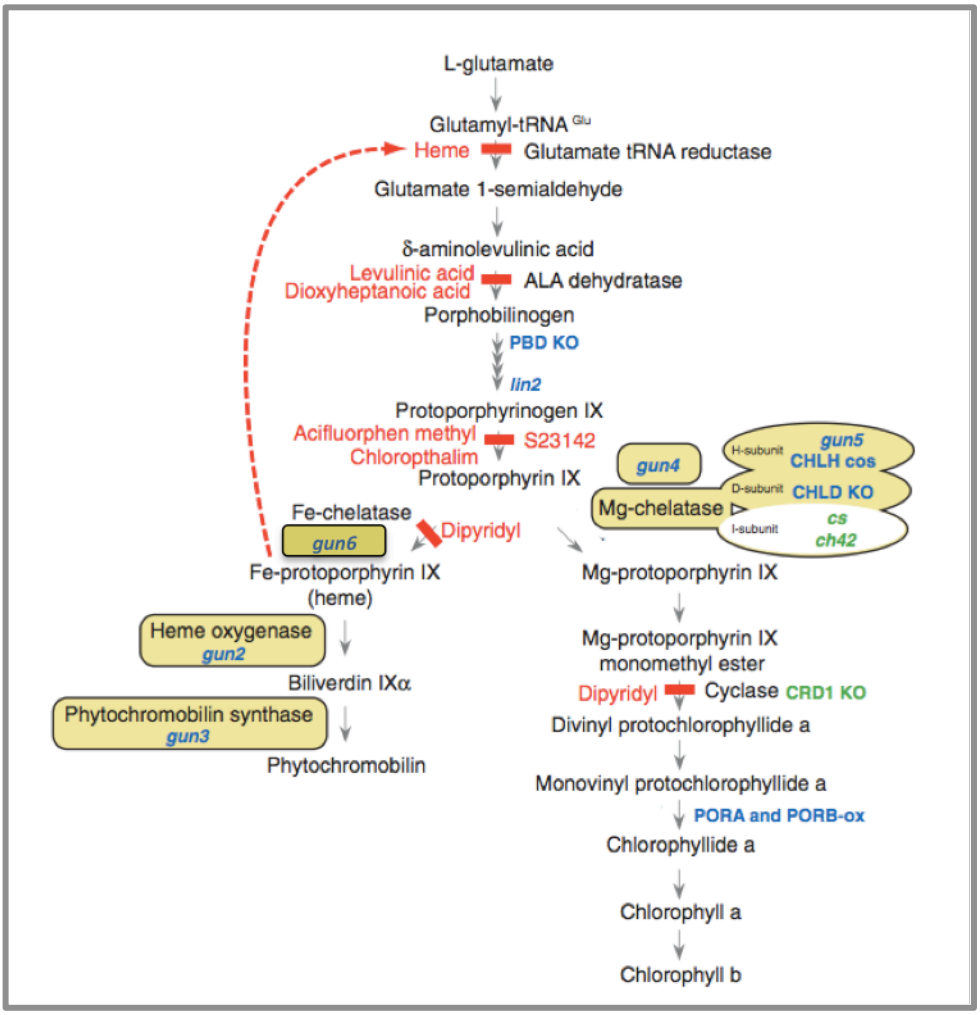

Figure 1.2. Tetrapyrrole biosynthesis pathway. Inhibitors are in red, mutants with a *gun* phenotype are shown in blue; mutants that do not show a *gun* phenotype are coloured in green (Adapted from Nott et al., 2006).

However, also the plastid protein synthesis has an influence on the retrograde signalling. The use of inhibitors of plastid translation, such as chloramphenicol, lincomycin (Lin), and erythromycin, revealed the existence of a plastid gene expression- (PGE) triggered pathway which, if perturbed, leads to the down-regulation of PhANGs as well (Oelmüller et al., 1986; Gray et al., 1995). For instance, mutations of the PGE machinery in Arabidopsis, such as *prpl11*

lacking the chloroplast ribosome large subunit 11 (Pesaresi et al., 2001), *sig2* and *sig6* lacking the sigma factors 2 and 6 (Woodson et al., 2013), *prin2* devoid of the Plastid Redox INsensitive2 protein (Kindgren et al., 2012) and *pap7/ptac14* without the Polymerase Associated Protein7 (Gao et al., 2011) all show the repression of the PhANGs expression. A key protein able to integrate the NF- and LIN-triggered retrograde pathways is GUN1 (Koussevitzky et al., 2007), whose name is derived from the first of the six gun mutants identified by Susek et al. (1993)

1.3 The GUN1 protein

The Arabidopsis GUN1 (GENOMES UNCOUPLED 1) is a chloroplast-located P-type PPR (pentatricopeptide-repeat-protein), of 918 amino-acids displaying a small MutS-related (SMR) domain (Moreira & Philippe, 1999) and a plastid transit peptide at the N terminus. GUN1 protein co-localizes with Plastid Transcriptionally Active Chromosome 2 (pTAC2), a protein marker of the plastid nucleoids. Nevertheless, GUN1 has been reported to behave as an atypical PPR protein, since no clear RNA binding activity has ever been identified. *In vitro* experiments demonstrated that GUN1 can bind DNA due to the SMR domain at the C-terminal (Koussevitzky et al., 2007), but any attempt to show an *in vivo* interaction of GUN1 with nucleic acids failed (Tadini et al., 2016). On the other hand, GUN1 appears to be involved in protein-protein interaction, being found associated with the plastid protein homeostasis machinery (Tadini et al., 2016). Furthermore, GUN1 is present in high abundance in differentiating chloroplasts during very early stages of the seedling development even before the accumulation of the chlorophylls (Wu et al., 2018). The half-life of GUN1 is about 4 hours and its degradation depends

on the ClpC1 (part of the Clp protease complex) activity: the main regulation of the GUN1 protein accumulation in fact, occurs at post-translational level (Wu et al., 2018). As single mutant, *gun1* displays a very subtle chlorophyll-deficiency phenotype in cotyledons at 6 days after sowing (DAS), with a very low penetrance (about 9% of the mutants show pale cotyledons) (Ruckle et al., 2007). Conversely, the introgression of *gun1* mutations in Arabidopsis mutants lacking plastid ribosomal subunits leads to drastic phenotypes, as proved by the albinotic seedling-lethal mutants of *gun1 prpl11* and *gun1 prpl24* and *gun1 prps17* double mutants (Tadini et al., 2016). Furthermore, Paieri et al. (2018) demonstrated a functional interaction between *GUN1* and *RH50*, a gene coding for a DEAD-box RNA helicase, involved in 23s and 4.5s rRNA maturation and the assembly of the plastid large subunit. Consistently, Zhao et al. (2018) showed that *gun1* mutant was more sensitive to lincomycin-mediated inhibition of chloroplast biogenesis, supporting the role of GUN1 in plastid protein translation. Overall, these findings together with the report by Llamas et al. (2017), where the combination of the *gun1* mutation with defects in Clp protease activity resulted in seedling lethality, clearly indicate that GUN1 protein has a more general role in the maintenance of the chloroplast protein homeostasis during early stages of chloroplast biogenesis.

1.4 The GUN1-containing protein complex

As described by Koussevitzky et al. (2007) GUN1 protein co-localizes with pTAC2 in plastid nucleoid structures, suggesting the interaction with relatively large protein complex(es) (Fig. 1.4). Indeed, Tadini et al. (2016) isolated a GUN1-GFP-containing complex and defined GUN1 putative interactors. Among possible interactors, they have found proteins involved in transcription, RNA metabolism and translation such as pTAC6, that together with pTAC2 and

other polymerase-associated proteins (PAPs), forms an active core of interaction with the Plastid Encoded RNA polymerase (PEP), named soluble RNA polymerase (sRNPase) complex (Pfalz et al., 2006). GUN1 interacts with proteins involved in plastid translation, such as the ribosomal proteins rpl2, rps3 and rps4 (plastid encoded) and PRPL10 (nuclear encoded) and the translation initiation factor2 (cpIF2; FUG1) (Miura et al., 2007). In the chloroplast nucleoids, and also in the list of GUN1 interactors there is the DEAD-box-containing RNA helicase 3 (RH3) involved in the splicing of group II introns present in the transcripts of the genes *rpl2*, *trnA*, *trnI*, and *rps12* and important for the maturation process of the 23S rRNA (Olinares et al., 2010; Asakura et al., 2012). GUN1 interacts as well with other PPR proteins, such as At3g49240 (AtPPR_3g49240), which results in embryo-lethality if the corresponding gene is silenced (Cushing et al., 2005). Furthermore, GUN1 interacts with the chloroplast protein import, folding and degradation machineries (Fig. 1.3, 2.) (Tadini et al., 2016). For instance, the two *Arabidopsis thaliana* Hsp93 proteins, ClpC1 and ClpC2 were found in the list of GUN1 interactors, but only ClpC2 was found in the nucleoids (Melonek et al., 2016). ClpC2 was classically coupled with Tic110 as an ATP-driven motor in the import process. Recently Flores-Pèrez and colleagues (Flores-Pèrez et al., 2016) demonstrated the interaction of ClpC1 with the other subunits of the Clp protease machinery core (ClpR, ClpP, ClpT and ClpD) and it's likely that ClpC1 works as a quality control point for the newly imported pre-proteins (Huang et al., 2016). In Arabidopsis two stromal chaperones Hsc70 are also present: cpHsc70-1 and cpHsc70-2 (Su & Li, 2008) both interactors of GUN1, but only cpHsc70-1 is part of the nucleoid proteome (Melonek et al., 2016). Because the double mutant lacking these two proteins has never been identified, it appears evident that cpHsc70-1 and cpHsc70-2 have an essential role in chloroplast biogenesis, possibly involved in the protein import of photosynthetic and non-

photosynthetic precursor proteins (Su and Li, 2010). In addition, these two stromal Heat shock proteins act as modulators of the proteins activity and prevent the formation of toxic protein aggregates in the stroma (Su and Li, 2008).

The chaperonins ptCpn60α1 and ptCpn60β1 are also in the list of GUN1 interactors. In Arabidopsis two members of the Cpn60α family exist, called ptCpn60α1 and ptCpn60α2, and four members of Cpn60β: ptCpn60β1–β4 (Suzuki et al., 2009). Only ptCpn60α1 and ptCpn60β2 have been found in the nucleoid proteome (Melonek et al., 2016). ptCpn60 and ptCpn10 together with other stromal chaperones like the cpHsc70-1 and cpHsc70-2 described above, seem to guarantee the correct folding of the imported plastid pre-proteins (Boston et al., 1996; Jackson-Constan et al., 2001).

Finally, in the list of the GUN1 interactors (Tadini et al., 2016) the FtsH1, FtsH2, FtsH5 and FstH8 subunits, that form the FTSH protease complex active in the turnover of D1 protein and involved in chloroplast biogenesis, were also identified, further supporting the role of GUN1 in the maintenance of protein homeostasis during early stages of chloroplast biogenesis.

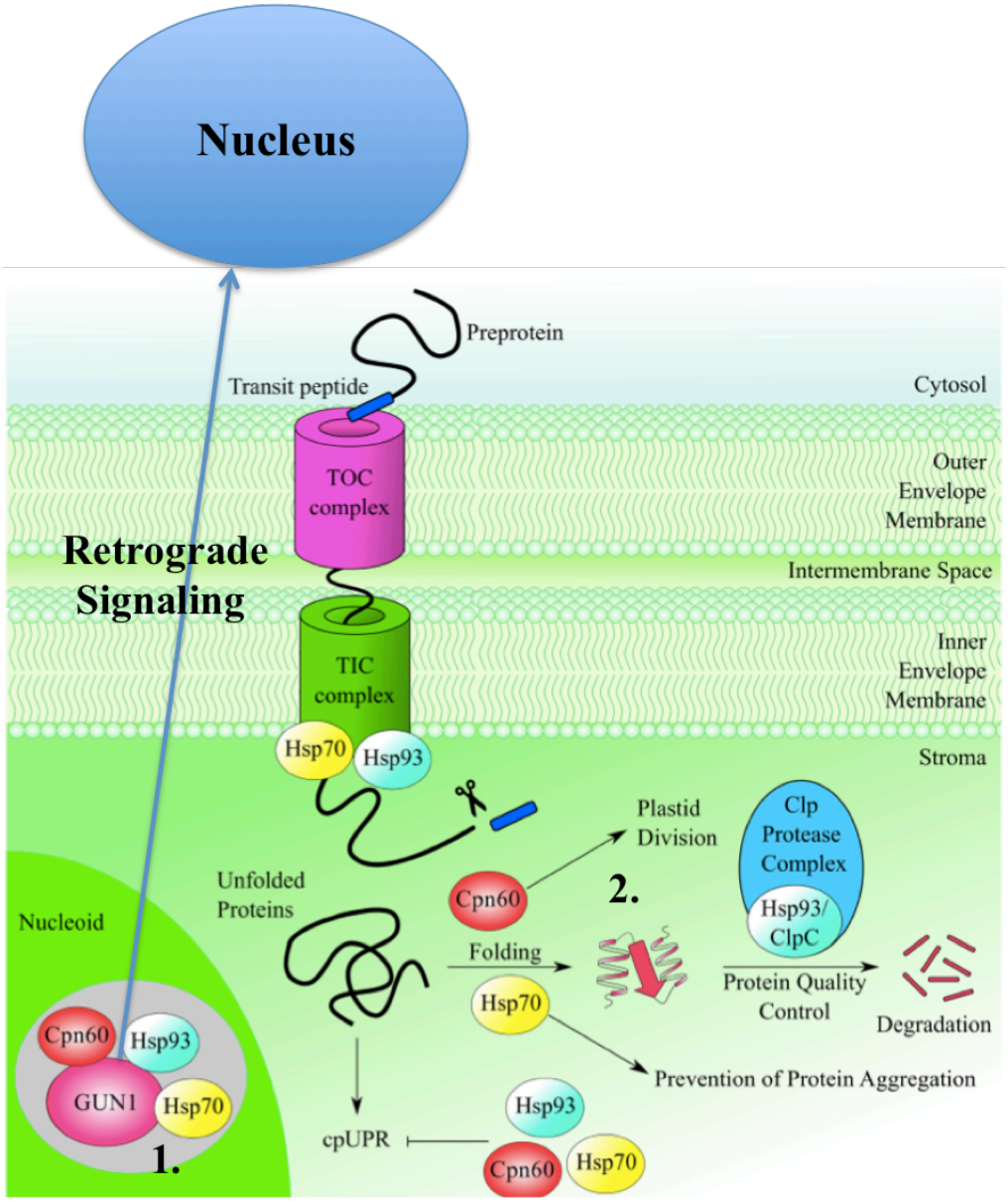

Figure 1.3. The protein complex(es) in which GUN1 exerts its function: **1.** Interactions with the transcriptional/translational machinery in the nucleoids, **2.** Maintenance of the chloroplast protein homeostasis (import, folding and degradation of the plastid proteins) (Adapted from Colombo et al., 2016)

1.5 The plastid transcription machinery

As anticipated in the paragraph 1.1, the nuclear genome encodes for most of plastid proteins and the anterograde signaling consists in the transcription, cytosolic translation and import into the plastid of proteins capable to regulate the expression of plastid genes, at transcriptional or post transcriptional level (Bräutigam et al., 2007).

In *A.thaliana* and higher plant chloroplasts, two complementary transcription systems exist. The Plastid-Encoded Polymerase (PEP) is a eubacteria-type multimeric RNA polymerase while the Nuclear-Encoded Polymerase (NEP) is instead a phage-type derived by the proteobacteria-like ancestor. PEP expression is under the control of NEP enzyme, implying that the nucleus exerts the activation of plastid transcription. PEP subunits are plastid-encoded and display a prokaryotic-derived gene organization. *rpoB*, *rpoC1, rpoC2* coding for subunits β (121 kDa), β' (79 kDa) and β'' (156 kDa) are clustered in an operon, while the gene *rpoA,* coding for the subunit α (38 kDa), is located in another operon, together with genes of ribosomal proteins. PEP promoters usually possess bacterial σ^{70} -10 and -35 consensus sequences (Fig. 1.4, B). On the other hand, NEP enzymes (RPOTm, RPOTp, RPOTmp) are monomeric and encoded in the nuclear genome, translated in the cytosol and imported in the plastids (Fig. 1.4, A). RpoTp, directed to the chloroplast, is mainly active in green tissues, RpoTm is active in the mitochondria and RpoTmp is targeted to both organelles (Hedtke et al., 2002).

NEP promoters exist in three different forms: class Ia, class Ib, class II; the first one has got a conserved motif called "YRTa" and located few nucleotides before the start codon (Fig. 1.4, C). The class Ib are characterized by having another kind of conserved motif: GAA-box located upstream the YRTa motif (Börner et al., 2015).

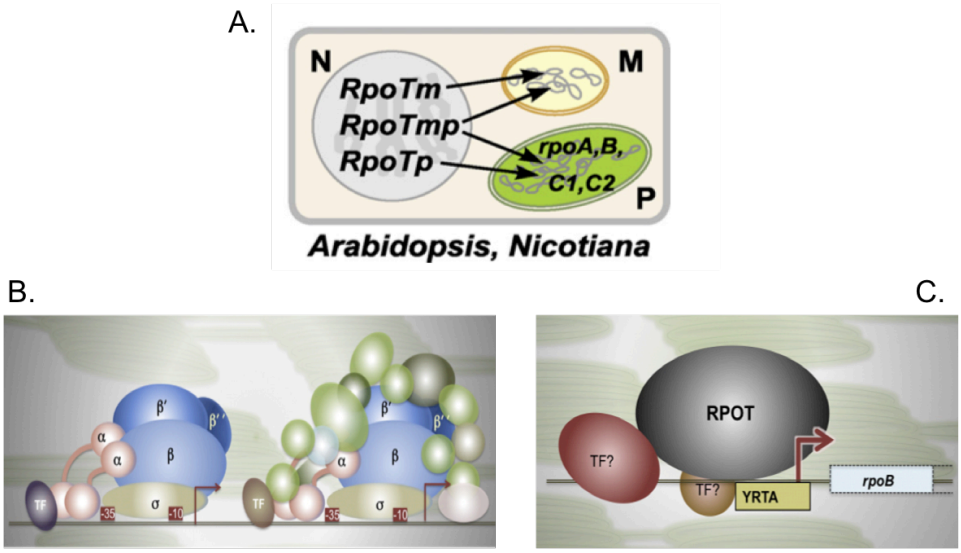

Figure 1.4. NEP and PEP RNA polymerases (**A**) Localization of the genes coding for the organellar RNA-polymerases in *Arabidopsis thaliana* and *Nicotiana tabacum*. Abbreviations: N, nucleus; M, mitochondrion; P, plastid (Liere et al., 2011), (**B**) PEP subunits, a sigma factor (σ), necessary for binding to the promoter region, protein factors (TF) (Börner et al., 2015), (**C**) NEP and the YRTA motif located few nucleotides upstream of the site of transcription initiation (red arrow) (Börner et al., 2015)

Moreover, the promoter specificity of the PEP enzyme is guaranteed by nuclear-encoded sigma-like transcription factors (SLFs) (Fig. 1.5, B). In *A. thaliana* six SLFs have been identified (SIG1 to SIG6). In particular, it has been shown that SIG2, SIG3, and SIG5 play an essential role during the embryonal photosynthesis. SIG2 is associated with PEP enzyme and active in the specific transcription of the *psaJ* and tRNA-Glu genes (Allorent et al., 2013). SIG3 is retained in dry seeds therefore is probably important during the seed development and/or germination (Allorent et al., 2013). The knock-out mutant *sig5* is embryo-lethal (Allorent et al., 2013). The *sig6* and *sig2* knockout plants show a pale-green cotyledon phenotype. These two sigma factors seems to be involved, in the specific de-etiolation step of the chloroplasts in cotyledons (Ishizaki et al., 2005).

For the correct development of the chloroplast, NEP and PEP have to cooperate and, although in the past it was thought that some operons could be transcribed specifically by one of the two polymerases, recent studies demonstrated that many plastid genes are transcribed by either polymerases (Börner et al., 2015). Immunoblots, performed using the antibodies against NEP and PEP subunits, clearly show that both NEP and PEP enzymes are present in dry seeds, and RPOTp and RPOTmp levels are high 2 days after germination (DAG), decrease at 5 DAG and rise again at 6 DAG, when true leaves emerge (Demarsy et al., 2006).

1.6 Import and folding of nuclear-encoded plastid proteins

Beside the coordination of plastid and nuclear gene expression through the chloroplast-nucleus communication, the import of nuclear-encoded proteins into the chloroplasts is a key event of chloroplast biogenesis. Nuclear-encoded preproteins, synthesized in the cytosol, and directed to the chloroplasts have a specific N-terminal amino-acid sequence called chloroplast transit peptide (cTP) that can be recognized and bound by TOC GTPase-receptors, the Translocon at the Outer membrane of the Chloroplasts (TOC), such as Toc159, Toc132, Toc120, Toc33 and Toc34. These different isoforms of the TOC receptors appear to be specialized in the translocation of preproteins with different functions (Demarsy et al., 2014). Once preproteins are recognized by receptors, they are driven through the channel protein Toc75 and reach the TIC complex, (Fig. 1.5, A). Receptors and channels are organized in a rigid complex of about 1000 kDa (Kikuchi et al., 2006).

The organization of the TIC complex is still under discussion and two main hypotheses have been formulated. According to the so-called classical model (Fig. 1.5, B.), Tic110, an inner envelope membrane protein, forms part of the protein-conducting channel together with Tic40. Tic110 function is associated with the channel protein Tic20, although a physical interaction has never been detected (Fig. 1.5, B) (Demarsy et al. 2014, Paila et al., 2015; Richardson et al. 2017; Kikuchi et al., 2009; Kikuchi et al. 2013). Tic110 and Tic40 interact with stromal molecular chaperones like ClpC, Hsp70 and Hsp90C, which act as ATP-driven import motor (Flores-Pérez and Jarvis 2013). According to the revised model, a 1 MDa TIC complex exists and it is composed of the channel Tic20, Tic56, Tic100 and Tic214 and this complex works in a strong association with the already described TOC complex (Fig. 1.5, B) (Kikuchi et al., 2013). Tic214 subunit is peculiar since is the only plastid-encoded import-related protein (Drescher et al., 2000).

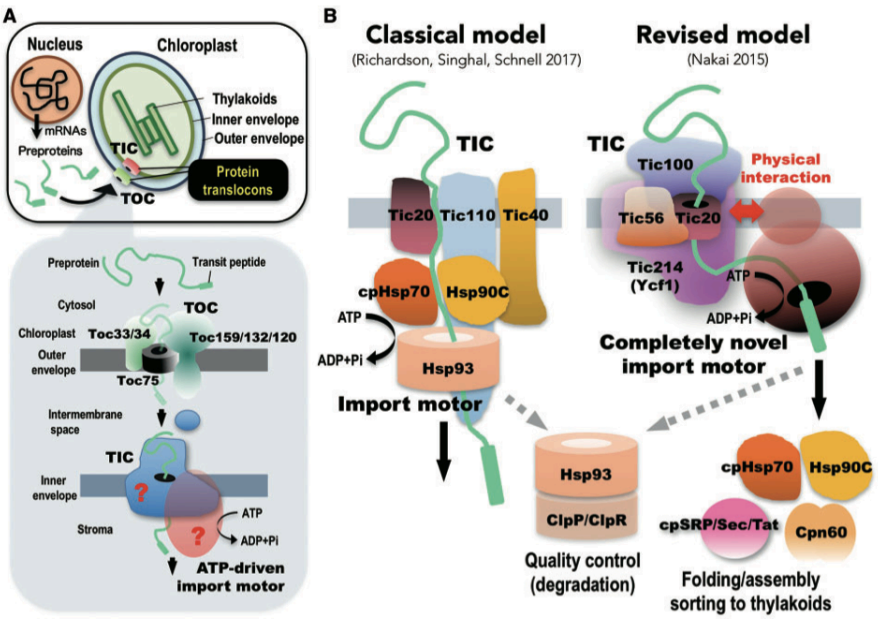

Figure 1.5. The chloroplast protein import machinery: (**A**) Chloroplast protein import machinery TIC-TOC, (**B**) comparison between the classical model (Richardson et al. 2017) and the revised model for TIC translocon (Nakai 2015a; Nakai 2015b; Nakai, 2018)

Once pre-proteins cross the inner envelope via TIC complexes, ClpC2 interacts with the precursor proteins binding their transit peptides and their mature regions (Huang et al., 2016). The two stromal cpHsc70-1 and cpHsc70-2 seems to be involved, together with ClpC2, in the translocation of the pre-proteins inside the chloroplast as part of the folding complex formed by ClpC2 and Hsp90C, proposed by Inoue et al. (2013). Despite that, there are no evidences about the direct physical interaction between cpHsc70s and the TIC complex or between cpHsc70s and the pre-proteins (Su & Li, 2010).

On the contrary, the ptCpn60-Tic110 complex, together cpHsc70s, is responsible for the maturation of the newly imported plastid proteins, in particular of the ones directed to the thylakoid membranes (Madueno et al.,

1993; Tsugeki and Nishimura, 1993; Peng et al., 2011). Moreover, ptCpn60 is able to form complexes with the thylakoid protein Plsp1-1, a peptidase involved in thylakoid formation, and to activate cpSec-1, responsible for the insertion of the FtsH5 protease and the subunit 3 of the photosystem I (PsaF) in the thylakoid membranes (Endow et al., 2015).

1.7 The thylakoid FtsH proteases

Chloroplast protein homeostasis is another important step in chloroplast biogenesis and chloroplast maintenance. In particular, there are three main families of proteases involved in the maintenance of chloroplast protein homeostasis: the prokaryotic-like proteases FtsH, Deg and Clp. The FtsH proteins are ATP-dependent zinc metalloproteases that have a relevant role in chloroplast biogenesis. The *A. thaliana* genome codes for 12 FtsH proteins, eight of them are destined to the chloroplast (FtsH1, FtsH2, FtsH5 FtsH6, FtsH7, FstH8, FtsH9, FtsH12), three proteases are mitochondria-located (FtsH3/4/10) and one, FtsH11 is dual-located (mitochondria and chloroplast) (Sakamoto et al., 2003; Wagner et al., 2012). The C-terminus domain of FtsH proteins contains the ATPase and the protease domains, which face the stroma, while the N-terminus region exhibits a transmembrane domain (Fig. 1.6, A) (Lindahl et al., 1996). FtsH1, FtsH2, FtsH5 and FstH8 are organized in the thylakoid membrane in homo or hetero-hexamers. The hetero-hexamers consist in two subunits of type A (FtsH1, FtsH5) plus four subunits of type B (FtsH2, FtsH8) (Fig. 1.6, B) (Zaltsman et al., 2005).

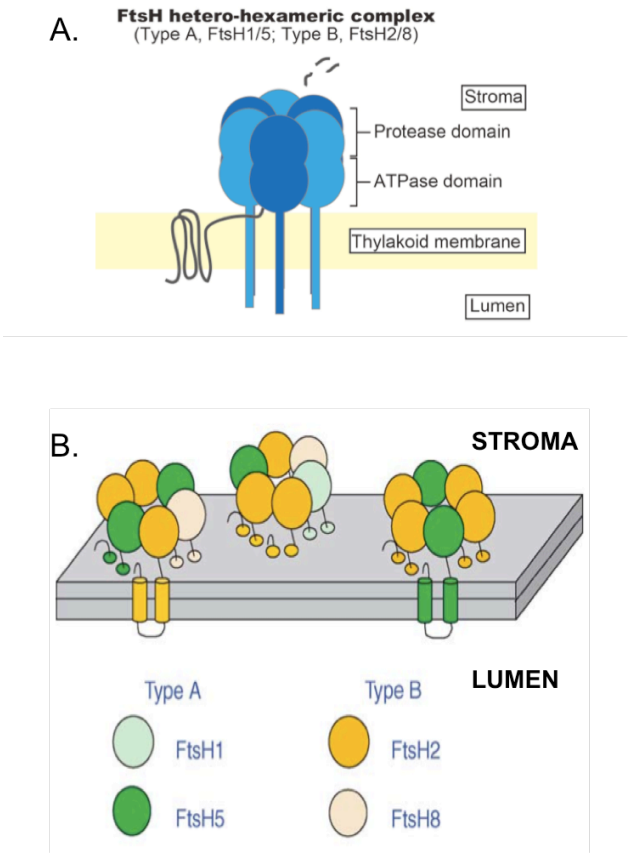

Figure 1.6. Thylakoid FtsH structure, the principal domains are indicated (**A**) (Adapted from Kato & Sakamoto, 2018) and organization in thylakoid hetero-complexes is shown (**B**) (Adam et al., 2006)

FtsH2 and 8 are homologous and functionally interchangeable and they are able to stabilize FtsH1 and 5, homologous and interchangeable as well, in the thylakoid membranes (Yu et al., 2004; 2005). The most abundant subunits are: FtsH2, FtsH5 followed by FtsH8 and FtsH1 (Sakamoto et al., 2003; Yu et al., 2004; Yu et al., 2005). Mutant lacking FtsH2 (*yellow variegated 2*, *var2*) shows the most severe phenotype with strong variegations on the true leaves (Chen et al., 2000). The white sectors characteristic of the *ftsh2* homozygous mutant leaves, contain abnormal plastids while, in the green sectors, the maturation of

the chloroplasts is very slow (Sakamoto et al., 2009). Knockout mutants of *FTSH5* gene (*var1*) show variegations in the true leaves, less dramatic than *ftsh2* (Sakamoto et al., 2002) while *ftsh1* and *ftsh8* knockout mutants show a wild-type-like phenotype. The combination of *ftsh1 ftsh5* and *ftsh2 ftsh8* mutations results in albinotic plants (Zaltsman et al., 2005). The reduction of the plastid protein synthesis rate, as in *fug1* knock-down mutants, is able to revert *var2* variegated phenotype (Miura et al., 2007).

The thylakoid FtsH protease complexes have several functions in the chloroplast physiology, one of the most characterized and better described is their role in the PSII repair cycle.

When the protein D1, part of the central core of the Photosystem II (PSII), is photo-damaged needs to be rapidly removed and replaced. The degradation of D1 requires the disassembly of the PSII, in order to allow D1 exposition to the proteases. Once degraded, the de-novo synthesis of D1 can occur. The D1 degradation can be exerted via two pathways (Fig. 1.7), one is entirely performed by the FtsH proteases (Kato et al., 2009) and a second pathway it is a team work between the FtsH and Deg proteases (Schuhmann & Adamska, 2012). Moreover, it has been demonstrated that the FtsH proteins are involved in the early stage of the assembly of the Photosystem I (PSI) as well (Järvi et al., 2016). Recently, Wang et al. (2016) reported that in oxidative stress conditions, thylakoid FtsH are also involved in the EX1-mediated retrograde signalling.

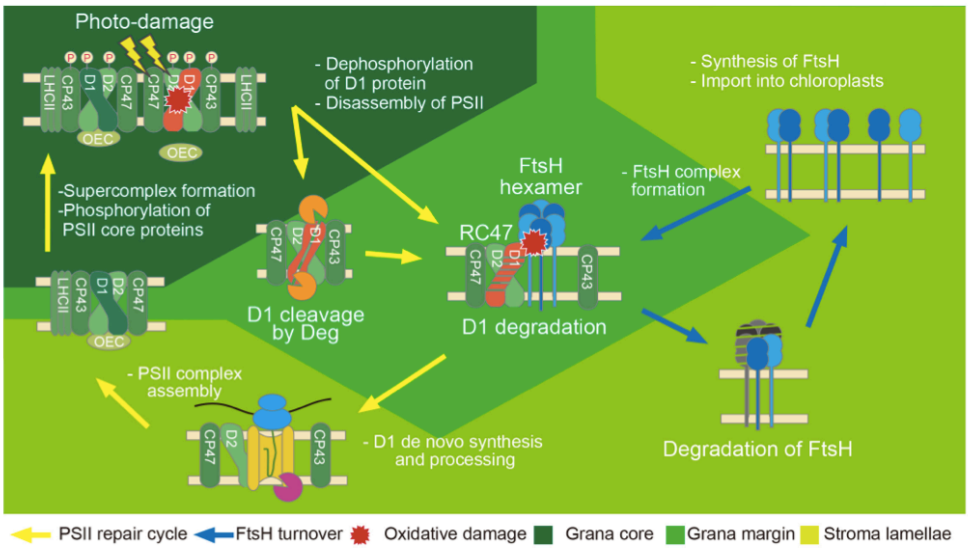

Figure 1.7. FtsH involvement in PSII repair cycle (Kato & Sakamoto, 2018)

1.8 The Chlorophagy

To guarantee that only properly developed and fully functional chloroplasts become part of cotyledons and leaves, all the damaged molecular components or even entire damaged chloroplasts have to be suddenly removed in order to avoid even more serious damages to the photosynthetic-competent tissues.

This is possible thanks to an evolutionarily conserved process in all the eukaryotes: the autophagy. In general, when this process occurs, entire portions of cytoplasm are included in newly-formed double membrane vesicles: the autophagosomes that, subsequently, release captured damaged cytosolic components in the lysosomes or in the vacuole and their content can be digested. In plant, when the entire damaged chloroplast is transported to the vacuole to be totally degraded, chlorophagy takes place (Ishida et al., 2014). This phenomenon was firstly observed studying the *Arabidopsis thaliana* mutant *atg4* in which the chlorophagy process is repressed during leaf senescence (Fig. 1.8 B; Wada et al., 2008).

Autophagy ATG proteins were well characterized in yeast, however, their orthologues in *Arabidopsis thaliana* have a very similar role and mechanism of action (Yoshimoto et al., 2004). These proteins function in two conjugation cascades and are active in budding and elongation of the autophagosomes (Nakatogawa et al., 2009). ATG proteins are involved in the response to photodamages of the chloroplast (UVB exposure but also natural light exposure) in fact *atg5* and *atg7* knock-out mutants, damaged with light, show deformed chloroplasts with disorganized thylakoidal membranes. In the extreme case, UVB-damaged chloroplasts are vehiculated to the vacuole for the chlorophagy (Fig. 1.8 C; Izumi & Nakamura, 2017).

There are other stresses to which chloroplasts must react, for example sugar starvation. To this kind of stress, the chloroplast reacts *in primis* activating a

specific pathway: Rubisco-containing bodies (RCBs) pathway (Izumi et al., 2010). The RCBs are autophagic compartments that contain portions of the stroma enriched with stromal proteins and involved in recycling of amino-acids (Izumi et al., 2010). Moreover, the RCBs pathway is activated during the early stages of the senescence process, when these vesicles literally "dry up" the old chloroplasts before their total vacuolar digestion (Fig. 1.8, A) (Wada et al., 2008).

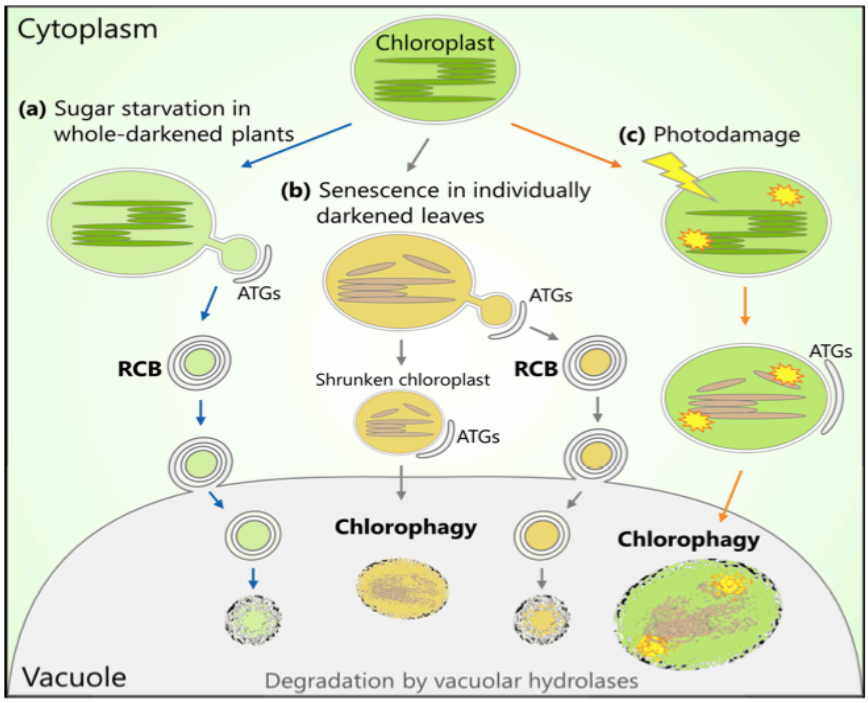

Figure 1.8. Different paths to chlorophagy: (**A**) in case of sugar starvation and necessity of energy, (**B**) accelerated senescence, (**C**) ultraviolet-B (UV-B)-induced photodamage. For details see the text. Abbreviations: RCB, Rubisco Containing Bodies. (Izumi & Nakamura, 2018)

The chlorophagy can also be mediated by others specific processes and actors:

1. ATI body

ATI1 (ATG8-interacting protein 1) produces plastid vesicle containing not only stroma (like the RCBs) but also parts of thylakoid membranes and pieces of the

envelope. ATI1 bodies (Fig. 1.9, A) can also be found inside the chloroplast (Michaeli et al., 2014).

2. Senescence-Associated Vacuoles (SAVs)

SAVs increase in number during the senescence in tobacco leaves (Carrion et al., 2013) and contain a specific protein: Senescence associated gene 12 (SAG12), a cysteine protease. SAVs could be considered an extra-pathway involved in plastid protein degradation in the last phases of the senescence (Fig. 1.9, A).

3. Vesicles chloroplast-derived

This pathway, mediated by the protein chloroplast vesiculation (CV), is autophagy-indipendent. In Arabidopsis, when CV protein is overexpressed, it interacts with thylakoids and envelope-located proteins and many CV-containing vesicles (CCVs) are generated (Fig.1.9, A) (Wang & Blumwald, 2014). These vesicles contain proteins from all the plastid compartments: envelope, thylakoids and stroma (Wang & Blumwald, 2014). Not less important, *CV* transcripts level increases during the senescence progression and in plants subjected to different stresses: oxidative and salt stress (Wang & Blumwald, 2014), UVB-damage (Izumi & Nakamura, 2017).

4. Ubiquitin proteasome system-associated chlorophagy

The first important E3-ubiquitin ligase identified to be involved in this pathway was suppressor of *ppi1* locus 1 (SP1) (Ling et al., 2012), inserted in the chloroplast outer envelope and involved in the TOC turnover: SP1 adds ubiquitin to the TOC components (for sure to atToc159, atToc75, and atToc33) (Fig. 1.9, B) inducing their 26S proteasome-mediated degradation, for instance upon oxidative stress conditions, thereby limiting the import of pre-proteins in the chloroplast and avoiding the production of ROS (Ling & Jarvis, 2015). A recently identified E3-ubiquitin ligase, cytosol-located, and also active in the chlorophagy is plant-u-box 4 (PUB4) (Fig. 1.9, B). Mutants like the

ferrochelatase 2 (*fc2*) knock-out plants are not able to control the oxidative stress and high levels of ROS finally induce cell death, however, in the double mutant *fc2 pub4-6* the chlorophagy events are markedly reduced (Woodson et al., 2015). However, how PUB4 triggers the ROS-damaged chloroplasts degradation and which are its target proteins in the chloroplast outer envelope remain to be clarified.

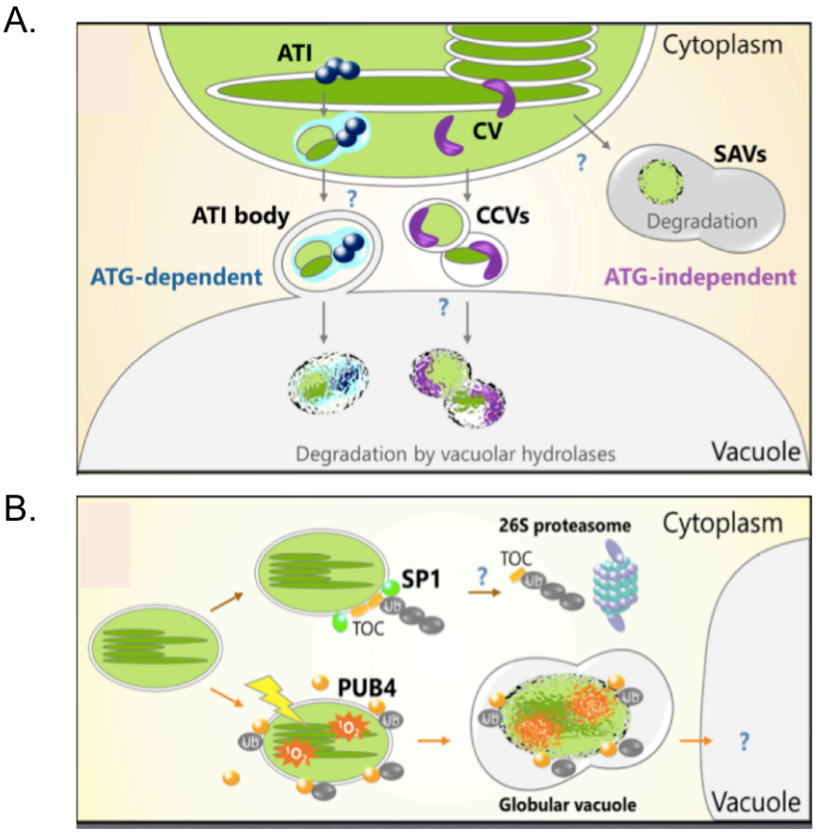

Figure 1.9. Alternative chlorophagy pathways: (**A**) simplified model for chloroplast protein turnover mediated by ATI bodies, CV-containing vesicles (CCVs) and senescence-associated vacuoles (SAVs). For details see the text, (**B**) chloroplast protein turnover and chlorophagy mediated by ubiquitination. For details see the text. (Adapted from Izumi & Nakamura, 2017)

Aims of the project

GUN1 protein plays a crucial role in the plastid-to-nucleus communication and in the maintenance of the chloroplast protein homeostasis as proven by the very dramatic phenotypes, i.e. seedling lethal, shown by Arabidopsis double mutants where the *gun1* mutation was combined with defect in plastid protein synthesis and plastid protein degradation. The first aim of this Ph.D. project is to further confirm the involvement of GUN1 protein in chloroplast biogenesis and chloroplast protein homeostasis. This will be obtained by verifying the existence of functional interactions between GUN1 and two main processes responsible of chloroplast protein homeostasis: i) the thylakoid protein quality control performed by the FTSH protease complex, and ii) the chloroplast protein import and protein folding carried out by the stromal located Hsp70 chaperone. To reach this goal:

1. A genetic approach will be carried out, double mutants *gun1 ftsh1, gun1 ftsh2, gun1 ftsh5*, *gun1 ftsh8* and *gun1 cphsc70* will be generated either by crossing and segregation analysis or by employing the CRISPR-Cas9 gene editing strategy, as in case of *gun1 ftsh2* since the two gene loci are adjacent on the same chromosome.
2. The generated double mutants will be characterised in terms of visible phenotype (greening capability, photosynthetic performance and chlorophyll content) and thylakoid protein content, via immunoblot analyses.
3. The analyses of chloroplast morphology will be performed via transmission electron microscope (TEM) in order to define the impact of double mutations on chloroplast biogenesis.

The second aim of this work will be to understand the molecular bases of the GUN1-dependent chloroplast biogenesis with respect to its role within the chloroplast and in relation to its activity in the retrograde communication with the nucleus. Due to the nucleoid localization of GUN1 and the molecular characteristics of GUN1 protein, i.e. it is a PPR protein that accumulates during the very early stages of chloroplast biogenesis in Arabidopsis cotyledons, we will focus our attention on:

4. The expression of chloroplast genes in cotyledons of the different single and double mutants and in Col-0 seedlings grown in the presence of different concentration of lincomycin, i.e. characterised by a partial or total block of plastid protein synthesis.
5. The accumulation of PhANG transcripts and transcription factors with a role in retrograde signalling.

I do believe that the achievement of these objectives will represent an important contribution to the comprehension of the chloroplast-to-nucleus communication and more in general will shed a new light into the intricate molecular network at the basis of chloroplast biogenesis and chloroplast protein homeostasis.

2. Materials and methods

2.1 Plant material and growth conditions

All the *A. thaliana* T-DNA insertion mutant lines used in this work are listed in the Table 2.1. In order to determine the insertion site, the regions flanking the T-DNA insertion (Fig. 2.1) were PCR amplified and sequenced (primer sequences in Table 2.2). Double and triple mutants *gun1-102 ftsh5-3, ftsh2-22 ftsh5-3, prps21-1 gun1-102 ftsh5-3, fug1-3 gun1-102 ftsh5-3* were all produced by manual crossing the single and double mutants, while *gun1-9 ftsh2-23* and *pub4-7 gun1-102 ftsh5-3* were produced employing the CRISPR-Cas9-gene editing technology.

Col-0 and mutant seeds were subjected to 2 days of vernalization on wet whatman paper at 4°C in darkness. After this step they were transferred on soil in a climate chamber at 22°C and 60% RH (Relative humidity) under a long-day regime (16 h light / 8 h dark cycle).

To obtain the transgenic lines, flowers of Col-0 plants were subjected to *Agrobacterium tumefaciens*-mediated transformations (floral dipping) with FtsH1, FtsH2, FtsH5, FtsH8 carrying-vectors (see paragraph 2.2) and of *gun1-102 ftsh5-3* plants with FtsH1 and FtsH5 carrying-vectors according to Clough and Bent (1998). Plants were transferred to the greenhouse and seeds were collected after 3 weeks. Transgenic plants were selected on the basis of their resistance to glufosinate-containing herbicide Basta (Bayer). Successful complementation was confirmed by measurements of chlorophyll fluorescence, chlorophyll quantification and growth. The presence of the transgene in the complemented mutant plants was confirmed by PCR using primers that specifically allowed the amplification of FtsH5 and FtsH1 cDNA fragments and by western blot analyses. The CRISPR-Cas9 mutant plants, carrying the

mutation of interest, were produced through floral dipping too and selected among the T3 generation. Primer sequences used for Guide RNA design are listed in Table 2.2.

The lines: *oeFtsH1-GFP gun1-102 ftsh1-1, oeFtsH1-GFP gun1-102 ftsh5-3*, *oeFtsH5-RFP gun1-102 ftsh5-3*, *oeFtsH2-GFP gun1-9 ftsh2-23* and *oeFtsH8 gun1-102 ftsh8-1,* were obtained crossing the double mutant lines with each FTSH-overexpressing line and isolating the plants by PCR-based segregation. Afterwards, the identified plants were subjected to western blot analyses.

For phenotypic analyses and growth in presence of lincomycin (Lin), plants were grown for 6 days (80 μmol $m^{-2}s^{-1}$ at 16h/8h light/dark cycle) on Murashige & Skoog (MS) (Murashige and Skoog, 1962) medium (Duchefa Biochemie) with 2% (w/v) sucrose, 1% (w/v) Phyto-Agar (Duchefa Biochemie) together with lincomycin (Sigma-aldrich) at the final concentration of 550 μM.

Locus	Gene	Allele	Line	Reference
AT2G31400	*GUN1*	*gun1-102*	Sail-742-A11	Tadini et al., 2016
AT2G31400	*GUN1*	*gun1-9*	Point mutation	Koussevitzky et al., 2007
AT1G50250	*FtsH1*	*ftsh1-1 (ftsh1)*	Arabidopsis Knockout Facility (University of Wisconsin, Madison)	Sakamoto et al., 2003
AT2G30950	*FtsH2*	*ftsh2-22*	SAIL_253_A03	This work
AT2G30950	*FtsH2*	*ftsh2-23*	CRISPR-Cas9-induced	This work
AT5G42270	*FtsH5*	*ftsh5-3* (*var1-3*)	SAIL_875_E04	Sakamoto et al., 2002
AT1G06430	*FtsH8*	*ftsh8-1 (ftsh8)*	Syngenta Arabidopsis Insertion Library (Torrey Mesa Research Institute, San Diego, CA)	Sakamoto et al., 2003
AT2G23140	*PUB4*	*pub4-2*	Salk054373	Wang et al., 2013
AT2G23140	*PUB4*	*pub4-7*	CRISPR-Cas9-induced	This work
AT1G17220	*FUG1*	*fug1-3*	SAIL_209_E08	Miura et al., 2007
AT3G27160	*PRPS21*	*prps21-1*	SAIL_1173_C03	Tadini et al., 2016
AT1G32990	*PRPL11*	*prpl11-1*	SAIL_504_G08	Pesaresi et al., 2001
AT4G24280	*cpHsc70-1*	*cphsc70-1*	Salk_140810	Su & Li, 2008

Table 2.1 List of the mutant alleles employed in this work.

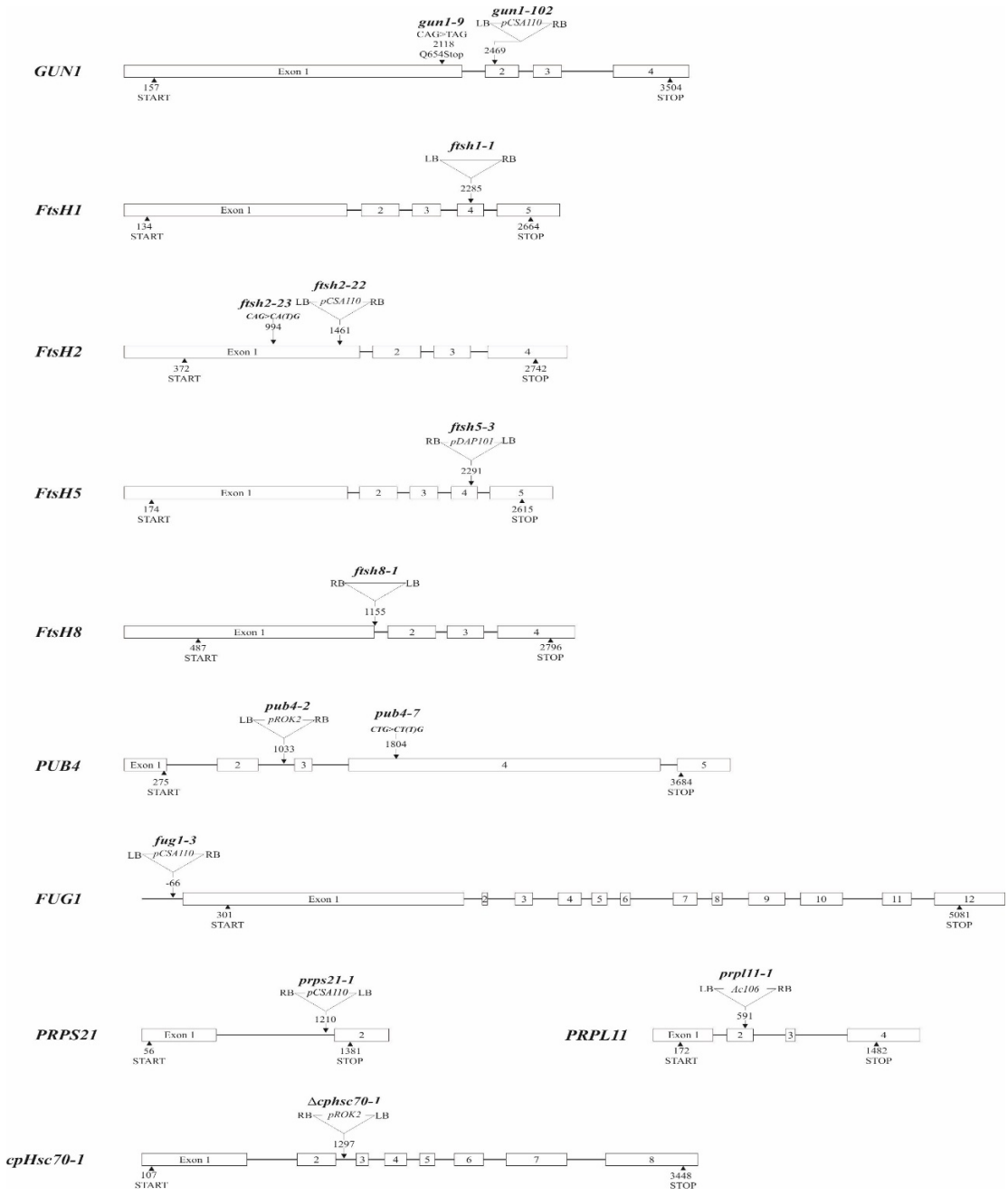

Figure 2.1. Schematic representation of T-DNA tagging and CRISPR-Cas9-induced mutations in *GUN1*, *FtsH*, *PUB4*, *PRPS21*, *PRPL11* and *CPHSC70-1* genes. Exons are indicated as numbered white boxes, introns as black lines. Arrowheads indicate the positions of translation initiation and stop codons. Sites, designations and orientations of T-DNA insertions

are indicated (RB, right border; LB, left border). The T-DNA insertions are not drawn to scale. Sequence modifications obtained by gene editing are indicated in parenthesis: CA(T)G and CT(T)G indicate the CRISPR-Cas9-mediated insertion of a single nucleotide in the first exon of *FtsH2* and in the fourth exon of *PUB4* genes, respectively. Note that the phenotypes of *gun1-9 ftsh2-23* and *pub4-1 gun1-102 ftsh5-3* cotyledons were fully complemented by the introduction of wild-type copies of *FtsH2* and *PUB4* genes, respectively, excluding the possibility of off-targets introduced by the CRISPR-Cas9 gene editing strategy.

Locus	Gene	Sense primer (5' to 3')	Antisense primer (5' to 3')	Use
AT2G31400	*GUN1*	GAGAGTAACAACCGAACGAC	AAAGTGCCAAAGCATGTCAG	*GUN1-102* genotyping
AT2G31400	*GUN1*	GAGAGTAACAACCGAACGAC	TAGCATCTGAATTTCATAACCAATCTCGATACAC	*gun1-102* genotyping
AT2G31400	*GUN1*	TTTGCCTTTCTCTTCTTCTG	GGACCATTGGTCCTATACAC	*gun1-9* genotyping (BsaXI cut)
AT1G50250	*FTSH1*	GCGGAAGGTTAGTTAGTAATGG	ACTCATGAACTCTTCACCGTC	*FTSH1-1* genotyping
AT1G50250	*FTSH1*	CGTCTTCAAAGCAAGTGGATTGATGTG	ACTCATGAACTCTTCACCGTC	*ftsh1-1* genotyping
AT2G30950	*FTSH2*	AGATGGCAGCTTCATCAGC	CGTCAACACTTACCTGCACC	*FTSH2-22* genotyping
AT2G30950	*FTSH2*	TAGCATCTGAATTTCATAACCAATCTCGATACAC	TGAACGTGTCGCGTACCTG	*ftsh2-22* genotyping
AT2G30950	*FTSH2*	CGCTTTTGATTGGTGGTTTG	AACCGCAGTGAATCTCTCAG	*ftsh2-23* genotyping
AT5G42270	*FTSH5*	GTGTGGTTTATTGCAGGTGC	CCTTCTGCGATGACATCTGC	*FTSH5-3* genotyping
AT5G42270	*FTSH5*	GTGTGGTTTATTGCAGGTGC	CTGAATTTCATAACCAATCTCGATACAC	*ftsh5-3* genotyping
AT1G06430	*FTSH8*	TTGATGCAGGTATCTGTTGACG	CCAAAGATGACTTCTTCGGC	*FTSH8-1* genotyping
AT1G06430	*FTSH8*	GCTTCATCGGCTTGTCTTCTC	CCAAGCCTCGCTAGTCAAAAGTGTA	*ftsh8-1* genotyping
AT3G27160	*PRPS21*	TCAATGATAGCTTGTGATGG	TTTCCAACTCACAATGTACC	*PRPS21* genotyping
AT3G27160	*PRPS21*	TCAATGATAGCTTGTGATGG	TAGCATCTGAATTTCATAACCAATCTCGATACAC	*prps21* genotyping
AT1G32990	*PRPL11*	CTTCTCTACATCCCAACTCC	GCGGGGTCTTGAGAATAAAC	*PRPL11-1* genotyping
AT1G32990	*PRPL11*	CTTCTCTACATCCCAACTCC	ATAATAACGCTGCGGACATCTACATTTT	*prpl11-1* genotyping
AT1G17220	*FUG1*	CTTAAATGTAGCCACGTGTG	ACTAAAGCATACGATGCATC	*FUG1-3* genotyping
AT1G17220	*FUG1*	TAGCATCTGAATTTCATAACCAATCTCGATACAC	ACTAAAGCATACGATGCATC	*fug1-3* genotyping
AT4G24280	*CPHSC70-1*	TGGTACCTTTGATGTCTCAG	TGGCCGTGATAAAAGGTAAG	*CPHSC70-1* genotyping
AT4G24280	*CPHSC70-1*	GCGTGGACCGCTTGCTGCAACT	TGGCCGTGATAAAAGGTAAG	*cphsc70-1* genotyping
AT2G23140	*PUB4*	TAGACCCGTTTGAGAAGTAC	TTAGCGATTAAGGCCTTCAC	*PUB4-2* genotyping
AT2G23140	*PUB4*	TAGACCCGTTTGAGAAGTAC	GCGTGGACCGCTTGCTGCAACT	*pub4-2* genotyping
AT2G23140	*PUB4*	GATTCTGATTGAAGCTGTTGC	TTAGCGATTAAGGCCTTCAC	*pub4-7* genotyping
At2G31400	*GUN1*	*TCCTTTCAATGGCGTCAACG	**ACAAAAGAAGAGGCTGTAAAGCAAACG	Subcellular localization, BiFC
AT1G50250	*FTSH1*	*ATGGCTTCTAACTCATTACTACG	**TCAAGAAATATACAACTCAGCTTGGC	Subcellular localization, BiFC
AT2G30950	*FTSH2*	*ATGGCAGCTTCATCAGCTTGTC	**AGACAGCAGCTGGTGTTGGTG	Subcellular localization, BiFC
AT5G42270	*FTSH5*	*ATGGCGACCACATCATCAAAC	**AAGAAACATATAACTCGGCTTGTCCG	Subcellular localization, BiFC
AT1G06430	*FTSH8*	*ATGGCTGCTTCATCGGCTTG	**AGACAGACGCTGGTGTTGGTG	Subcellular localization, BiFC
AT1G49240	*ACT8*	CTCAGGTATTGCAGACCGTATGAG	CTGGACCTGCTTCATCATACTCTG	qtRT-PCR
AT1G13320	*PP2A*	TATCGGATGACGATTCTTCGTGCAG	GCTTGGTCGACTATCGGAATGAGAG	qtRT-PCR
At2G26150	*HSFA2*	TCGTCAGCTCAATACTTATGGATTC	CACATGACATCCCAGATCCTTGC	qtRT-PCR
At4G27670	*HSP21*	TGGACGTCTCTCCTTTCGGATTG	TTTGTCGCATCGTCCTCATTGG	qtRT-PCR
At4G24280	*CPHSC70-1*	CTCGTGAGGAAGGTGACTGG	AACACCACCTAGGGTCTCCA	qtRT-PCR
At5G49910	*CPHSC70-2*	GCTGACTCCGTCGTTTACCA	CCTGGTTGGGGTTGGTTGTA	qtRT-PCR
At4G16520	*ATG8f*	CGTTCTTTGTAGTCTACAGG	CGGAATCCTATCAGGATACT	qtRT-PCR
AT5G17290	*ATG5*	CATGTCTCAGAGTGATCAAG	CTCATCTTCGACTGTTCC	qtRT-PCR
AT2G44140	*ATG4*	AGCTCTAGGATTCTATTGCC	CGTTTGATTCCTCAGCTAGT	qtRT-PCR
AT2G45980	*ATI1*	TCATCATCAATCTCCGGATC	CTCATTGTTAGCCATCCTCA	qtRT-PCR
AT2G25625	*CV*	CGTCAAAGATCTCTTGTAGG	CATCATTGATCTGAATCCCG	qtRT-PCR
AT2G23140	*PUB4*	CTTCTCAGAAGTATCTCGTC	CATCTGCTATAGGCTTCAAC	qtRT-PCR
AT1G50250	*FTSH1*	TTCTCCGTCTGTCGTTATAG	GCTGAATCTAACTCTCTCGA	qtRT-PCR
AT2G30950	*FTSH2*	GCTAGACAGATGGTAACAAC	CTCAGACATGGAGTTTCTTG	qtRT-PCR
AT5G42270	*FTSH5*	TCTTTGGAGACGAGAATGTG	CTTTGACCCAAGAAAGGGTT	qtRT-PCR
AT1G06430	*FTSH8*	TAACCGGATTCAGCGTGTAC	GAGTATTGGAGAACCTTGGT	qtRT-PCR
AT2G07739	*Tic214*	ACTGATAAAGAGCCACATGG	TGAAGAATTTGTCCACTCCAAG	NB
ATCG00740	*rpoA*	AGGCATTGCGATGCGAAGAG	GACTATATCCGCGATTCCTC	NB
ATCG00190	*rpoB*	TCAAGAAGAACAGGCTGTTC	GTTTCAACCCACGATCCTAG	NB
AtCG00905/ AtCG01230	*rpS12-3'*	ACTATCACCCCCAAAAAACC	AACGCCCTTGTTGACGATCC	NB
AtCG00670	*clpP1*	ATGCCTATTGGCGTTCCAAAAG	TTATTGAACCGCTACAAGATCAAC	NB

ATCG00490	*rbcL*	AACTCCTCAACCTGGAGTTCC	CCATCTAATTTATCGATGGTTGG	NB
ATCG00020	*psbA*	CTTCTGCAGCTATTGGATTGC	CATTTTCTGTGGTTTCCCTGA	NB
AT1G29920	*Lhcb1*	GACTTTCAGCTGATCCCGAG	CGGTCCCTTACCAGTGACAA	NB
ATCG00120	*atpA*	TTCTTCCGTGGCTCAGGTAG	AATAGCAGGTCTGATTCCAG	NB
ATCG00350	*psaA*	AGGCTTCCACAGTTTTGGTTT	CCCAAACATCTGACTGCATTT	NB
AT2G30950	*FTSH2*	**ATTG** CCTGGTAACCCACTTCAGTT	**AAAC** AACTGAAGTGGGTTACCAGG	CRISPR-Cas9 guide RNA
AT2G23140	*PUB4*	**ATTG** TCATTACTTCAAGTGACAGA	**AAAC** TCTGTCACTTGAAGTAATGA	CRISPR-Cas9 guide RNA
	attB sites: **GGGGACAAGTTTGTACAAAAAAGCAGGCT***; **GGGGACCACTTTGTACAAGAAAGCTGGGT**** **ATTG/AAAC**, SIgned in bold, are sticky ends for cloning procedure			

Table 2.2 List of the primers used in this work. In the last column the experiment(s) for which they were used is reported. NB, Northern Blot; qRT-PCR, Real-time PCR.

2.2 Construction of vectors

To obtain *oeFtsH1-GFP*, *oeFtsH2-GFP*, *oeFtsH5-RFP* and *oeFtsH8-GFP* transgenic lines, the FtsH1, FtsH2, FtsH8 cDNA were ligated into the plant expression vector pB7FWG2 while FtsH5 cDNA was ligated into the vector pB7RWG2, purchased by Flanders Interuniversity Institute for Biotechnology (Gent, Belgium). All these genes were placed under the transcriptional control of the cauliflower mosaic virus 35S promoter (*35S-CaMV*).

The double mutant *gun1-9 ftsh2-23* was generated by targeting the first exon of *FtsH2* genomic locus in *gun1-9* mutant background, using the pDe-CAS9 vector, using the cloning procedure described by Fauser et al., (2014). The triple mutant *pub4-7 gun1-102 ftsh5-3* was generated by targeting the fourth exon of *PUB4* genomic locus, in *gun1-102 ftsh5-3* mutant background, exploiting the pHEE401E vector and using the cloning procedure described by Xing et al., (2014).

2.3 Chlorophyll fluorescence measurements and chlorophyll quantification

In vivo chlorophyll *a* fluorescence of cotyledons (6 Days After Sowing, DAS) was measured employing a Dual-PAM-100 (Walz) after 30 min of dark incubation of the seedlings at room temperature (23 to 25°C). Using the dark-adapted plants, the minimal fluorescence (*F0*) was measured. With a pulse (0.8 sec) of saturating white light (3000 μmol photon m^{-2} s^{-1}), the maximum fluorescence (*Fm*) was determined. The ratio $(F_m\text{-}F_0)/ F_m$ was calculated as F_v/F_m, the maximum quantum yield of PSII. After 10 min of actinic red light (80 μmol photon m^{-2} s^{-1}), the steady state fluorescence (*Fs*) was measured and with a second saturation pulse the *Fm'* was determined. The PSII effective quantum yield (ΦII) was then calculated (Pesaresi et al., 2009).

For pigment extraction, 6 days old plants growth in soil, (80 mg of each samples -fresh weight-) were collected and frozen in liquid nitrogen. Chlorophyll and carotenoids were extracted adding 800 μl of 100% (v/v) acetone to each pulverized sample, these were vortexed and centrifuged at max speed, 4°C, for 10 min. The supernatant was collected and diluted in a final volume of 1 mL using 80% (v/v) acetone. Absorbance of chlorophyll *a* and *b* were measured spectroscopically and measurements were performed in triplicate.

Concentration of chlorophyll *a* and *b* was obtained using the extinction coefficients from previous studies (Porra et al., 1989).

Total chlorophyll content was calculated and expressed in μg/mg using this formula:

$$Chla + Chlb = \frac{17{,}76 \cdot A_{646} + 7{,}43 \cdot A_{663}}{m \cdot V} \cdot DF$$

Where:

A_{663} is the Chla absorbance, A_{646} is the Chlb absorbance, m is the mass material (mg), V is the volume of acetone (mL), DF is the dilution factor

2.4 Transmission electron microscopy

Tissue fragments (1-2 mm^2) from fully expanded seedlings of Col-0, *gun1-102*, *ftsh2-22*, *ftsh5-3*, *pub4-2, gun1-102 ftsh5-3*, *gun1-9 ftsh2-23*, *+/ftsh1-1 ftsh5-3*, *ftsh2-22 ftsh5-3*, *pub4-7 gun1-102 ftsh5-3* Arabidopsis plants were fixed in 1.2% glutaraldehyde and 3.3% paraformaldehyde in 0.1 M phosphate buffer pH 7.4 at 4°C for 2 h, postfixed in 1% OsO_4 (w/v) in the same buffer for 2 h, dehydrated in an ethanol series and embedded in Spurr's resin. Thin sections (1-2 m thick) were stained with 0.1 % tolouidine blue and examined with an Olympus BX-50 light microscope (Olympus, Japan). Ultrathin sections were stained with 2% uranyl acetate and lead citrate, before being examined with a Jeol 100SX TEM (Jeol, Japan) operating at 80 KV.

2.5 Nucleic acid analyses

The 6 DAS Col-0 and mutant seedlings were collected and grounded in liquid nitrogen, the total RNA was extracted from pulverized tissues adding to them one volume of extraction buffer [300 mM NaCl, 50 mM TRIS-HCl pH 7.5, 20 mM EDTA, 0.5% (w/v) SDS] and one volume of Phenol-Chloroform-Isoamylalcohol (PCI). After this step, the samples were solubilized at 65°C for 5 min and centrifuged for 10 min at 7.000 *g*. The supernatant collected after the

centrifugation, was mixed with one volume of 8 M LiCl, incubated for two h at -20°C and finally centrifuged for 30 min at 4°C at 7.000 *g*. The pellet was then washed with 75% ethanol and resuspended in 80 µl of DEPC-treated water.

RNA gel blot analyses were performed according to Meurer et al. (2002), using 5 µg of total RNA for each sample. ^{32}P-labeled DNA probes were generated using primers listed in Table 2.2.

A quantitative Real-Time PCR was performed on total RNA extracted from 6 days old plants using the DNA, RNA and protein purification kit (NucleoSpin® TriPrep, Machery-Nagel), according to the supplier's recommendations. Total RNA (4 µg) was used as template to synthesize cDNA, employing the GoScript Reverse Transcription system kit (Promega). For the quantitative Real-time PCR, the housekeeping genes *ACTIN8* (AT1G49240) and *PP2A* (AT1G13320) were used as internal standards, and gene specific primers are listed in Table 2.2. The final volume of the Real-time PCR reactions was 20 µL using the iTaq Universal SYBR Green Supermix (Bio-Rad), 10 mM of both 5' and 3' primers, and the cDNA was diluted 5 times in distilled, deionized water. The PCR program used for all the analyses was: 3 min, 95°C (thermo-start); 40 cicles (5 s, 95°C; 30 s, 60°C); and 1 sec, 55°C; and ended with an 95°C-step dissociation. All the experiments were performed in triplicate using a CFX96 Real-Time system (Bio-Rad) and the replicates were analysed through Bio-Rad CFX Manager software (V3.1).

2.6 Protein samples preparation and immunoblot analyses

For immunoblot analyses, total proteins were extracted from 6 DAS seedlings, as described by Martinez-Garcia et al. (1999). Seedling material was homogenized in Laemmli sample buffer [20% (v/v) glycerol, 4% (w/v) SDS,

160 mM Tris-HCl 6.8, 10% (v/v) 2-mercaptoethanol] to a concentration of 0.1 mg μl^{-1} (fresh weight/Laemmli sample buffer). Samples were incubated at 65°C for 15 min and, after a centrifugation step (10 min at 16.000 *g*), the supernatant was then incubated for 5 min at 95°C and loaded onto SDS-PAGE. For immunoblot against TIC and TOC proteins (Toc159, Toc75, Toc34, Tic110, Tic40, Tic100, Tic56, Tic20-1), seedlings material was homogenized in a modified Laemmli sample buffer [4% (w/v) SDS, 160 mM Tris-HCl pH 6.8, 100 mM dithiothreitol; 0.1 mg μl^{-1} (fresh weight/Laemmli sample buffer)] Samples were incubated at 65°C for 15 min and followed by centrifugation step (10 min at 16.000 *g*). The supernatant was then loaded avoiding the denaturation step at 95°C. Proteins, corresponding to 4 mg of seedlings fresh-weight, were fractionated by SDS–PAGE 10% (w/v) acrylamide; (Schägger and von Jagow, 1987) and then transferred to polyvinylidene difluoride (PVDF) membranes (Ihnatowicz et al., 2004). Replicate filters were immunodecorated with specific antibodies.

Intact chloroplast isolation was performed, with minor changes, according to Kunst, 1998. 0.5 g of 6 DAS seedlings were homogenized in 2 ml of 45 mM Sorbitol, 20 mM Tricine-KOH pH 8.4, 10 mM EDTA, 10 mM $NaHCO_3$ and 0.1% (w/v) BSA fraction V and centrifuged for 7 min at 700 *g*. The supernatant was collected as extra-chloroplast fraction while the intact chloroplast pellet was washed with 1 ml of the same buffer. After a centrifugation step (7 min at 700 *g*), the pellet was collected as intact chloroplast fraction.

To perform immunoblot to analyze HY5 transcription factor accumulation (Lee et al., 2017), total protein extracts were prepared, grinding the samples (6 DAS seedlings grown as described in paragraph 2.1, with and without lincomycin) in urea buffer [50 mM Tris-HCl pH 7.5, 4 M urea, 150 mM NaCl, 0.1% (v/v) Nonidet P-40, 50 μM MG132 (Sigma-aldrich) and Protease inhibitor cocktail tablets (Roche)], samples were incubated at 65°C for 15 min and, after a

centrifugation step (10 min at 16.000 *g*), the supernatant was then incubated for 5 min at 95°C and separated by SDS-PAGE 12% (w/v) acrylamide (Schägger and von Jagow, 1987), and immunoblotted over night with anti-HY5 antibody (1:500 dilution). In the immunoblot analyses of the transcription factors, the detection system used was the Liteablot Turbo chemiluminescent substrate (Euroclone) while for all the other proteins was used the Chemiluminescent substrate (Euroclone).

AtHsp90-1 (AS08 346), Tic40 (AS10 709), Toc34 (AS07 238), Toc75 (AS06 150), ClpB3 (AS09 459), VIPP1 (AS06 145), UBQ11 (AS08 307A), ptCpn60 (AS12 2613), Hsc70-1 (AS08 348), PsaD (AS09 461), D1 (AS05 084), PsbO (AS06 142-33), PetA (AS08 306), PetC (AS08 330), ATPase-β (AS05 085), Lhca1 (AS01 005), Lhca2 (AS01 006), Lhca3 (AS01 007), Lhca4 (AS01 008), Lhcb1 (AS01 004), Lhcb2 (AS01 003), Lhcb3 (AS01 002), Lhcb4 (AS04 045), Lhcb5 (AS01 009) and RbcS (AS07 259), HY5 (AS12 1867) antibodies were obtained from Agrisera. The GFP antibody was purchased from Thermo Fisher Scientific, AtHsc70-4 antibody from Antibodies-online and the RFP antibody was obtained from Chromotek. Tic 100, Tic 56, Tic20-1 antibodies were donated by Masato Nakai (Osaka University), Tic110, Toc159 and ClpC2 antibodies were obtained from Paul Jarvis (University of Oxford), FtsH1 antibody from Zach Adam (The Hebrew University of Jerusalem), while FtsH2 and FtsH5 were donated by Wataru Sakamoto (Okayama University), GLK1 antibody was donated by Takehito Inaba (University of Miyazaki).

2.7 Immunoprecipitation of Toc34

Toc34 immunoprecipitation was performed on 0.5 g of frozen Col-0 and *gun1-102* 6 DAS seedlings grown in presence of 550 µM lincomycin. The tissue powder was homogenized in 500 µl of immunoprecitation (IP) buffer [30 mM

Hepes–KOH pH 8.0, 150 mM NaCl, 60 mM KOAc, 10 mM MgOAc, 1% (v/v) Nonidet P-40 and proteinase inhibitor cocktail (Sigma-Aldrich, P9599)]. Samples were incubated on ice for 15 min and subjected to a centrifugation step (10 min at 16.000 *g*). The supernatant was incubated (1 h, at 4°C) with 3 µl of Toc34 specific antibody. A mixture of magnetic anti-rabbit IgA and IgG Dynabeads^{TM} (Thermo Fisher Scientific) was then added to the samples. After 1 h incubation at 4°C, the magnetic beads were washed 3 times for 10 min with 1 ml of IP buffer and eluted with Laemmli sample buffer.

2.8 Protoplast isolation, BiFC and localization analyses

Protoplasts were isolated from leaves of *A. thaliana* (Col-0), which were grown on soil. The plants were grown in a temperature-controlled incubator (22°C) with a photoperiod of 16 h light (75 µmol photons m^{-2} s^{-1}) and 8 h dark**.** The cell wall was digested and the protoplast carefully extracted from the mesophyll according to the protocol described in Sheen, J. (2002). In detail, rosette leaves were collected from 3- to 5-week-old plants and cut into strips of 0.5–1 mm with a fresh razor blade. Leaf tissue was digested using an enzyme solution containing 1.25% (w/v) cellulase Onozuka R-10 (Duchefa) and 0.3% (w/v) Macerozyme R-10 (Duchefa) for a period of 3 h at 23 °C in the darkness. The protoplast suspension was filtered through a 50 µm nylon mesh washed three times with W5 solution (154 mM NaCl, 125 mM CaCl2, 5 mM KCl, 2 mM Mes, pH 5.7 adjusted with KOH) and used for PEG-mediated transformation. For each protoplast transformation, 10 µg of a MidiPrep purified DNA (Qiagen) carrying the constructs for the BIFC analyses were used. To produce the constructs for the experiment, *FTSH2, FTSH5* and *GUN1* genes were cloned into pVyNE or pVyCE vectors (Gehl et al., 2009), which carry sequences

encoding the N-terminal or the C-terminal portion of the Venus protein (a YFP derivative), respectively. Protoplasts, transformed with each construct combination (FTSH2 ^{YC}-GUN1^{YN}, FTSH5^{YC}-GUN1^{YN}, FTSH5^{YN}-FTSH2^{YC} as positive control), were incubated in the dark for 16–24 h at 23 °C, before performing confocal microscopy.

The localization of the FtsH proteins was performed using the plasmids (see paragraph 2.2) harboring the *35S*::*GUN1-GFP, 35S*::*FTSH1-GFP, 35S*::*FTSH2-GFP, 35S*::*FTSH8-GFP* and *35S*::*FTSH5-RFP* cassettes; the protoplast transformation was carried out as described above (10 µg of a MidiPrep purified DNA), followed by confocal microscopy analyses.

Arabidopsis protoplasts expressing the FTSH2 ^{YC}-GUN1^{YN}, FTSH5^{YC}-GUN1^{YN}, FTSH5^{YN}-FTSH2^{YC} BiFC complexes were analysed with a 63× oil-immersion objective (HCX PL APO 63X, N.A. 1.32) of an inverted Leica DMIRE2 microscope, equipped with a Leica TCS SP2 laser scanning device (Leica, Germany). For the detection of reconstituted YFP fluorescence the protoplasts were excited with the 514-nm line of the Argon laser and the emission was collected between 525 and 545 nm. The same laser line was also used to excite chlorophyll which emission was collected between 650 and 750 nm.

2.9 Thylakoids isolation

The thylakoids were extracted according to Järvi et al. (2011) working in dim light at 4°C. Six-days-old plants (growth on soil in the climate chamber) were collected and grinded in ice-cold grinding buffer [50 mM Hepes/KOH pH 7.5, 330 mM sorbitol, 2 mM EDTA, 1 mM $MgCl_2$, 5 mM ascorbate and 0.05% (w/v) BSA]. The homogenized samples were filtered using Miracloth layer, followed the centrifugation of the samples at 5.000 *g* at 4°C for 4 min. The

pellets were resuspended in an osmotic-shock buffer (50 mM Hepes/KOH pH 7.5, 5 mM sorbitol and 5 mM $MgCl_2$) and centrifuged at 5.000 *g* at 4°C for 4 min. The resulting pellets were resuspended into storage buffer (50 mM Hepes/KOH pH 7.5, 100 mM sorbitol and 10 mM $MgCl_2$) and finally centrifuged at 5.000 *g* at 4°C for 4 min. The isolated thylakoid membranes were resuspended and stored in the storage buffer at –80°C. The quality of the samples was evaluated measuring the chlorophyll content as described in the paragraph 2.3.

2.10 Biochemical analyses of thylakoid protein complexes: Blue Native and 2D SDS-PAGE

The thylakoid membranes (5 μg of total chlorophyll) were centrifuged at 4° for 10 min at 14.000 rpm and first resuspended in the same volume of storage buffer (see paragraph 2.9) and 25BTH20G [25 mM BisTris/HCl pH 7.0, 20 % (v/v) glycerol and 1M Pefabloc, with 10 mM sodium fluoride] (1:1 proportion) to reach a final chlorophyll concentration of 1 μg/μL. After gentle resuspension the detergent solution [25 mM BisTris/HCl pH 7.0, 20 % (w/v) glycerol, 1M Pefabloc, 10 mM sodium fluoride] together with 2% Dodecyl-maltoside (DM) to reach a final chlorophyll concentration of 0.5 μg/μL and a final detergent concentration of 1% (w/v) DM, was added. The thylakoid extracts were left to solubilize in the detergent solution for 5 min in ice and darkness. The samples were then centrifuged at max speed (14.000 rpm) for 25 min at 4°C, to remove the insoluble material.

The supernatant was then carefully collected into a separate tube, which already contained the one-tenth volume of Serva Blue G buffer [100 mM BisTris/HCl pH 7.0, 0.5 mM aminocephalosporanic acid, 30% (w/v) sucrose, 50 mg · ml $^{-1}$ Serva Blue G].

The native-PAGE gels were prepared as described in Schägger et al. (1991): to obtain an optimal protein complex separation the gel gradient used was 3.5-12.5% (w/v) total concentration of both acrylamide (AA) and bisacrylamide (Bis) monomers. The stacking gel solution was prepared with a final concentration of 3.5% (w/v) AA/Bis. Methods and solutions used to separate the protein complexes in the first (Large-pore BN-PAGE) and the second dimension (2D SDS-PAGE) are described into details in Järvi et al. (2011).

2.11 Soluble protein extraction

The soluble proteins were isolated from fresh six-days-old cotyledons according to Kangasjärvi et al. (2008). The cotyledons were grinded and poured into a new tube. Ice-cold extraction buffer [25 mM Hepes-KOH pH 7.5, 10mM $MgCl_2$, 1 tablet/10 mL protease inhibitor (1X) (complete Mini, Roche), 1 tablet/10 mL phosphatase inhibitor (1X) (phosSTOP, Roche), milliQ to reach the volume] was added to the pulverized sample, maintaining the homogenized solution as concentrated as possible. The extract was kept in ice for 10 min and then centrifuged for 15 min at 14.000 rpm. The supernatant was collected and used for mass spectrometry analyses.

2.12 Mass spectrometry analyses

Identification by data dependent acquisition (DDA) and analysis by selected reaction monitoring (SRM) of the FtsH bands (Appendices S6 and S7) have

been carried out essentially as in Trotta *et al.*, 2016. The list of masses used as inclusion list during the DDA analysis of the bands is reported in Appendix S4, for FtsH2 and Appendix S5, for FtsH2. The list of peptides and relative transitions monitored in SRM can be found in Appendix S8.

For the analysis of total foliar soluble extract (Appendices S2 and S3), the procedure described for total thylakoids analysis in Trotta *et al.*, 2016 has been used, with the exception that 50 µg of proteins per each genotype and treatment, with three biological replicates, have been digested with a trypsin in a ratio 1:10 µg. The following modification were in use: for the nLC-ESI-MS/MS analysis, a single column 40 cm x 75 µm, packed with 1.9 µm C18 120 Å (Dr Maisch) and a column oven at 60°C was used as in Geyer, 2016. Flow rate at 800 bar was 600 nl/min and the solvent B was 80% ACN 0.1% formic acid. The grandient was 3 to 43% B for 60 min, followed by 5 min increase to 100% and 10 min of 100% B. The mass spectrometer used was a Q-Exactive HF (Thermo Scientific), with resolution set to 120000 and scan range 300 to 1800 m/z for MS1 and resolution 15000 with scan range 200 to 2000 m/z for MS2. Dynamic exclusion window was set to 20 s and up to 30 masses with m/z >2+ were selected for MS2 for every MS1 scan. All the other conditions, including the Mascot searches, were conducted as previously described (Trotta et al., 2016).

The mass spectrometry analyses (Appendix S9) performed to study the accumulation of the cytosolic chaperones (Hsp90-2, Hsp70-1) in the different genetic backgrounds were so organized: differentially 1D-gel lines from Col-0 and *gun1-102* were cut and digested enzymatically with trypsin as described by Marsoni et al. (2008) with some modifications. Briefly the gel pieces were washed in H_2O HPLC-grade and subsequently in 50% acetonitrile (ACN) for 10 min. The gel fragments were incubated for 5 min in 100% ACN for 5 min; liquid was discarded and gel pieces were reduced in 25 mM Dithiothreitol

(DTT) for 20 min at 56°C and subsequently alkylated for 20 min with 55 mM of iodacetamide (IAA) at T amb in the dark. The gels pieces were washed in 20 volumes of H_2O in order to eliminate any residue of IAA and after in a solution 1:1 of ACN and NH_4HCO_3 100 mM for 15 min. The gel pieces were dried under vacuum on a centrifugal evaporator. For the protein digestion trypsin solution [Sequencing Grade Modified Trypsin V5111, Promega, Madison; 12.5 ng/µl in digestion buffer (25 mM NH_4HCO_3, 2.5 mM $CaCl_2$)] was added and samples were incubated at 4°C. After 120 min the supernatants (SN) were replaced with of digestion buffer and the proteins were digested O/N at 37°C. In order to extract the tryptic fragments, the gel pieces were sonicated for 5 min in a cool water bath and SN collected (fraction I). The gel pieces were incubated for 15 min at 37°C in 25 mM NH_4HCO_3 and, after addition of one volume of ACN, were incubated for 10 min at Tamb, vortexing occasionally. The SN were collected and pooled with the fraction I and the samples were washed for 10 min in in 5% formic acid and, after addition of one volume of ACN, incubated for further 10 min (vortexing occasionally). The SN were pooled again and DTT were added to give a final concentration of 1 mM. Finally, the samples were dried under vacuum on a centrifugal evaporator and the resulting tryptic fragments were dissolved in 0.1% formic acid analyzed by Liquid chromatography – Mass Spectrometry (LC-ESI MS/MS).

LC-ESI-MS/MS was performed with a Finningan LCQ DECA XP Mass spectrometer, equipped with a Finningan Surveyor MS HPLC system (Thermo Electron Corporation, California, USA). Chromatography separations were conducted on a Discovery Bio wide pore C18 column (150 µm I.D. × 150 mm length and 5 µm particle size; SIGMA, USA), using a linear gradient from 5% to 75% ACN, containing 0.1% formic acid with a flow of 2 µL min^{-1}. Acquisitions were performed in the data-dependent MS/MS scanning mode (full MS scan range of 400–1400*m*/*z* followed by Zoom scan for the most

intense ion from the MS scan and full MS/MS for the most intense ion from the zoom scan), thus enabling a dynamic exclusion window of 3 min. Fragmentation spectra were searched against NCBI Arabidopsis thaliana database using TurboSEQUEST Bioworks™ 3.2 software (Thermo Electron Corporation, California, USA) with these settings: two missed cleavages, fixed modification of cysteine (carbamidomethylation) and variable modification of methionine (oxidation). The precursor ion tolerance was set at 1.4 AMU. For an accurate protein identification the results were filtered as follow: peptides X-correlation *vs* charge > 1.5 (+1 charge), 2.0 > (+2 charge), > 2.5 (+3 charge), peptide probability < $1e^{-003}$, ΔCN > 0.1, Sf > 0.7, almost two different peptides. Only protein present in all biological replicates were considered for further analysis. Protein relative quantification between Col-0 and *gun1-102* sample were done considering the number of peptides assigned to each protein normalized using the total number of peptide /per gel (70-Col-0+90 Col-0+70 *gun1-102*+90 *gun1-102*). Statistical significance was evaluated by T Student test ($p<0.05$).

2.13 Nuclear proteins extraction

Plants were grown for 6 days on Murashige & Skoog (MS) (Murashige and Skoog, 1962) medium (Duchefa Biochemie) with 2% (w/v) sucrose, 1% Phyto-Agar (Duchefa Biochemie) with and without lincomycin (Sigma-aldrich) added to the medium in the final concentration of 550 μM at 80 μmol $m^{-2}s^{-1}$ at 16h/8h dark/light cycle.

Seedlings (1 g of material) were carefully transferred to liquid MS supplemented with 2% (w/v) sucrose and 50 μM MG132 (Sigma-aldrich). The petri dishes were transferred for 5 h to the growth chamber (80 μmol $m^{-2}s^{-1}$).

Samples were collected from the liquid MS and grinded in liquid nitrogen. Samples frozen powder was resuspended in 4 mL of Extraction Buffer 1 (EB1) [0.4 M sucrose, 10 mM Tris-HCl pH 8, 10 mM MgCl2, 1 mM EDTA, 5 mM β-mercaptoethanol and 1 tablet/50 mL protease inhibitor cocktail (Roche), 100 μM MG132], and left in ice for 5 min. The suspension was then filtered through Miracloth into new 2 mL tubes. Samples were centrifuged at 3.000 *g* for 20 min at 4°C.

The obtained pellet was gently resuspended in 1 mL of Extraction Buffer 2 (EB2) [0.25 M sucrose, 10 mM Tris-HCl pH 8, 10 mM MgCl2, 1 mM EDTA, 1% (v/v) triton X-100, 5 mM β-mercaptoethanol and 1 tablet/50 mL protease inhibitor cocktail (Roche), 100 μM MG132], and then transferred in a new 1.5 mL tube. Nuclei were pelleted again spinning the samples at 12.000 *g* for 10 min at 4 °C.

Nuclei pellet was then resuspended in 300 μL of Extraction Buffer 3 (EB3) [1.7 M sucrose, 10 mM Tris-HCl pH 8, 2 mM MgCl2, 1 mM EDTA, 0.15% (v/v) triton X-100, 5 mM β-mercaptoethanol and 1 tablet/50 mL protease inhibitor cocktail (Roche), 100 μM MG132]

300 μL of EB3 were laid into a clean 1.5 mL tube, and the 300 μL resuspended pellet were carefully layered on the top and subjected to 1 h of centrifugation at 14.000 *g* at 4°C.

The nuclei pellet was gently resuspended in 350 μL of Laemmli sample buffer (for the composition see the paragraph 2.6). Nuclear protein samples were first incubated at 65°C for 15 min and, afterwards, for 5 min at 95°C and loaded onto SDS-PAGE.

3. Results

3.1 GUN1 and the thylakoid FtsH protease complex are essential for proper greening of cotyledons

To further investigate the function of GUN1 in chloroplast protein homeostasis and chloroplast-to-nucleus signaling, we focused our attention on the functional relationship between GUN1 and the thylakoid FtsH protease complex at the seedling stage, i.e. the two-cotyledon stage used to characterize the *gun* mutant phenotype (Figure 3.1, A). To this end, *gun1-102* was introduced into genetic backgrounds carrying mutations in nuclear genes for FtsH1 (*ftsh1-1*), FtsH2 (*ftsh2-22*), FtsH5 (*ftsh5-3*) and FtsH8 (*ftsh8-1*) proteins. The *gun1-102 ftsh1-1*, *gun1-102 ftsh5-3* and *gun1-102 ftsh8-1* double mutants were obtained by crossing manually T-DNA insertional mutants, while the CRISPR-Cas9 based gene editing strategy was used to generate the *ftsh2-23* mutant allele in the *gun1-9* genetic background, since the two genes are in linkage on chromosome 2 (Figure 2.1, Materials and methods). Notably, *gun1-102, ftsh1-1, ftsh5-3* and *ftsh8-1* single mutants displayed wild-type-like cotyledons in terms of chlorophyll content (Figure 3.1, F) and photosynthesis (Figure 3.1, E), while *ftsh2-22* had a slight reduction in chlorophyll content and photosynthetic performance. Furthermore, while *gun1-102 ftsh1-1* and *gun1-102 ftsh8-1* were indistinguishable from Col-0 seedlings (Figure 3.1, A and B), *gun1-102 ftsh5-3* and *gun1-9 ftsh2-23* displayed exacerbated phenotypes characterized by white-yellow cotyledons, i.e. reduced chlorophyll content and low photosynthesis efficiency (Figure 3.1, F). The enhanced variegated phenotype of *gun1-102 ftsh5-3* double mutant was observable till the four-leaves rosette stage, while plants became identical to the *ftsh5* mutants at later stages (21 DAS). On the

contrary, the exacerbated *gun1-9 ftsh2-23* albinotic phenotype resulted in lethality at the two-leaves rosette stage (Figure 3.1, B). Interestingly, the additive effects on cotyledon pigmentation and photosynthesis, observed in *gun1-9 ftsh2-23* and *gun1-102 ftsh5-3* genetic backgrounds, were intermediate compared to plants with a reduced content of type A (+/*ftsh1-1 ftsh5-3*, carrying one functional copy of *FtsH1* allele), type B (+/*ftsh8-1 ftsh2-22*, carrying one functional copy of *FtsH8* allele) or both type A and type B (*ftsh2-22 ftsh5-3*) FtsH subunits, and plants lacking either type A (*ftsh1-1 ftsh5-3*) or type B (*ftsh2-22 ftsh8-1*) proteins, characterized by seedling lethal-albino phenotypes (Figure 3.1, A). These observations, together with the fact that the *gun1-102 ftsh5-3* cotyledon phenotype could be fully rescued by overexpressing the *FtsH1* gene (*oeFtsH1 gun1-102 ftsh5-3*), as in the case of *oeFtsH5 gun1-102 ftsh5-3* line (Figure 3.1, C, D, E, F), suggest that GUN1 protein might have a role in proper accumulation of thylakoid FtsH protease complex in Arabidopsis cotyledons. Interestingly, a partial rescue of *gun1-102 ftsh5-3* variegated cotyledons could be also observed through the introduction of the CRISPR-Cas9 induced *pub4-7* mutant allele, giving rise to the *pub4-7 gun1-102 ftsh5-3* triple mutant, lacking a broadly expressed cytosolic E3 ubiquitin ligase reported to control chloroplast degradation (Figure 2.1; Woodson et al., 2015). Overall, it appears that GUN1 and the thylakoid FtsH protease complex are essential for proper chloroplast development and that the observed phenotype of *gun1-9 ftsh2-23*, and *gun1-102 ftsh5-3* cotyledons might derive, at least in part, by the PUB4-mediated degradation of altered chloroplasts. Interestingly, this process seems to be peculiar of Arabidopsis cotyledons, since no rescue occurred in *gun1-102 ftsh5-3* seedlings, by introducing the *fug1-3* (*fug1-3 gun1-102 ftsh5-3*) and *prps21-1* (*prps21-1 gun1-102 ftsh5-3*) mutations (Figure 3.1, C), both involved in plastid protein synthesis and known (from

literature) to suppress the leaf variegated phenotypes of *ftsh2* and *ftsh5* single mutants (see also Figure 3.1, D).

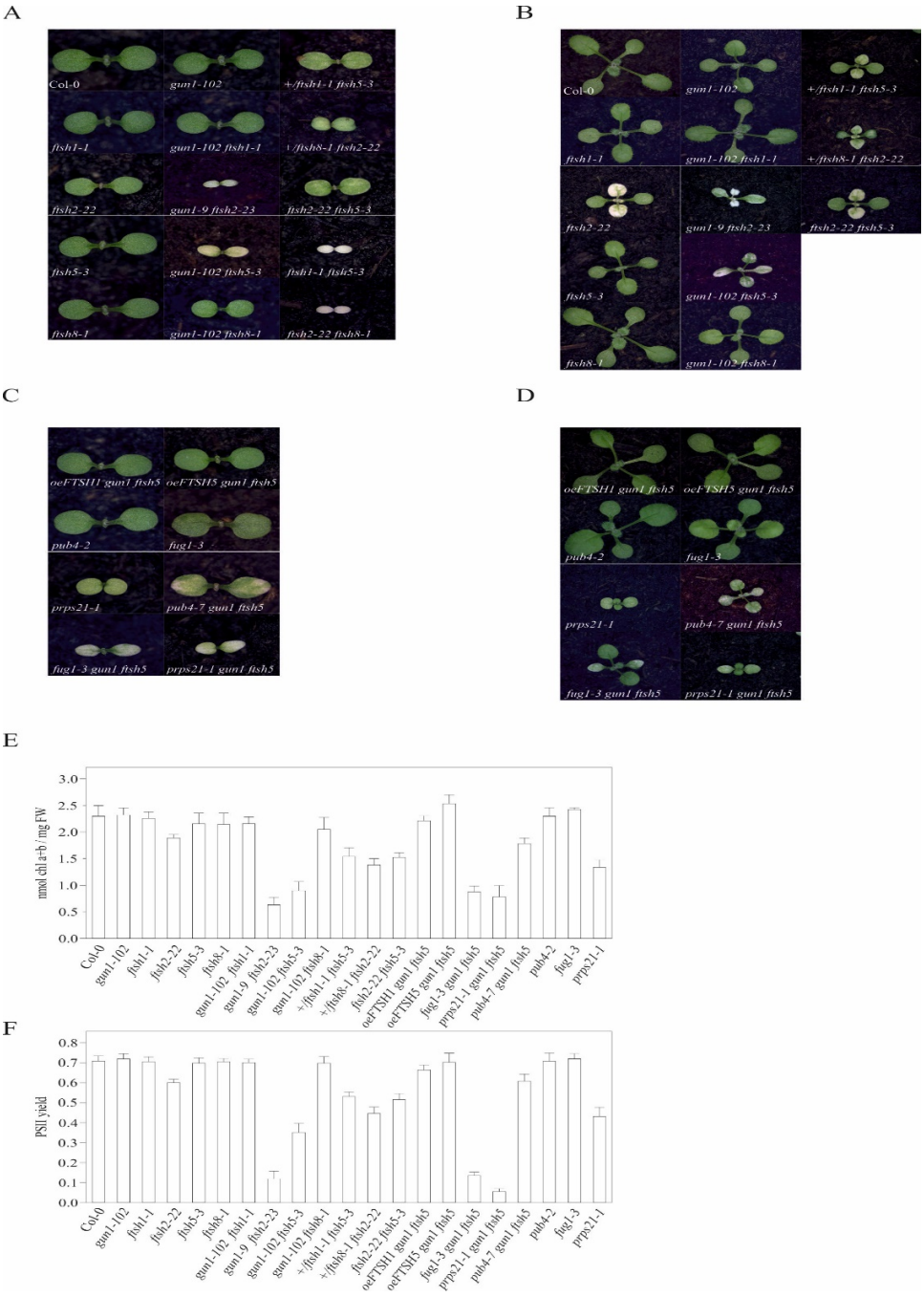

Figure 3.1. Genetic interaction between GUN1 and the FtsH2 and FtsH5 subunits of the thylakoid protease complex. A, and B, Phenotypes of *gun1-102* and *ftsh* single and double mutants at 6 (**A**) and 12 (**B**) days after sowing (DAS). At 6 DAS, only cotyledons are formed (**A**) while, at 12 DAS, the first two leaves are present (**B**). C, and D, Phenotypes of fully complemented *oeFtsH1 gun1-102 ftsh5-3* and *oeFtsH5 gun1-102 ftsh5-3* seedlings, partially reverted *pub4-7 gun1-102 ftsh5-3* line and no rescued *fug1-3 gun1-102 ftsh5-3*, and *prps21-1 gun1-102 ftsh5-3* cotyledons, together with the *pub4-2*, *fug1-3* and *prps21-1* single mutants at 6 (**C**) and 12 (**D**) days after sowing. (**E**), Cotyledon chlorophyll content of lines shown in A and C measured at 6 DAS. The total chlorophyll content was normalized on cotyledon fresh weight (nmol chl a+b /mg FW). (**F**), The cotyledon photosynthetic performance of lines shown in (**A**) and (**C**) was measured as effective quantum yield of PSII, employing a DUAL-PAM-100 (WALZ). Note that the absence of chlorophyll in *ftsh1-1 ftsh5-3* and *ftsh2-22 ftsh8-1* double mutant cotyledons did not allow the measurement of PSII photosynthetic efficiency.

3.2 GUN1 and the thylakoid FtsH protease complex are essential for the accumulation of fully developed lens-shaped chloroplasts

To better understand the cotyledon phenotypes of mutant seedlings, we analyzed the ultrastructure of mesophyll cell chloroplasts by transmission electron microscopy (TEM; Figure 3.2). TEM of thin sections of cotyledons from Col-0, *gun1-102*, *pub4-2* and *ftsh5-3* seedlings (grown at 100 μmol photons m^{-2} sec^{-1}) showed the characteristic chloroplast organization, including stacked granal thylakoids, stroma lamellae and starch granules. On the contrary, the paler cotyledons of *ftsh2-22*, +/*ftsh1-1 ftsh5-3* and *ftsh2-22 ftsh5-3* seedlings were characterized by highly vacuolated, round-shaped chloroplasts lacking the typical thylakoid organization in grana and stroma lamellae. In addition, vesicle-like structures were observed at the border between the chloroplast and the tonoplast in the case of *ftsh2-22* and *ftsh2-22 ftsh5-3*

chloroplasts. The introduction of *gun1-102* mutation into the *ftsh5-3* background led to the appearance of several cotyledon mesophyll cells, where fully developed WT-like chloroplasts were replace by plastids devoid of thylakoid membranes and characterized by large vesicles budding from the organelle and delivered to the vacuole. Interestingly, the enhanced greening of *gun1-102 ftsh5-3* cotyledon when the *pub4-7* mutation was introduced in this mutant background (see fig.3.2) indicates that the lack of PUB4 E3-ubiquitin ligase partially rescues the double mutant phenotype. In particular, a large part of chloroplasts of *pub4-7 gun1-102 ftsh5-3* cotyledon cells displayed irregular shapes and vesicles, but retained the thylakoid membranes, together with the partition in grana and stroma lamellae, and starch granules, suggesting that the concomitant absence of GUN1 and FtsH5 proteins leads to the degradation of altered chloroplasts, also through the PUB4-mediated chloroplast digestion pathway. A more exacerbated cotyledon phenotype was shown by *gun1-9 ftsh2-23* seedlings, where highly vacuolated irregular-shaped chloroplasts were rarely observed in mesophyll cells, and a considerable number of highly electron-dense structures inside vacuoles were visible, possibly as result of peroxisomes digestion.

Overall, the TEM observations support the notion that GUN1 and the optimal functionality of the thylakoid FtsH protease complex are essential for the accumulation of fully functional lens-shaped chloroplasts and that abnormal plastids are digested by the PUB4-dipendent pathway, although the involvement of other chloroplast degradation pathways cannot be excluded.

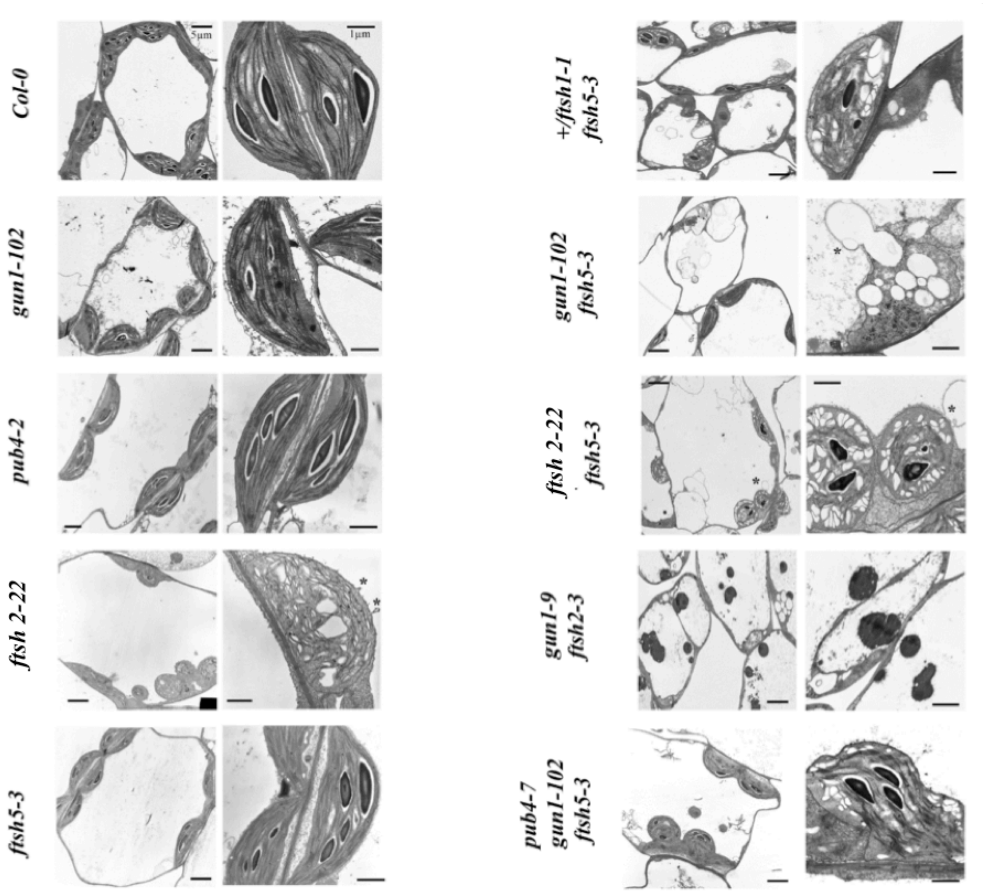

Figure 3.2. TEM micrographs of chloroplasts in 6 DAS Arabidopsis cotyledon mesophyll cells from Col-0, *gun1-102*, *ftsh5-3*, *ftsh2-22*, *pub4-2* single mutants, *+/ftsh1-1 ftsh5-3*, *ftsh2-22 ftsh5-3*, *gun1-102 ftsh5-3* and *gun1-9 ftsh2-23* double mutants and the *pub4-7 gun1-102 ftsh5-3* triple mutant. Ultrathin sections of cotyledons from Col-0 and mutant seedlings stained with 2% uranyl acetate and lead citrate observed by TEM. Scale bars for each sample correspond to 5 μm, right image, and 1 μm, left image.

3.3 The principal proteins involved in autophagy pathways are not so drastically changed at transcriptional level in the *gun1* mutant background

The expression of genes involved in the main pathways responsible to export chloroplast material in membrane-bound organelles and to deliver it to vacuoles for degradation was monitored. Quantitative Real-Time PCR (qRT-PCR) analyses (Fig. 3.3) performed on Col-0, *gun1-102*, *ftsh5-3* and *gun1-102 ftsh5-3* cotyledons, however, showed only minor differences in transcript levels of genes involved in the autophagy pathway, *ATG4*, *ATG5*, *ATG8f*, in the ATI-bodies mediated pathway (*ATI1*), in the autophagy-independent vesicle pathway, i.e. *chloroplast vesciculation* (*CV*) gene, and in the *PUB4*-mediated chloroplast digestion pathway, implying that some of these pathways are not activated or are even partially inhibited in *gun1-102 ftsh5-3* cotyledons, or that their regulation takes place at the post-transcriptional level, as in the case of *PUB4* gene (Figure 3.3).

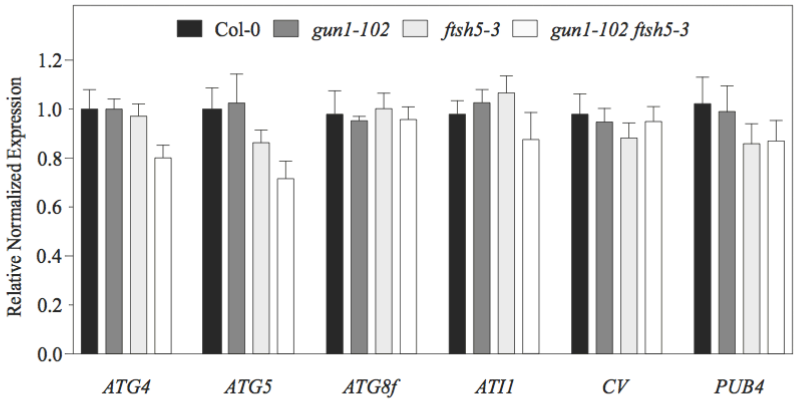

Figure 3.3. Expression of genes involved in chloroplast degradation in Col-0, *gun1-102*, *ftsh5-3* and *gun1-102 ftsh5-3* cotyledons. qRT-PCR analyses have been performed to monitor

the expression of genes involved in the autophagy pathways: *ATG4*, *ATG5*, *ATG8f, ATI1*, *CV* and *PUB4* genes. Primer pair sequences used for the analysis are described in Table 2.2 (Materials and methods). Values are the average of three biological and 9 technical replicates. Lines indicate the Standard deviation (SD). The *ACT8* and *PP2A* expression levels were used as internal standards.

3.4 The absence of GUN1 influences FtsH protein levels and has a general impact on thylakoid protein accumulation and organization

Genetic and phenotypic evidences (see Figure 3.1), together with chloroplast ultrastructure (see Figure 3.2) indicate that GUN1 protein has a role in the correct accumulation of the thylakoid FtsH protease complex. Intriguingly, immunoblot analyses performed using antibodies raised against the FtsH1, FtsH2 and FtsH5 subunits, support the notion that the absence of GUN1 protein decreases FtsH1 and FtsH5 levels in *gun1-9 ftsh2-23* cotyledons with respect to the *ftsh2-22* single mutant by about 20% and FtsH1 and FtsH2 abundance in *gun1-102 ftsh5-3* cotyledons in comparison to *ftsh5-3* by 17 and 32 %, respectively (Figure 3.4, A and Table 3.1). In addition, the level of FtsH1 protein in *gun1-9 ftsh2-23* was exactly half of the amount detected in *ftsh2-22 ftsh5-3* cotyledons, implying that the *gun1* mutation has a higher destabilizing effect on the accumulation of thylakoid FtsH protein complex than the concomitant absence of the two major subunits, FtsH2 and FtsH5. The crucial role played by GUN1 protein in mutant backgrounds defective in the thylakoid FtsH protease complex is further supported by the significant differences in PSII-LHCII supercomplex organization observed in cotyledons of Col-0, *gun1-102,* and *ftsh* seedlings. Indeed, thylakoids isolated from *ftsh2-22*, *gun1-102*

ftsh5-3 and *ftsh2-22 ftsh5-3* cotyledons and fractionated by large-pore Blue Native PAGE in the first dimension (Fig 3.4, B) and by SDS-PAGE in the second (Fig 3.4, C) showed a prominent reduction of PSII-LHCII supercomplexes (see asterisks) and a larger accumulation of CP43-less PSII-core (see crosses) in comparison with Col-0, *gun1-102* and *ftsh5-3* thylakoids. As expected, immunoblot analyses showed also a marked decrease of PSII (D1, PsbO), PSI (PsaD), Cyt b_6f (PetA, PetC), ATPase (ATPase-β), light harvesting complex of PSII (Lhcb4, Lhcb3) and light harvesting complex of PSI (Lhca2) in *gun1-9 ftsh2-23*, *gun1-102 ftsh5-3* and, although to a lesser extent, in *ftsh2-22 ftsh5-3* cotyledons with respect to the levels observed in Col-0, *gun1-102*, *ftsh2-22* and *ftsh5-3* thylakoids (see Table 3.1 for the quantification of protein amount). Interestingly, the marked decrease of the mature form of Lhcb3 protein (25 kDa), observed in *gun1-9 ftsh2-23* and *gun1-102 ftsh5-3* samples, was concomitant with the appearance of a Lhcb3 form migrating at around 90 kDa. This signal, although much fainter, was also visible in *ftsh5-3* and *ftsh2-22 ftsh5-3* thylakoids, possibly as result of post-translational modifications. Immunoblot analyses were also performed on the same set of genotypes to monitor the accumulation of the outer (Toc34) and inner (Tic40, Tic56, Tic100) translocon subunits of the chloroplast envelope. The Tic100 abundance was clearly reduced in *gun1-9 ftsh2-23* and *gun1-102 ftsh5-3* cotyledons, with respect to the related *ftsh* single mutants, by 20 and almost 90%, respectively. On the contrary, the levels of Tic40 and Tic 56 did not change significantly between *gun1-9 ftsh2-23*, *gun1-102 ftsh5-3* and the *ftsh2-22*, *ftsh5-3 s*ingle mutants. Furthermore, and similarly to Lhcb3, the Toc34 specific antibody was able to recognize three major forms of the protein in all the mutant analyzed: one at 34 kDa, the expected molecular weight of the mature form, and other two around the 80 kDa region, implying the occurrence of post-translation modifications. Also in the case of Toc34, the two higher bands were especially

abundant in *gun1-9 ftsh2-23* and *gun1-102 ftsh5-3* cotyledons, although they were clearly detectable also in *ftsh5* and *ftsh2 ftsh5* samples.

The abundance of proteins essential for thylakoid membrane formation, ClpB3 and VIPP1, together with the cytosolic protein folding and degradation machinery, AtHsc70-4, AtHsp90-1 and ubiquitin 11 (UBQ11), were also monitored. In general, their levels increased in *gun1-9 ftsh2-23* and *gun1-102 ftsh5-3* in comparison to *ftsh2-22*, *ftsh5-3* single mutants and Col-0, thus behaving in the opposite way of the thylakoid electron transport chain and translocon subunits (Table 3.1). Similarly, the abundance of ClpB3, AtHsc70-4 and ubiquitinated proteins (UBQ11) increased in *ftsh2-22 ftsh5-3* double mutant with respect to Col-0, while the VIPP1 and AtHsp90-1 levels remained unchanged. Overall, it is interesting to observe that the lack of GUN1 protein, per se, affects the abundance of a limited number of the proteins, manly subunit of the plastid translocation machinery, such as Tic100 and Toc34, supporting further the notion that GUN1 activity is needed when defects in plastid protein homeostasis are present.

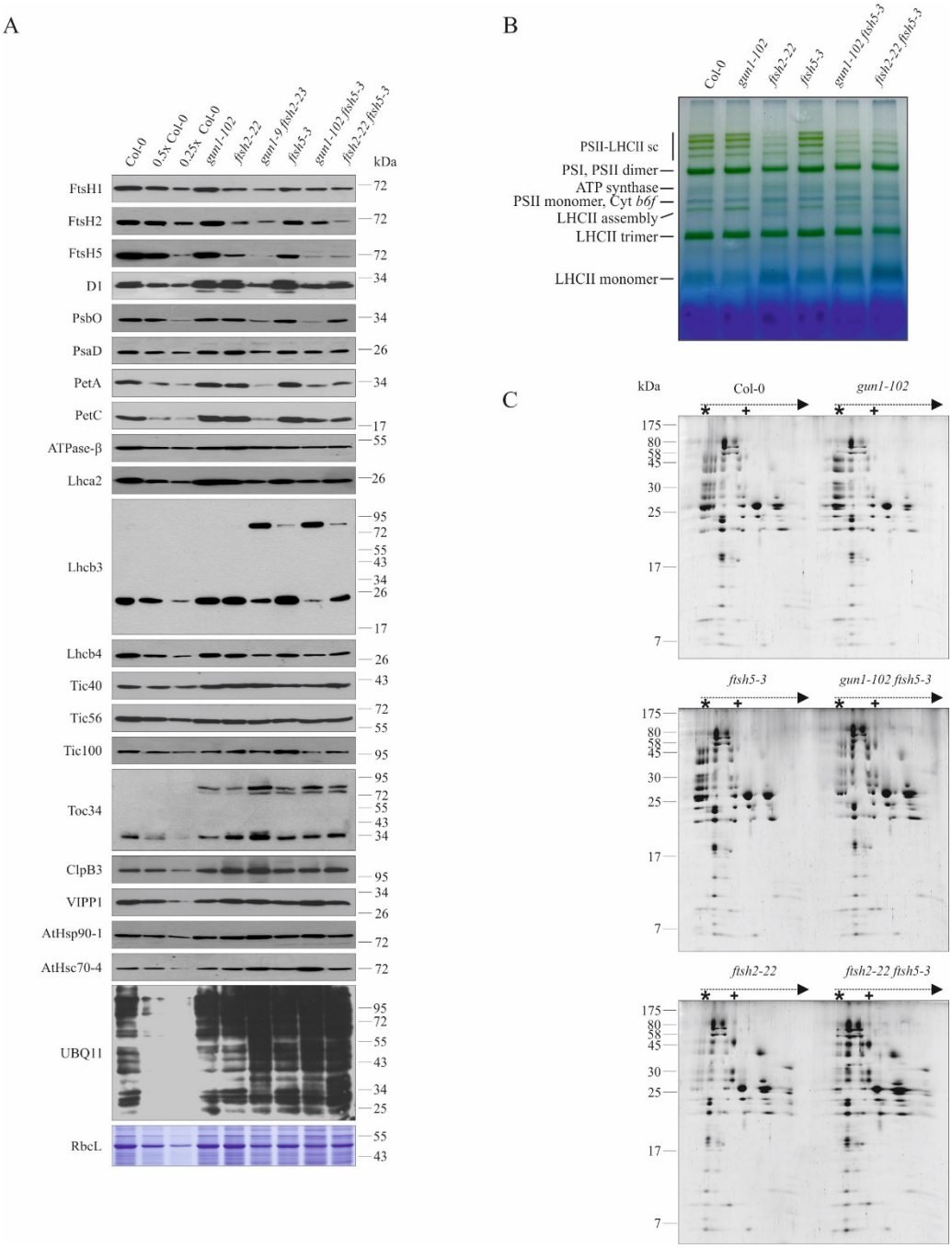
A
Col-0
0.5x Col-0
0.25x Col-0
gun1-102
ftsh2-22
gun1-9 ftsh2-23
ftsh5-3
gun1-102 ftsh5-3
ftsh2-22 ftsh5-3
kDa
FtsH1
FtsH2
FtsH5
D1
PsbO
PsaD
PetA
PetC
ATPase-β
Lhca2
Lhcb3
Lhcb4
Tic40
Tic56
Tic100
Toc34
ClpB3
VIPP1
AtHsp90-1
AtHsc70-4
UBQ11
RbcL
B
Col-0
gun1-102
ftsh2-22
ftsh5-3
gun1-102 ftsh5-3
ftsh2-22 ftsh5-3
PSII-LHCII sc
PSI, PSII dimer
ATP synthase
PSII monomer, Cyt b6f
LHCII assembly
LHCII trimer
LHCII monomer
C
kDa
Col-0
gun1-102
ftsh5-3
gun1-102 ftsh5-3
ftsh2-22
ftsh2-22 ftsh5-3

Figure 3.4. Immunoblot analyses and thylakoid protein complex organization in Col-0, *gun1-102* and mutant cotyledons with altered FtsH protease complex. (**A**). Immunoblot analyses on total protein extracts of thylakoid-located FtsH1, FtsH2, FtsH5 proteins, subunits of photosynthetic complexes (D1, PsbO, PsaD, PetA, PetC, ATPase-β, Lcha2, Lhcb3 and Lhcb4), subunits of the envelope translocation machinery (Tic40, Tic56, Tic110, Toc34), proteins involved in thylakoid membrane formation (ClpB3, VIPP1) and the two cytosolic chaperones, AtHsc70-4 and AtHsp90-1. The ubiquitination level was detected with ubiquitin 11 (UBQ11) specific antibody. Coomassie Brilliant Blue (C.B.B.) staining, displaying the rubisco large subunit (RbcL), is shown as loading control. Plant material, corresponding to 5 mg of seedlings fresh weight and collected at 6 DAS was used for the analyses. Decreasing amounts of Col-0 protein extracts were loaded into lanes indicated as 0.5x Col-0 and 0.25x Col-0. (**B**) Blue Native PAGE (BN-PAGE) analyses of thylakoid membrane protein complexes in Col-0, *gun1-102*, *fths2-1* and *ftsh5-3* single mutants, *gun1-102 ftsh5-3* and *ftsh2-22 ftsh5-3* double mutants, isolated from cotyledons of 6 DAS seedlings. Thylakoid samples were normalized to 5 µg of chlorophyll and solubilized with 1% β-DM (n-Dodecyl-β-D-maltoside), prior to fractionation by large-pore Blue Native PAGE (lpBN-PAGE). (**C**) The BN gel lanes from Col-0 and mutants shown in (**B**) were then fractionated on 2D SDS-PAGE under denaturing conditions and proteins were visualized with SYPRO orange protein gel stain. Arrows indicate the direction of the BN run. Asterisks indicate PSII-LHCII super-complexes, crosses the CP43-less PSII-core.

Protein	*gun1-102*	*ftsh2-22*	*gun1-9 ftsh2-23*	*ftsh5-3*	*gun1-102 ftsh5-3*	*ftsh2-22 ftsh5-3*
FtsH1	0.95 ± 0.18	0.36 ± 0.04	0.14 ± 0.02	0.48 ± 0.03	0.31 ± 0.05	0.28 ± 0.03
FtsH2	1.17 ± 0.12	0.08 ± 0.02	0.09 ± 0.03	0.46 ± 0.02	0.14 ± 0.02	0.03 ± 0.01
FtsH5	0.88 ± 0.09	0.30 ± 0.04	0.12 ± 0.01	0.41 ± 0.03	0.16 ± 0.02	0.21 ± 0.02
D1	1.22 ± 0.11	1.27 ± 0.09	0.36 ± 0.03	1.32 ± 0.11	0.53 ± 0.07	0.91 ± 0.08
PsbO	0.95 ± 0.11	0.92 ± 0.1	0.31 ± 0.07	0.84 ± 0.03	0.23 ± 0.09	0.74 ± 0.03
PsaD	1.16 ± 0.15	1.54 ± 0.11	0.35 ± 0.01	1.02 ± 0.08	0.43 ± 0.06	0.59 ± 0.02
PetA	1.09 ± 0.08	0.91 ± 0.07	0.18 ± 0.02	1.02 ± 0.11	0.43 ±0.02	0.66 ± 0.03
PetC	0.98 ± 0.10	1.16 ± 0.10	0.47 ± 0.02	0.98 ± 0.05	0.63 ± 0.04	0.65 ± 0.02
ATPase-β	0.87 ± 0.05	0.92 ± 0.08	0.59 ± 0.04	0.57 ± 0.03	0.41 ± 0.04	0.53 ± 0.04
Lhca2	1.02 ± 0.08	0.98 ± 0.06	0.39 ± 0.01	0.81 ± 0.01	0.41 ± 0.02	0.83 ± 0.03
Lhcb3	1.00 ± 0.10	0.98 ± 0.02	0.33 ± 0.02 (0.65 ± 0.03)[a]	1.01 ± 0.03 (0.05 ± 0.01)[a]	0.11 ± 0.01 (0.63 ± 0.01)[a]	0.44 ± 0.02 (0.15 ± 0.02)[a]
Lhcb4	1.05 ± 0.08	0.97 ± 0.07	0.39 ± 0.02	0.92 ± 0.05	0.41 ± 0.02	0.53 ± 0.02
Tic40	1.15 ± 0.14	1.35± 0.09	1.35 ± 0.11	0.91 ± 0.08	0.76 ± 0.07	1.29 ± 0.10
Tic56	0.96 ± 0.04	0.98 ± 0.05	0.92 ± 0.10	0.78 ± 0.05	0.83 ± 0.04	0.89 ± 0.05
Tic100	0.48 ± 0.03	0.83 ± 0.08	0.61 ± 0.06	1.82 ± 0.070	0.21 ± 0.050	0.49± 0.05
Toc34	0.58 ± 0.07 (0.55 ± 0.04)[a]	1.34 ± 0.13 (0.49 ± 0.02)[a]	2.41 ± 0.08 (2.15 ± 0.12)[a]	1.11 ± 0.06 (0.81 ± 0.04)[a]	1.15 ± 0.07 (1.45 ± 0.03)[a]	1.36 ± 0.09 (0.85 ± 0.09)[a]
ClpB3	1.00 ± 0.07	1.97 ± 0.11	2.3 ± 0.09	1.43 ± 0.11	1.54 ± 0.08	1.69 ± 0.11
VIPP1	0.71± 0.09	1.08 ± 0.08	1.13 ± 0.11	0.98 ± 0.09	1.35 ± 0.08	0.89 ± 0.06
AtHsp90-1	1.00 ± 0.07	1.16 ± 0.11	1.91 ± 0.11	1.12 ± 0.09	1.87 ± 0.08	0.98 ± 0.07
AtHsc70-4	0.89 ± 0.10	1.08 ± 0.08	1.77 ± 0.09	1.18 ± 0.12	2.2 ± 0.06	1.12 ± 0.13
UBQ11	0.98 ± 0.04	1.09 ± 0.12	2.22± 0.09	1.28 ± 0.08	1.56 ± 0.07	2.45 ± 0.09

Table 3.1. **Quantification of proteins in light-adapted cotyledons of Col-0 and mutant seedlings.**

Col-0 levels are set to 1 (100%). Values are means ± SD from three independent protein gel blots (see Figure 3.4).

[a]Abundance of proteins migrating at higher molecular weights as observed in the case of Lhcb3 and Toc34 subunits

3.5 GUN1 and the two most abundant thylakoid-located FtsHs do not show a direct physically interaction

First of all, it was of interest to understand where the FtsH proteins (FtsH1, FtsH2, FtsH8 proteins fused to GFP and FtsH5 protein fused to the RFP) and GUN1 protein fused to GFP localize within the chloroplast. As observable in the figure 3.5, A, the GUN1-GFP signal accumulates in distinct fluorescent foci within the chloroplasts, visualized by the red chlorophyll autofluorescence (Merged), resembling the pattern of chloroplast nucleoids, whereas the FtsH-GFP showed a more uniform distribution inside the chloroplasts.

Subsequently, in order to clarify if GUN1 directly interacts with the FTSH protease complex, a BiFC assay was performed: GUN1 was fused to the N-terminal (YN) end of the YFP protein, whereas the FtsH2 and FtsH5 proteins were fused to the C-terminal (YC) end and co-transformed into Arabidopsis protoplasts. Reconstitution of YFP fluorescence (YFP, signaling positive interactions), chlorophyll auto fluorescence (CHL), overlay of YFP and CHL signals (YFP/CHL) and bright fields are shown. Clearly, (Fig. 3.5, B) no YFP signal could be observed in the presence of either FtsH2^{YC}-GUN1^{YN} or FtsH5^{YC}-GUN1^{YN}. On the contrary the FtsH2^{YC}-FtsH5^{YN} combination, used as control, was able to reconstitute the YFP protein as shown by the strong YFP signal detected inside the chloroplasts. Reciprocal experiments exchanging YN and YC provided identical results.

However, the absence of physical interactions between GUN1 and the FtsH2 and FtsH5 subunits does not allow to exclude the possibility that other proteins or specific conditions are needed for establishing the GUN1-FtsH subunit interactions.

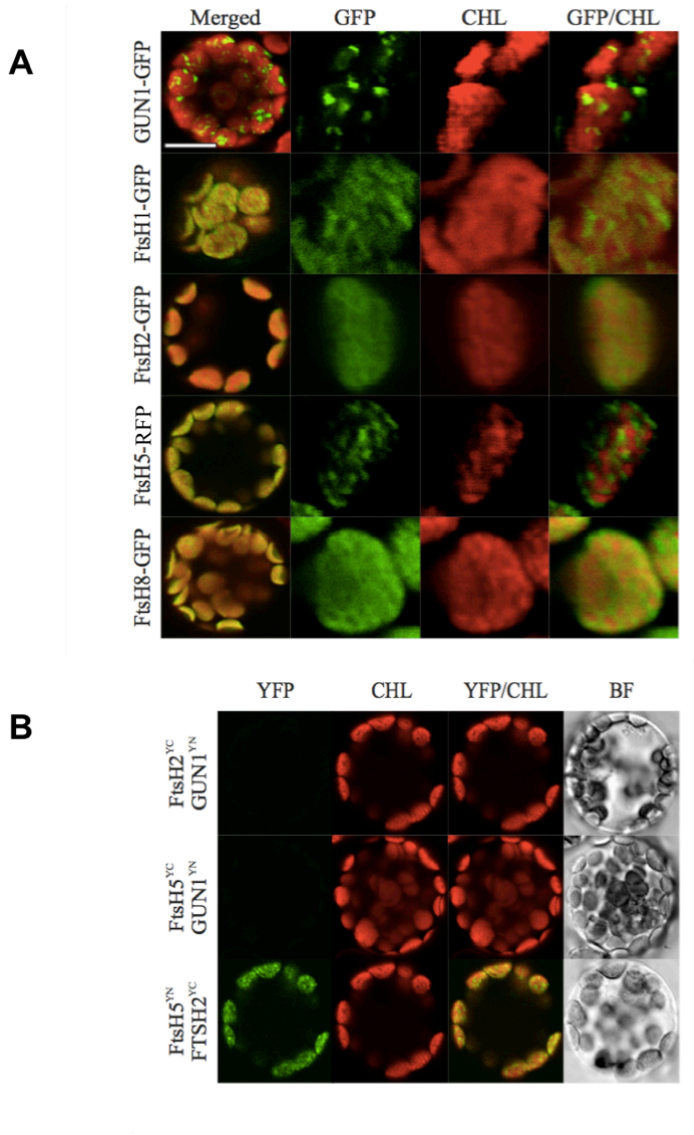

Figure 3.5. Sub-localization of GUN1 and FtsH proteins and characterization of protein interactions by BiFC assay. (**A**) Series of confocal laser scanning images (CLSM) of the subcellular localization of the GUN1, FtsH1, FtsH2, FtsH8 proteins fused to GFP and FtsH5 fused to RFP (the signal was converted in a "GFP signal" in order to obtain an homogeneous

final image), obtained from transiently transformed Arabidopsis (ecotype Col-0) leaf mesophyll protoplasts. GFP, details of the protein chimer distributions at the level of thylakoid membranes (CHL). GFP/CHL, overlay of both signals. (**B**) BiFC in Arabidopsis protoplasts detected by fluorescence confocal microscopy. Scale bar = 5 μm

3.6 GUN1 does not affect the FtsH genes expression at transcriptional level

The hypothesis according to which GUN1 could affect the *FtsH1,2,5,8* mRNAs accumulation and, as a consequence, protein abundance was also tested. Quantitative Real-Time PCR (qRT-PCR) analyses performed on Col-0, *gun1-102*, *ftsh5-3* and *gun1-102 ftsh5-3* seedlings, however, showed that the accumulation of *FtsH1*, *FtsH2* and *FtsH8* transcripts did not change between Col-0 and mutant cotyledons, implying that the increased reduction of FtsH protein levels observed in *gun1-102 ftsh5-3* cotyledons cannot be ascribed to changes in transcript accumulation (Figure 3.6).

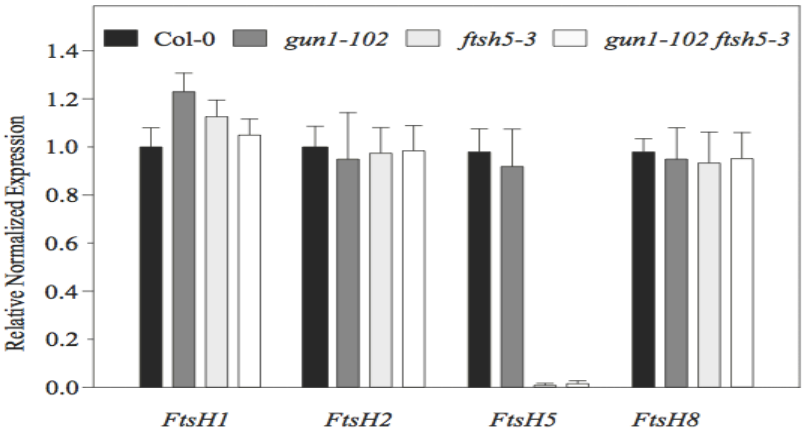

Figure 3.6. Expression of *FtsH* genes in Col-0, *gun1-102*, *ftsh5-3* and *gun1-102 ftsh5-3* cotyledons. qRT-PCR analyses have been performed to monitor the expression of nuclear *FtsH* genes encoding the thylakoid FtsH protease complex. cDNA was prepared from 6 DAS Col-0

and mutant seedling grown on MS medium at long-day conditions. Primer pair sequences used for the analysis are described in Table 2.2 (Materials and methods). Values are the average of three biological and 9 technical replicates. Lines indicate the standard deviation (SD). The *ACT8* expression level was used as internal standard.

3.7 Thylakoid FtsH precursor proteins accumulate in mesophyll cells of *gun1* cotyledons

The possible existence of a GUN1-mediated post-transcriptional mechanism, responsible to control FtsH protein accumulation, was verified by immunoblot analyses on Col-0 and *gun1-102* seedlings grown on MS medium in the presence or absence of lincomycin (+/-Lin), i.e. the same conditions that allow to detect the molecular phenotype of *gun1* mutants (Fig 3.7, A). As expected, Col-0 and *gun1-102* cotyledons, characterized by the lincomycin inhibition of plastid protein synthesis, showed no accumulation of the large (see C.B.B. stained gel: the most abundant band migrating between 55 and 43 kDa is absent in lincomycin treated samples) and small (RbcS) subunits of RUBISCO, as well as of the antenna proteins of PSI (Lhca1-to-Lhca4) and PSII (Lhcb1-to-Lhcb5), and only a modified form of Lhcb3, migrating at around 90 kDa in the SDS-PAGE, was observable in Col-0 and, significantly more abundant, in *gun1-102* cotyledons. Furthermore, a marked reduction of FtsH proteins could also be observed in cotyledons of Lin-grown seedlings, together with the appearance of FtsH-specific Higher molecular Weight bands (hwFtsH), migrating between 70 and 80 kDa and compatible with the predicted molecular weights of FtsH precursor proteins. Interestingly, the hwFtsH forms were largely abundant in Lin-grown *gun1-102* cotyledons, but they were also detectable in *gun1-102* seedlings grown on standard MS medium, when the FtsH1, FtsH2 and FtsH5

antibodies were employed for immunodecoration. The hwFtsH proteins could be fully recovered in the extra-plastidial (Sup) soluble fraction of cotyledon proteins extracted from Lin-grown seedlings, suggesting that they could represent the FtsH1, FtsH2 and FtsH5 proteins together with their chloroplast (cTP) and thylakoid (tTP) transit peptides (Fig 3.7, B). On the contrary, the larger form of Lhcb3 could be detected in both the extra-plastidial and the plastid enriched fraction (Pellet) of *gun1-102* cotyledon protein extracts. To overcome the problems due to the cross-reactivity of FtsH antibodies, the coding sequences of *FtsH1*, *FtsH2, FtsH5* and *FtsH8* genes were placed under the control of the 35S-CaMV promoter and fused in frame to either *GFP* (*oeFtsH1-GFP*, *oeFtsH2-GFP* and *oeFtsH8-GFP*) or *RFP* (*oeFtsH5-RFP*). These constructs were introduced, via Agrobacterium-mediated transformation, in Col-0 and in the corresponding *gun1-102 ftsh* double mutants and the accumulation pattern of chimeric proteins was monitored in control (not-transformed Col-0 seedlings) and transformed seedlings grown on MS medium with and without lincomycin (Fig 3.7, C). In agreement with the observations made on the endogenous FtsH proteins (see Fig 3.7, A), higher molecular weight proteins could be detected in *gun1-102 ftsh1-1* cotyledons, carrying the FtsH1-GFP chimer (*gun1-102 ftsh1-1* + *oeFtsH1-GFP*), as well as in *gun1-9 ftsh2-23* + *oeFtsH2-GFP* and *gun1-102 ftsh5-3* + *oeFtsH5-RFP* seedlings, grown on MS medium in the presence of lincomycin, using GFP and RFP specific antibodies, respectively. In addition, high molecular weight FtsH2-GFP and FtsH5-RFP specific signals were also detected in *gun1-9 ftsh2-23* + *oeFtsH2-GFP* and *gun1-102 ftsh5-3* + *oeFtsH5-RFP* genetic backgrounds grown in the absence of plastid translation inhibitor, suggesting a possible indirect role of GUN1 in plastid protein import.

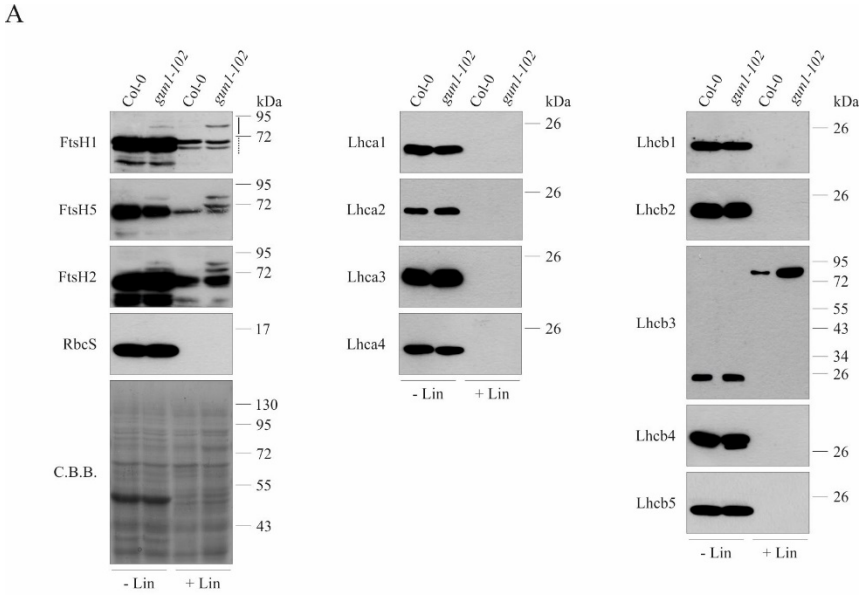
A
Col-0
gun1-102
kDa
FtsH1
FtsH5
FtsH2
RbcS
C.B.B.
95
72
17
130
55
43
- Lin
+ Lin
Lhca1
Lhca2
Lhca3
Lhca4
26
Lhcb1
Lhcb2
Lhcb3
Lhcb4
Lhcb5
34

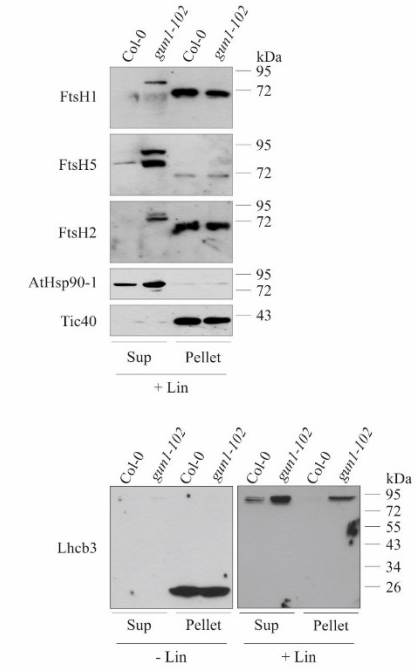
B
Col-0
gun1-102
kDa
FtsH1
FtsH5
FtsH2
AtHsp90-1
Tic40
95
72
43
Sup
Pellet
+ Lin
Lhcb3
55
34
26
- Lin

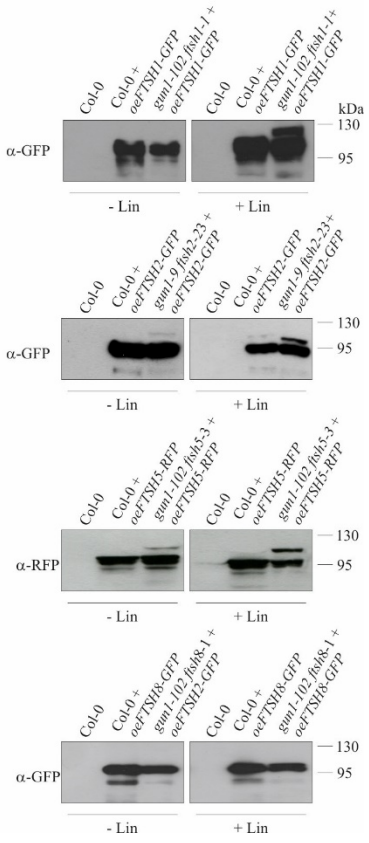
C
Col-0
Col-0 + oeFTSH1-GFP
gun1-102 fsh1-1 + oeFTSH1-GFP
kDa
α-GFP
130
95
- Lin
+ Lin
Col-0 + oeFTSH2-GFP
gun1-9 fsh2-23 + oeFTSH2-GFP
Col-0 + oeFTSH5-RFP
gun1-102 fsh5-3 + oeFTSH5-RFP
α-RFP
Col-0 + oeFTSH8-GFP
gun1-102 fsh8-1 + oeFTSH8-GFP

Figure 3.7. **FtsH precursor protein accumulation in Col-0 and *gun1-102* seedlings grown on MS medium with and without lincomycin.** (**A**) Immunoblot analyses on total proteins extracted from Col-0 (+/- Lin) and *gun1-102* (+/- Lin) cotyledons. Filters were immunodecorated with antibodies specific for the FtsH1, FtsH2, FtsH5 proteins, the small subunit of RUBISCO (RbcS), the light harvesting complex of PSI (Lhca1, Lcha2, Lhca3, Lhca4) and PSII (Lhcb1, Lhcb2, Lhcb3, Lhcb4 and Lhcb5). Coomassie Brilliant Blue (C.B.B.) staining, displaying the Rubisco large subunit (RbcL), is shown as loading control. The continuous line on the right side of the FtsH1 immunoblot indicate the hwFtsH region, with the dotted line the mFtsH portion (the bands corresponding to the mature protein). (**B**) The plastid enriched fraction (Pellet) and the protein extra-chloroplast soluble fraction (Sup) were isolated from Col-0 and *gun1-102* cotyledons obtained from seedlings grown on MS medium + Lin. After SDS-PAGE protein fractionation and blotting, filters were immunolabeled with FtsH1, FtsH2 and FtsH5 specific antibodies. The AtHSP90-1 antibody was used as a marker for the extra-chloroplast soluble fraction, while Tic40 for the plastid enriched fraction. In the case of Lhcb3 immunoblot, the Pellet and Sup fractions were also isolated from cotyledons grown on MS medium without Lin. (**C**) Immunoblots of cotyledon total protein extracts from not-transformed Col-0 seedlings, Col-0 and *gun1 ftsh* seedlings transformed with *oeFtsH-GFP* (*oeFtsH5-RFP*) constructs, under the control of 35S-CaMV promoter, grown on MS medium with and without Lin. Commercially available GFP and RFP specific antibodies were used to detect the accumulation of the FtsH chimeras. Plant material, corresponding to 5 mg of cotyledon fresh weight and collected at 6 DAS was used for the analyses.

3.8 The absence of GUN1 leads to FTSH5 precursor protein accumulation in the cytosol

The possible accumulation of FtsH precursor proteins was verified through nLC-ESI-MS/MS analysis of trypsin digested gel slices isolated from the 75-to-90 kDa region of both Col-0 (+/- Lin) and *gun1-102* (+/-Lin) lanes, indicated as hwFtsH bands (see continuous line in Fig 3.7, A), and from the 60-to-70 kDa region, indicated as mature protein bands (mFtsH, see dotted line in Fig 3.7). The lists of proteins identified in the four hwFtsH and the four mFtsH bands are

provided in Appendices S2 and S3, respectively. The four subunits of the thylakoid FtsH protease complex were identified with a high confidence in the mFtsH bands of the four samples (Appendix S3), and the peptide spectrum matches (PSMs) were largely more abundant in both Col-0 and *gun1-102* lanes (FtsH1: Col-0, 130 PSM; *gun1-102*, 122; FtsH2: Col-0, 165; *gun1-102*, 140; FtsH5: Col-0 168; *gun1-102*, 159; FtsH8: Col-0, 93; *gun1-102*, 88) than in Col-0 + Lin and *gun1-102* + Lin lanes (FtsH1: Col-0, 30 PSM; *gun1-102*, 23; FtsH2: Col-0, 30; *gun1-102*, 26; FtsH5: Col-0 37; *gun1-102*, 28; FtsH8: Col-0, 21; *gun1-102*, 21), confirming the marked reduction of the thylakoid FtsH protein complex in seedlings grown in the presence of lincomycin, as shown by immunoblot analysis (see Fig 3.7). However, only the FtsH1 subunit was found with a high confidence in the hwFtsH band of *gun1-102* + Lin (Appendix S2). To increase the accuracy of our analyses, all eight samples (four hwFtsH and four mFtsH bands) were re-analyzed by monitoring, exclusively, the presence of FtsH2 and FtsH5 peptides, predicted by *in silico* digestion of FtsH2 and FtsH5 subunits (see Appendices S4 and S5), in both mature and precursor bands (Appendices S6 and S7). Peptides of FtsH5 mature protein could be identified in all 4 mature and 4 precursor bands (Appendix S7). In addition, the precursor band of *gun1-102* + Lin sample contained two peptides of the FtsH5-cTP: [K].SLPFSVISR.[K] and [R].YQISQSEK.[L]. Similarly, the FtsH5-cTP peptide [K].SLPFSVISR.[K] was also detected in the precursor band of *gun1-102* sample, supporting further a role of GUN1 in chloroplast protein import. On the contrary, the FtsH2 peptides were manly found in the mFtsH bands of the four samples (Appendix S6). No FtsH2-cTP peptide could be detected in any of the 8 bands analyzed, although the [K].ILLGNAGVGLVASGK.[A] peptide, part of the thylakoid transit peptide, was detected in the mature band of *gun1-102* + Lin. To quantify the abundance of FtsH2 and FtsH5 subunits, together with the FtsH5-cTP, in both precursor and mature bands of Col-0 (+/-

Lin) and *gun1-102* (+/- Lin) samples, we selected a subset of FtsH1, FtsH2 and FtsH5 unique and relatively abundant peptides (Appendix S8) for targeted quantification by means of the Selected Reaction Monitoring (SRM) method. Peptides of the mitochondrial Ftsh3 protease, co-migrating with the hwFtsH bands, due to the molecular weight of its mature form, were also included as internal standard. In agreement with immunoblot data and PSM values (see Fig. 3.8 and Appendix S3), the FtsH1, FtsH2 and FtsH5 subunits resulted to be highly abundant in the mFtsH bands of the Col-0 and *gun1-102* samples, grown in the absence of lincomycin (Fig 3.8), whereas the amount of the mitochondrial located FtsH3 protease was not influenced by both the genetic background and the presence of lincomycin in the growth medium. Furthermore, the cTP-containing FtsH5 precursor protein was clearly detectable in the hwFtsH band of *gun1-102* and its abundance was increased by more than three folds in *gun1-102* + Lin sample (Fig 3.8). A 3-folds increase of FtsH5 precursor protein induced by lincomycin was also detachable in Col-0 + Lin in comparison to Col-0 sample, however the total abundance of FtsH5 precursor protein in Col-0 + Lin was even lower than the one present in *gun1-102* seedlings grown on standard MS medium, implying that the lack of GUN1 protein and the lincomycin treatment are the two major factors that influence the accumulation of FtsH5 precursor protein (Fig 3.8).

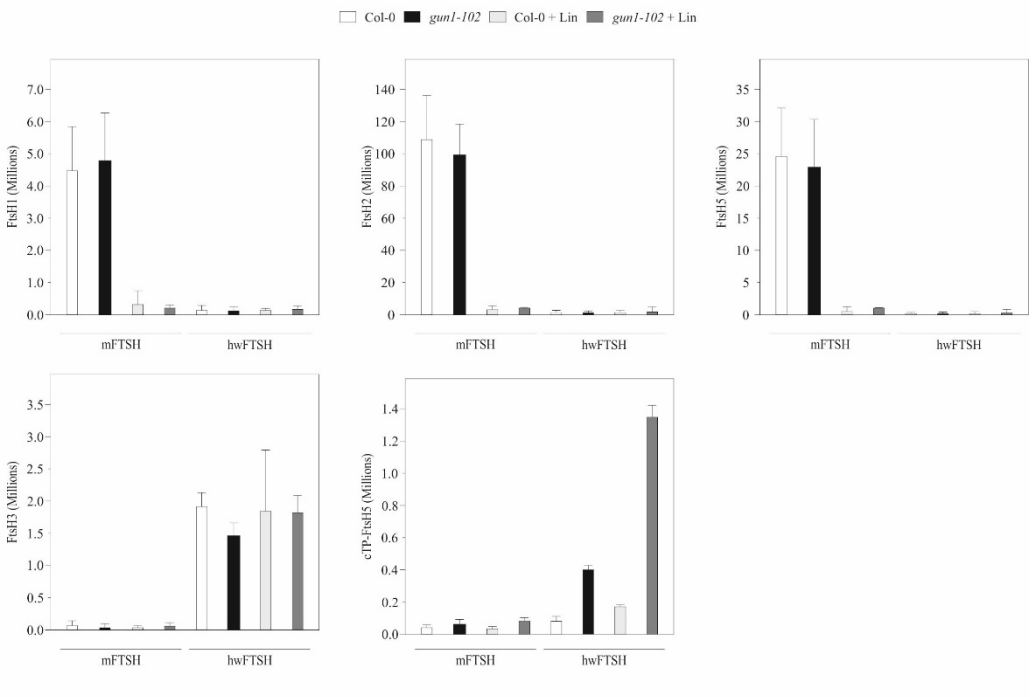

Figure 3.8. **Targeted quantification of FtsH mature and precursor proteins in Col-0 (+/- Lin) and *gun1-102* (+/- Lin) cotyledons by means of the Selected Reaction Monitoring (SRM) method.** FtsH1, FtsH2, FtsH5 and the precursor protein cTP-FtsH5 have been quantified using a subset of unique and relatively abundant peptides (see also Appendix S8) through the SRM strategy. Quantification of the mitochondrial FtsH3 protein has also been performed, as internal standard. Note, that the high abundance of the FtsH3 protein in the hwFtsH bands is due to the fact that the FtsH3 mature protein migrate in that specific region of the SDS-PAGE. Values are means ± SD from three biological replicates.

3.9 A broad range of plastid precursor proteins accumulate in *gun1* cotyledons

To verify the possibility that other chloroplast-targeted proteins accumulated in the cytosol of *gun1-102* cotyledon mesophyll cells, the soluble fraction of total proteins extracted from cotyledons of Col-0 (+/- Lin) and *gun1-102* (+/- Lin) seedlings was analyzed by nLC-ESI-MS/MS. The identified peptides were then mapped on the aminoacid sequences of 1241 proteins available in Uniprot (https://www.uniprot.org/proteomes/UP000006548) and known to have a cTP and on other 721 nuclear-encoded proteins predicted to be imported into chloroplast by ChloroP 1.1 (www.cbs.dtu.dk/services/ChloroP/). In Table 3.2 a list of chloroplast-imported proteins for which at least 1 peptide was found in each of the 3 biological replicates of at least one of the four samples is reported (for raw data see Appendix S9). The numbers refer to PSMs found in each sample, which can be used for a semi-quantification of precursor protein accumulation. In total, the presence of cTP was detected in 37 cotyledon proteins, of which 14 accumulated preferentially in *gun1-102* + Lin samples (see underlined ATG code in Table 3.2). Among them, subunits of the thylakoid electron transport chain and enzymes of the Calvin-Benson cycle. Sixteen precursor proteins were detected in all four genotypes, although in the case of the Acetyl-CoA enzyme, the Ankyrin repeat-containing protein 2 and the NAD(P)-binding Rossmann-fold superfamily protein accumulated much less in Col-0 than the other 3 samples. Only in three cases, peptides of cTPs could be identified exclusively in Col-0 and *gun1-102* seedlings grown on MS medium without lincomycin. In general, 93 PSMs were found in Col-0 cotyledons, 109 in *gun1-102*, 120 in Col-0 + Lin and 190 in *gun1-102* + Lin, implying that the lack of GUN1 protein in combination with the presence of lincomycin on the

growth medium favor the accumulation of chloroplast precursor proteins in the cytosol.

This finding was also corroborated by the increased accumulation of the cytosolic Heat Shock Protein 90 (AtHsp90) and the Heat Shock cognate protein 70 (AtHsc70) in *gun1-102* + Lin cotyledons, detected by trypsin digestion of gel slices (see asterisks in Fig. 3.9, A) from Col-0 + Lin and *gun1-102* + Lin samples, followed by Liquid chromatography – Mass Spectrometry (LC-ESI MS/MS) analyses (Fig. 3.9, B and Table 3.2). Moreover, immunoblot analysis performed by using AtHsp90-1 and AtHsc70-4 specific antibodies confirmed further the larger accumulation of heat-shock proteins in the cytosol of *gun1-102* cotyledon cells grown in the presence of lincomycin (Fig. 3.9, C). Indeed, members of Hsp90 protein family are reported to assist the transport of precursor proteins to organelles or, as in the case of Hsc70-4, to be involved in the degradation of chloroplast pre-proteins that accumulate in the cytosol.

Protein	Col-0			Col-0 + Lin			*gun1-102*			*gun1-102* + Lin			cTP (ChloroP)	Identified cTP Peptides
AT1G01090.1	nd	nd	nd	2	1	1	nd	nd	nd	1	1	nd	1-61	56-67
AT1G06680.1	nd	nd	nd	1	1	3	nd	2	2	3	3	4	1-77	42-55, 72-90
AT1G25220.2	nd	nd	1	1	nd	1	1	nd	1	1	1	1	1-50	2-8
AT1G32200.1	2	1	3	1	nd	1	2	nd	1	1	nd	1	1-90	65-95, 72-96
AT1G42970.1	1	1	1	1	2	1	1	1	1	1	1	1	1-80	67-75
AT1G50900.1	nd	1	1	nd	nd	nd	1	1	2	nd	nd	nd	1-68	65-80
AT2G02740.1	nd	2	1	1	1	1	1	nd	1	1	1	nd	1-75	60-66, 69-84
AT2G04400.1	1	nd	1	1	1	1	1	nd	nd	1	1	1	1-65	60-77
AT2G21330.1	nd	nd	nd	nd	1	1	nd	nd	nd	1	2	2	1-48	37-47
AT2G22230.1	nd	nd	nd	1	1	1	nd	nd	nd	nd	nd	1	1-49 (ChloroP)	43-49
AT2G28000.1	nd	nd	nd	nd	nd	nd	nd	nd	1	1	1	1	1-46	21-31
AT2G34460.1	nd	nd	nd	nd	nd	nd	nd	nd	nd	1	1	2	1-51	38-45, 49-60
AT2G39730.1	nd	nd	nd	nd	nd	nd	nd	nd	nd	1	1	2	1-58	14-36, 37-43
AT3G01500.2	nd	nd	nd	nd	nd	nd	nd	nd	4	3	6	7	1-113	52-58, 59-92, 93-101
AT3G04000.1	1	1	nd	2	1	1	nd	nd	2	2	2	1	1-53	18-26, 31-42, 43-56
AT3G12780.1	nd	nd	nd	nd	nd	nd	nd	nd	nd	1	1	1	1-75	15-26
AT3G13470.1	nd	nd	nd	nd	nd	nd	nd	nd	nd	1	1	1	1-50	2-21
AT3G52960.1	nd	nd	nd	1	2	2	nd	nd	nd	1	1	3	1-70	63-78
AT3G53900.1	4	2	5	2	2	3	5	6	3	1	2	2	1-61	2-13, 26-32, 33-42, 43-50, 51-58
AT3G54050.1	nd	nd	nd	nd	nd	nd	nd	nd	nd	1	2	2	1-59	20-33, 58-69
AT3G63540.1	3	5	3	nd	nd	nd	2	4	4	nd	nd	nd	1-52	19-31, 34-46
AT4G18440.1	1	1	1	3	3	2	1	1	2	nd	1	1	1-64 (ChloroP)	63-72
AT4G24280.1	3	4	4	4	4	6	4	3	4	4	7	6	1-92	37-43, 80-110[a]
AT4G29060.1	1	2	2	1	1	2	1	1	4	1	2	2	1-80 (ChloroP)	74-103
AT4G33030.1	nd	nd	nd	1	1	1	nd	nd	nd	nd	nd	1	1-86	62-85
AT4G35450.5	1	1	2	1	nd	2	2	1	5	2	3	3	1-62 (ChloroP)	8-17, 24-62
AT5G01530.1	nd	nd	nd	nd	nd	nd	nd	nd	nd	1	2	2	1-40	19-29, 30-38

AT5G16290.1	1	1	1	nd	nd	1	nd	1	1	nd	nd	1	1-62	59-73
AT5G16390.1	3	3	3	3	2	2	3	2	3	2	2	2	1-82	67-77, 68-87
AT5G22790.1	1	nd	nd	nd	nd	nd	1	1	1	nd	nd	nd	1-63	
AT5G35360.1	nd	nd	nd	1	1	1	nd	nd	1	nd	1	1	1-71	62-76
AT5G36880.2	1	nd	1	3	3	4	1	nd	1	2	5	4	1-84	24-31, 58-71, 72-96
AT5G40870.1	1	1	1	2	nd	1	1	nd	1	2	1	1	1-47	15-24[b], 44-60
AT5G49910.1	3	4	4	4	4	6	4	3	4	4	7	5	1-92	80-110
AT5G54770.1	nd	nd	nd	1	2	3	nd	1	nd	4	6	4	1-55	18-40, 46-68
AT5G63890.2	nd	nd	nd	nd	nd	nd	nd	nd	nd	1	1	1	1-30	25-33
AT5G66570.1	nd	nd	nd	nd	nd	nd	nd	nd	nd	4	2	5	1-58	17-23, 37-46, 47-61
Tot. Peptides		93			120			109			190			

Table 3.2. List of nuclear-encoded proteins targeted to chloroplast from total cotyledon soluble extracts for which at least one tryptic peptide belonging to the chloroplast transit peptide (cTP) has been found in each of the three biological replicates of at least one of the four samples. The results are presented as the number of peptides spectra matches (PSMs) corresponding to any cTP peptide found in each of the three biological replicate. The list of peptides identified in the total soluble extract have been manually screened for sequences falling in the cTP of one of the 1241 *Arabidopsis thaliana* entries with a known cTP available in Uniprot, or in one of the remaining 721 accessions annotated as targeted to the chloroplast. In the latter case, the sequence of the theoretical transit peptide have been predicted using ChloroP 1.1 (www.cbs.dtu.dk/services/ChloroP/). cTP (ChoroP): sequence of the cTP as reported in Uniprot or, when marked (ChoroP), as predicted by ChloroP 1.1. Identified cTP peptides: starting- and ending-amino acid position of the sequences covered by the identified tryptic peptides in the cTP aa portion. [a]Shared with AT5g49910.1; [b]Shared with AT3G27190.

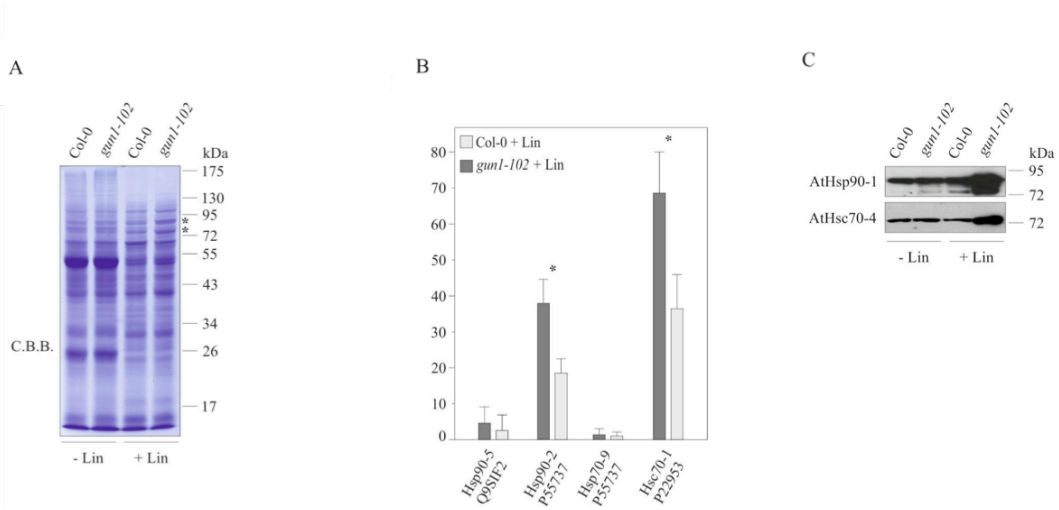

Figure 3.9. **Cytosolic chaperones AtHsp90-1 and AtHsc70-4 are accumulated in the *gun1-102* mutant seedlings grown in presence of lincomycin.** (**A**) C.B.B. stained SDS-PAGE of total protein extracts from Col-0 (+/- Lin) and *gun1-102* (+/- Lin) cotyledons, used to isolate the protein bands at ~ 80 kDa and ~ 90 kDa (see asterisks), highly abundant in *gun1-102* + Lin seedlings. (**B**) Gel slices (asterisks) enzymatically digested with tripsin were analysed by Liquid chromatography – Mass Spectrometry (LC-ESI MS/MS). The chart shows the differential accumulation (number of peptides/number of total peptides per gel slice) of four detected HSP protein families in Col-0 + Lin and *gun1-102* + Lin samples. The family name was assigned taking into account the top rank hits. Mean values ± SD are provided. Asterisks indicate the statistical significance evaluated by T-Student test ($p<0.05$). (**C**) Immunoblots of cotyledon total protein extracts from Col-0 (+/- Lin) and *gun1-102* (+/- Lin) seedlings, using antibodies specific for the two cytosolic chaperones, AtHsc70-4 and AtHsp90-1. Images of filters representative of three biological replicates are shown.

3.10 The translocation machinery of the plastid envelope is altered in *gun1-102* cotyledons

The detection of plastid precursor proteins in the cytosol of *gun1-102* and even more in *gun1-102* + Lin cotyledon cells, together with the reduction of Toc34 and Tic100 subunits observed in *gun1-102* cotyledons under optimal growth conditions (see Fig 3.10, A), prompted us to investigate into details the protein subunit composition of the two distinct chloroplast translocation complexes, TOC and TIC, together with the stromal chaperon system, in *gun1-102* and Col-0 seedlings grown on MS medium with and without lincomycin (Fig. 3.10, A). The Toc34 and Toc159 GTP-dependent receptor subunits, responsible to interact with distinct regions of the N-terminal cTP of cytosolic pre-proteins, were decrease by about 40 and 50% in *gun1-102* cotyledons in comparison to Col-0, respectively. Furthermore, a Toc34 specific band could also be detected at higher molecular weight in *gun1-102*, as already observed in Figure 3.4, A. Interestingly, the protein conducting channel Toc75 was also reduced by 50% in *gun1-102*, indicating that the entire heterotrimeric TOC complex is destabilized by the lack of GUN1 protein in Arabidopsis cotyledons. On the contrary, the inner membrane channel Tic110 and the associated protein Tic40 showed a slight increase in *gun1-102* sample, while the channel protein of the 1 MDa-complex, Tic20-I, together with Tic100 were both reduced to 50% of the control level. Besides the TIC and TOC complexes, the plastid translocation machinery requires the activity of various stromal chaperons, mainly the chloroplast cpHsc70, Hsp90 (ClpB3), Hsp93 (also known as ClpC2) and ptCpn60, as being involved in the folding of newly-imported proteins and/or consuming the energy, required for protein translocation, via ATP hydrolysis

(for details, see the paragraph 1.6 of the introduction). Notably, the levels of ClpB3, cpHsc70-1 and ptCpn60 were almost unchanged between *gun1-102* and Col-0 cotyledons, only ClpC2, showed a two-fold increase in *gun1-102* chloroplasts. However, differences at the level of TIC-TOC translocation machinery were more pronounced when Col-0 and *gun1-102* seedlings were grown on MS medium with lincomycin. In particular, the heterotrimeric TOC complex was markedly destabilized in *gun1-102* + Lin cotyledons, since Toc75 was reduced by more than three folds in comparison to Col-0 and only about 10% of Toc34 subunit was retained in its mature-unmodified form, with the majority of it detected in four distinct bands, migrating between 50 and 90 kDa. In addition, subunits of the 1 MDa-complex such as Tic20-I and Tic100 were under the limit of detection in *gun1-102* + Lin cotyledons and only a very faint band could be observed for Tic100 in Col-0 + Lin samples. Similarly, the level of Tic56 was reduced to 12% of Col-0 amount in Col-0 + Lin and to 4% in *gun1-102* + Lin cotyledons. It can be argued that the lincomycin inhibition of the chloroplast Tic214 (YCF1) synthesis prevents the stable accumulation of the entire 1 MDa TIC complex, although such an effect is more pronounced in *gun1-102* than in Col-0 cotyledons. Indeed, total protein ubiquitination was markedly increased in Col-0 + Lin and even more in *gun1-102* + Lin cotyledons with respect to the Col-0 and *gun1-102* samples, where no major differences could be observed (Fig. 3.10, B), supporting further the higher sensitivity of *gun1-102* seedlings to lincomycin. Furthermore, immunoprecipitation of Toc34 subunit in Col-0 + Lin and *gun1-102* + Lin samples, followed by immunoblot analysis with the UBQ11 specific antibody, allowed to clarify that the high molecular bands observed between 50 and 90 kDa are the result of Toc34 ubiquitination (Fig. 3.10, C). Overall, it appears clear the GUN1 protein plays a role in the organization of the plastid translocon machinery, particularly evident

under lincomycin growth conditions, possibly explaining the accumulation of plastid precursor proteins in the cytosol of GUN1 devoid cells.

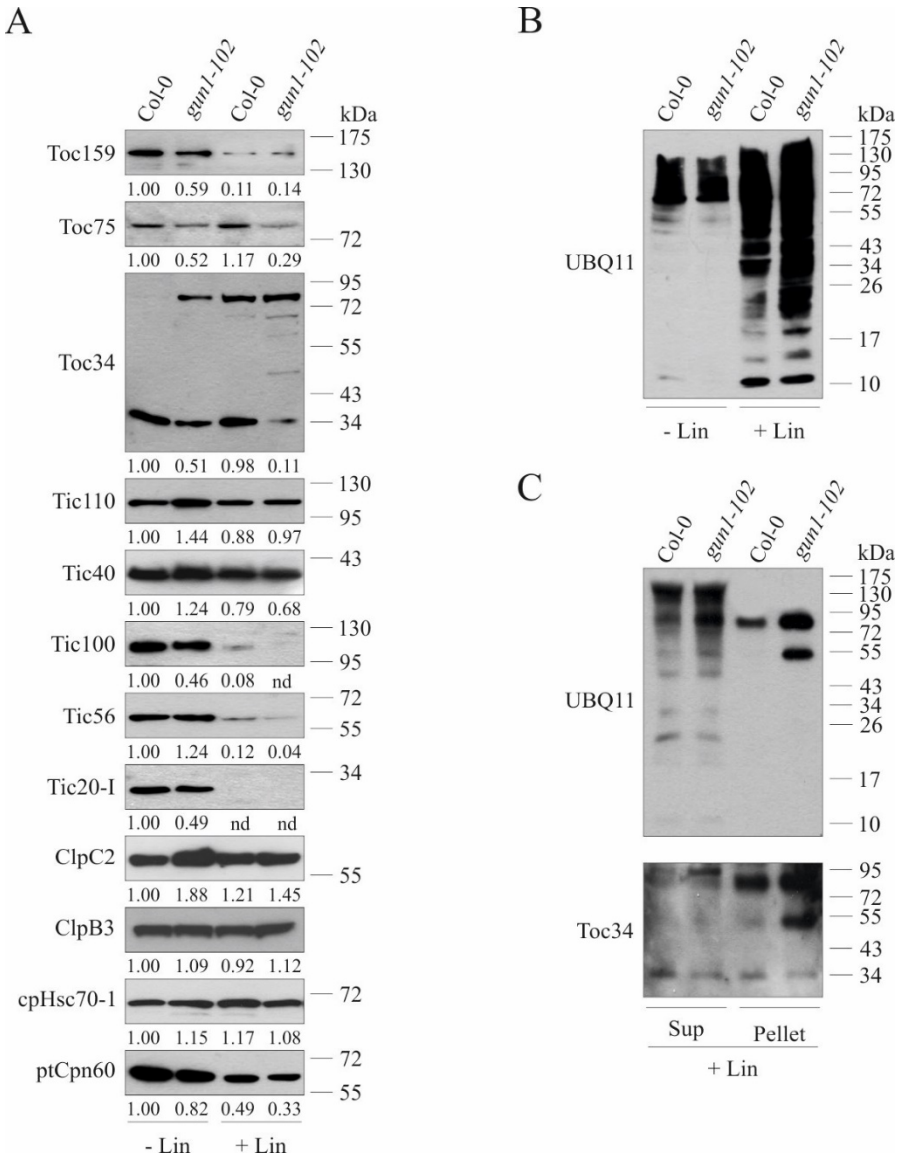

Figure 3.10. Chloroplast translocation machinery composition and ubiquitination in Col-0 (+/- Lin) and *gun1-102* (+/- Lin) cotyledons. (**A**) Immunoblot analyses of Tic and Toc translocation machinery together with the stromal chaperone system. Nitrocellulose filters

carrying fractionated cotyledon total proteins were probed with antibodies directed against subunits of the TOC (Toc159, Toc75, and Toc34), TIC (Tic110, Tic40) and 1 MDa TIC (Tic100, Tic56, Tic20-I) complexes. Furthermore, antibodies specific for the stromal chaperon system responsible of protein import and protein folding were also used (ClpC2, ClpB3, cpHsc70-1, ptCpn60). Quantification of signals (by ImageJ) relative to Col-0 (=1.00) is provided below each panel. Filter images are representative of three biological replicates. Standard deviation was below 10%. (**B**) Ubiquitination level of cotyledon total protein extracts from Col-0 and *gun1-102* seedlings, grown on MS medium with and without lincomycin, detected with the UBQ11 specific antibody. (**C**) Immunoblot analysis of protein fractions from Col-0 + Lin and *gun1-102* + Lin cotyledons obtained through immunoprecipitation experiments using the Toc34 antibody. Equal volumes of supernatant and pellet preparations were loaded onto the gels and replica filters were probed with UBQ11 and Toc34 specific antibodies. The protein bands migrating between 50 and 90 kDa in *gun1-102* and Col-0 samples, recognized by the UBQ11 antibody, were completely overlapping with signals detected by the Toc34 antibody, demonstrating that these two bands represent ubiquitinated forms of Toc34 subunit.

3.11 GUN1 controls the accumulation of NEP-dependent transcripts in a regulatory process

As a member of the PPR protein family, a possible role of GUN1 as a key regulator of the plastid post-transcriptional processing can be envisaged. To this aim, we tested the accumulation of NEP- and PEP-dependent plastid transcripts in cotyledons of Col-0, *gun1-102*, *ftsh5-3* and *gun1-102 ftsh5-3* seedlings by RNA gel-blot hybridization: Col-0 and mutant seedlings were grown on MS medium with and without lincomycin, and gel blot analyses were performed on total RNA extracted from cotyledons of seedlings at 6 DAS, by employing the same set of PEP and NEP mRNA specific probes (Fig. 3.11, A). Transcripts, encoding the large subunit of RUBISCO (*rbcL*), the *α* subunit of ATPase (*atpα*), the A subunit of PSI core (*psaA*) and the D1 subunit of PSII reaction

center (*psbA*), were selected, as representative of the bacterial type plastid-encoded RNA polymerase-dependent (PEP-dependent). In absence of lincomycin, the abundance of *rbcL* transcripts did not change in the four genetic backgrounds, whereas the accumulation of *atpβ*, *psaA* and *psbA* was markedly reduced in *gun1-102 ftsh5-3* and, although to a less extent, in *ftsh5-3* cotyledons with respect to Col-0 and *gun1-102* seedlings, where the PEP-dependent transcript levels were identical. Probes specific for *Tic214* (*Ycf1*), encoding a constituent of 1 MDa TIC complex, the 3' portion of *rps12* (*rps12-3'*) encoding the S12 subunit of plastid ribosomes, *rpoA* and *rpoB* responsible of the α and β subunits of PEP RNA polymerase, respectively, and *clpP1* encoding the proteolytic subunit 1 of the ATP-dependent Clp protease were, instead, selected to monitor the accumulation of Nuclear Encoded Polymerase-dependent (NEP-dependent) specific transcripts. Unlike the PEP transcripts, identical amounts of NEP-dependent mRNAs were observed in Col-0, *gun1-102* and *gun1-102 ftsh5-3* cotyledons, while all of them showed a slight increased accumulation in *ftsh5-3* seedlings, resembling the negative regulatory feedback loop reported, previously, in *C. reinhardtii* (Ramundo et al., 2013). As expected, in presence of lincomycin, the accumulation of PEP-specific transcripts was almost completely abolished in all four genotypes, with the only exception of *atpα* that accumulated as precursor mRNAs, particularly abundant in *gun1-102* cotyledons (see asterisk in Fig. 3.11, A). Furthermore, the increased accumulation of transcripts of the nuclear *Lhcb1* gene, encoding one of the antenna proteins associated to PSII, observed in *gun1-102* and *gun1-102 ftsh5-3* cotyledons, together with the lack of plastid rRNAs, as revealed by the methylene blue (MB) stained filter, confirmed the efficacy of the inhibitory activity of lincomycin on plastid translation. By contrast, the levels of NEP-dependent transcripts increased substantially in Col-0 and *ftsh5-3* cotyledons when grown on MS medium with lincomycin, concomitantly with the

appearance of highly abundant transcript precursor forms (see asterisks in Fig. 3.11, A) at the expense of mature mRNAs (see crosses in Fig. 3.11, A). Strikingly, the licomycin-induced increased of NEP-dependent transcripts did not occur in *gun1-102* and *gun-102 ftsh5-3* cotyledons, where the total amount of mature mRNAs were maintained at levels similar to the ones of the seedlings grown on optimal MS medium, although the enrichment in precursor RNAs was retained, too. To obtain independent evidences on the specific role of GUN1 in the regulation of NEP-dependent transcript accumulation, total RNA was isolated from cotyledons of Arabidopsis mutants lacking the S21 (*prps21-1*) and L11 subunits (*prpl11-1*) of plastid ribosomes (see Pesaresi et al., 2001 and Romani et al., 2012), and from the corresponding *gun1-102 prps21-1* and *gun1-102 prpl11-1* double mutants (Tadini et al., 2016), all grown on MS medium without lincomicyn (Fig. 3.11, B). RNA gel blot hybridizations, performed with probes specific for PEP- (*rbcL*, *psbA*) and NEP- (*rpoA* and *rps12-3'*) dependent transcripts, corroborate the substantial increase of NEP-dependent mRNA levels upon defects in plastid protein synthesis, i.e. in *prps21-1* and *prpl11-1*, and the major role played in this regulatory mechanism by the GUN1 protein, as revealed by the strong reduction of *rpoA* and *rps12-3'* transcripts in *gun1-102 prps21-1* and *gun1-102 prpl11-1* cotyledons. Moreover, the increase of NEP-dependent transcripts in Col-0 cotyledons could be already observed at minimal concentrations of lincomycin (5,5 μM) in the growth medium, when the inhibitory effect on plastid translation and cotyledon greening was only slightly visible (Fig. 3.12, A-B). In the case of *rpoA* mRNAs, the increase of the total transcript amount, together with the appearance of RNA precursors and the concomitant reduction of mature RNAs, went hand in hand with the increased concentration of lincomycin and the progressive impairment of cotyledon greening, reaching its maximum at 550 μM of lincomycin, when the accumulation of plastid rRNA (see the methylene blue stained filter, Fig.

3.12, B) and the proplastid-to-chloroplast transition is completely abolished (Fig. 3.12, A-B). By contrast, *rps12-3'* transcripts reached the highest abundance in Col-0 cotyledons at 11 μM lincomycin, possibly as consequence of the reduced stability of these mRNAs at higher lincomycin concentrations that prevent plastid ribosome accumulation (Fig. 3.12, B). A similar transcript accumulation pattern in response to different lincomycin concentrations was also observed in *gun1-102* cotyledons, although the total accumulation levels of *rpoA* and *rps12-3'* transcripts were markedly reduced. Nevertheless, increase in NEP-dependent transcripts could be still observed in the *gun1-102* seedlings grown on MS medium with different concentration of lincomycin, implying that other plastid factors are involved in this regulatory process. To obtain a more general view on the GUN1-dependent control of NEP transcript accumulation, the knock-out mutant for the nuclear gene *cpHsc70-1* (At4g24280), encoding the chloroplast heat shock protein 70-1 with an important role in the protein precursor import into chloroplasts (Fig. 3.12, C), was used. As in the case of the *gun1-102 ftsh5-3* and *gun1-9 ftsh2-23*, *gun1-102 cphsc70-1* seedlings showed as well altered greening of cotyledons as highlighted by the appearance of white sectors typical of the variegated phenotype, supporting further the important role of GUN1 in the maintenance of chloroplast protein homeostasis in Arabidopsis cotyledons. Moreover, the abundance of NEP-dependent transcripts such as *Tic214*, *rpoA* and *rps12-3'* was substantially increased in *cphsc70-1* cotyledons and reduced to Col-0 levels in *gun1-102 cphsc70-1* seedlings, implying that the perturbation of key players of plastid protein homeostasis is enough to activate the GUN1-dependent increase of NEP-related transcripts (Fig. 3.12, D). Into details, the very large accumulation of NEP-dependent transcripts, observed when plastid protein translation and, as consequence, PEP transcription is impaired, prompted us to assume that the GUN1-dependent regulatory mechanism is needed upon

alteration of chloroplast gene expression. Strikingly, this regulatory mechanism seems to be specific for cotyledons, since the abundance of *rpoA* mRNAs did not change between *prps21-1* and *gun1-102 prps21-1* leaves (Fig. 3.11, C).

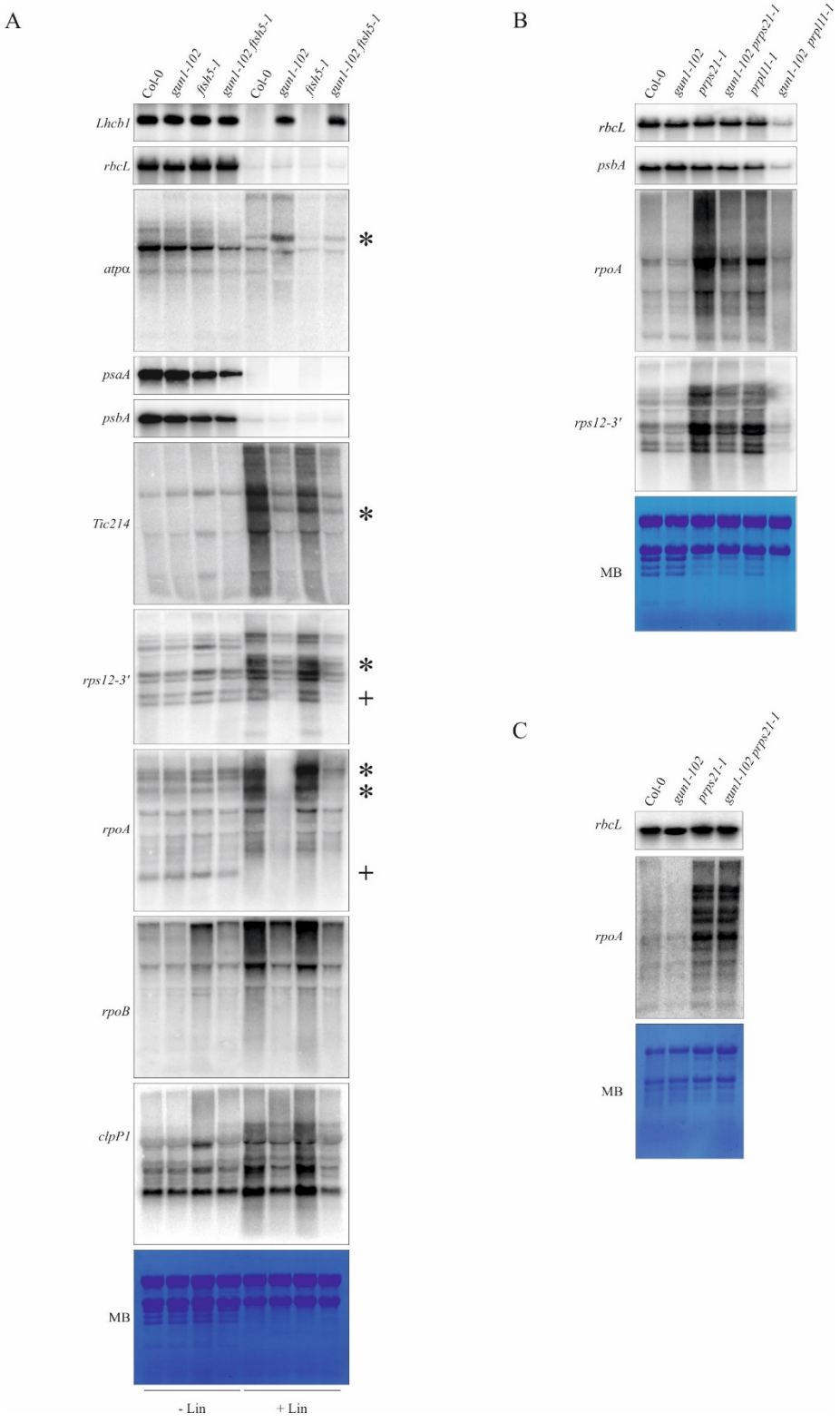
A
Col-0
gun1-102
ftsh5-1
gun1-102 ftsh5-1
Col-0
gun1-102
ftsh5-1
gun1-102 ftsh5-1
Lhcb1
rbcL
atpα
psaA
psbA
Tic214
rps12-3′
rpoA
rpoB
clpP1
MB
- Lin
+ Lin
B
Col-0
gun1-102
prpx21-1
gun1-102 prpx21-1
prpl11-1
gun1-102 prpl11-1
rbcL
psbA
rpoA
rps12-3′
MB
C
Col-0
gun1-102
prpx21-1
gun1-102 prpx21-1
rbcL
rpoA
MB

Figure 3.11. Transcript accumulation in Col-0 and mutant seedlings altered in chloroplast protein homeostasis. (**A**) Gel blots analysis of total RNA isolated form cotyledons of Col-0, *gun1-102*, *ftsh5-3* and *gun1-102 ftsh5-3* grown on MS medium with and without Lin. Probes specific for the nuclear gene *Lhcb1*, used as control for the *gun* phenotype, the plastid genes *rbcL*, *atpA*, *psaA*, *psbA*, transcribed by the PEP enzyme, and the NEP-dependent *Tic214* (*Ycf1*), *rps12-3'*, *rpoA*, *rpoB*, and *clpP1* genes were used for hybridization. (**B**) Gel blot analysis of total RNA isolated from cotyledons of Col-0, *gun1-102*, and mutants with defects in plastid protein translation such as *prps21-1* and *prpl11-1*, together with *gun1-102 prps21-1* and *gun1-102 prpl11-1* double mutants grown on MS medium. Probes specific for the PEP-dependent *rbcL*, *psbA* and NEP-dependent *rpoA*, *rps12-3'* plastid genes were used for hybridization. (**C**) Gel blot analysis of total RNA isolated from the first four leaves of Col-0, *gun1-102*, *prps21-1* and *gun1-102 prps21-1* plants grown on MS medium. The *rbcL* and *rpoA* probes were employed for hybridization. RNA-blots were stained with methylene blue (MB) as loading control. A representative result from three independent experiments is shown.

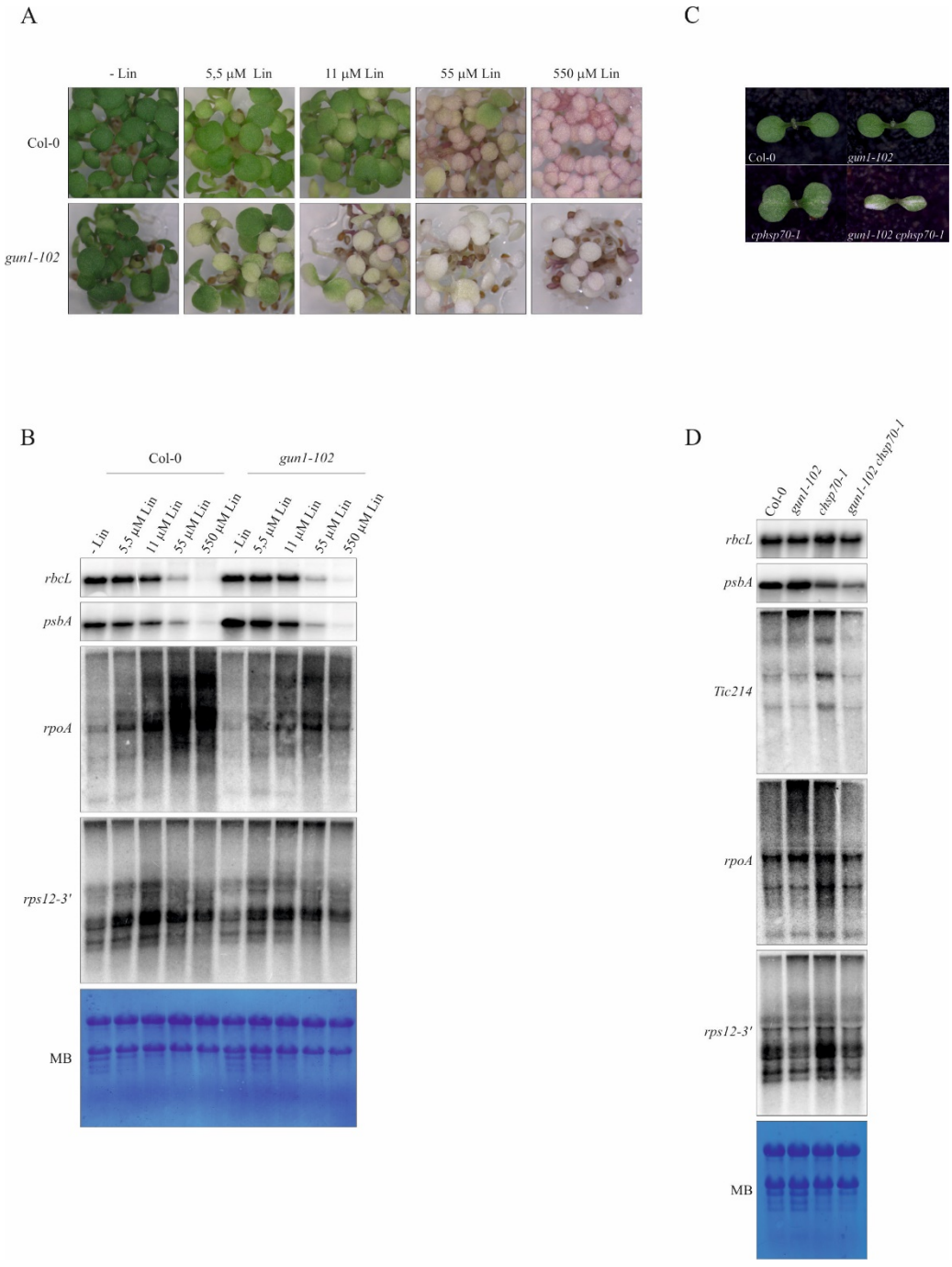
A
- Lin
5,5 µM Lin
11 µM Lin
55 µM Lin
550 µM Lin
Col-0
gun1-102
C
Col-0
gun1-102
cphsp70-1
gun1-102 cphsp70-1
B
Col-0
gun1-102
- Lin
5,5 µM Lin
11 µM Lin
55 µM Lin
550 µM Lin
rbcL
psbA
rpoA
rps12-3'
MB
D
Col-0
gun1-102
chsp70-1
gun1-102 chsp70-1
rbcL
psbA
Tic214
rpoA
rps12-3'
MB

Figure 3.12. Transcript accumulation in Col-0, *gun1-102*, *Δcphsc70-1* and *gun1-102 Δcphsc70-1* cotyledons grown under different conditions. (**A**) Phenotypes of Col-0 and *gun1-102* seedlings at 6 DAS grown on MS medium in the absence (- Lin) and at different concentration of lincomycin (5,5 μM Lin, 11 μM Lin; 55 μM Lin; 550 μM Lin). (**B**) Gel blot analysis of total RNA isolated from cotyledons of plants shown in (A). Probes specific for the PEP-dependent *rbcL*, *psbA* and NEP-dependent *rpoA*, *rps12-3'* plastid genes were used for hybridization. (**C**) Phenotypes of Col-0 and *gun1-102*, *cphsc70-1* and *gun1-102 cphsc70-1* seedlings at 6 DAS grown on soil under optimal growth-chamber conditions. (**D**) Gel blot analysis of total RNA isolated from cotyledons of plants shown in (C). Probes specific for the PEP-dependent *rbcL*, *psbA* and NEP-dependent *Tic214*, *rpoA*, *rps12-3'* plastid genes were used for hybridization. Note that Col-0, *gun1-102*, *cphsc70-1* and *gun1-102 cphsc70-1* seedlings showed the same phenotypes and RNA hybridization patterns when grown on MS medium. To control for RNA loading, blots were stained with methylene blue (MB). A representative result from three independent experiments is shown.

3.12 The chloroplast alterations caused by *gun1* mutation are sensed by the nucleus: protein ubiquitination level rises and the accumulation of main nuclear TFs is decreased

In order to characterize the effect of *gun1-102* mutation on the accumulation of nuclear transcription factors involved in GUN1 signaling pathway, biochemical analyses were performed on the isolated nuclear fraction of 6 DAS Col-0 and *gun1-102* mutant seedlings, grown in absence and presence of lincomycin. Immunoblot analyses were then performed using antibodies specific for GLK1 and HY5. To prevent the ubiquitination-mediated degradation of GLK1, the nuclei isolation was performed in presence of MG-132, an inhibitor of the 26S proteasome (Fig. 3.13, A). As documented by Tokumaru et al. (2017), GLK1

accumulation was completely abolished in presence of lincomycin, possibly due to ubiquitination-mediated degradation of GLK1 itself.

Furthermore, to follow the ubiquitination level of such samples, immunoblots using the UBQ11 specific antibody was performed. Interestingly, *gun1-102* seedlings showed a higher ubiquitination level of nuclear proteins, compared to Col-0, in either the presence or absence of lincomycin. The C.B.B. staining gel revealed the presence of two bands, of 72 kDa and 95 kDa size, more abundant in lincomycin-treated seedlings than in the other samples. This effect was observed in total protein extract and the two bands were identified as AtHsp90-1 and AtHsc70-4 (Fig.3.9) that seem to accumulate as well in the nuclei (Fig.3.13, A, light blue arrow).

Moreover, immunoblot analyses were also performed using the HY5-specific antibody, on total protein extract of 6 DAS Col-0 and *gun1-102* mutant seedlings, grown as well in absence and presence of lincomycin.

The band corresponding to the unmodified form of HY5 protein (17 kDa) was not detected in Col-0 and *gun1-102* seedlings grown under optimal conditions, however, in Col-0 seedlings grown with lincomycin, HY5 accumulates to higher levels than in *gun1-102* mutant background, grown under the same conditions (Fig.3.13, B). Srivastava et al. (2015) observed that HY5 has a high predisposition to being ubiquitinated in the dark; in this sense, when the plastid gene expression is repressed in *gun1-102* mutant seedlings, the level of ubiquitinated nuclear proteins rises and, probably, the 26S proteasome activity too. In this scenario, HY5 can be easily subjected to fast 26S proteasome degradation and this could explain why its unmodified form diminishes. Taken together, these preliminary observations suggest that the ubiquitin-mediated degradation of proteins, such as transcription factors (HY5), occurs in nuclei as well, and that such a machinery, probably, is particularly active in lincomycin-treated *gun1-102* seedlings.

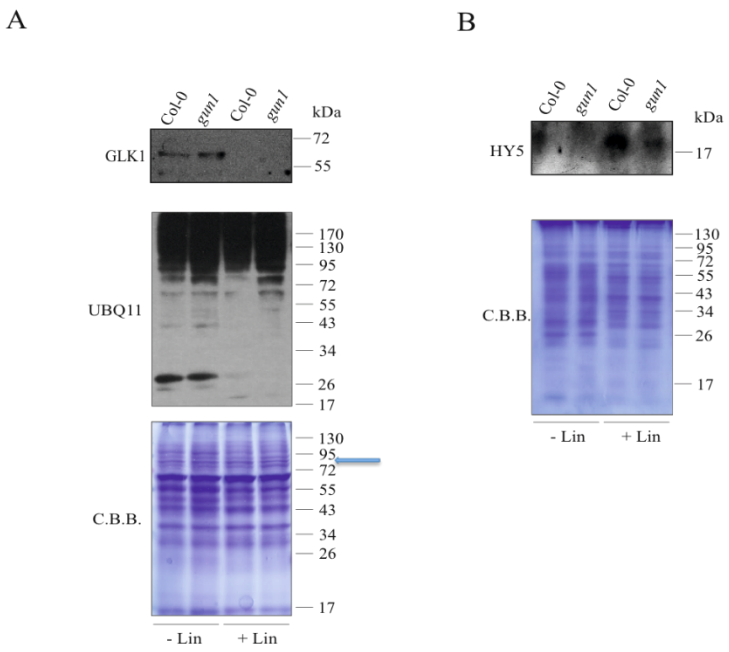

Figure 3.13. Nuclear transcription factors and ubiquitination level in the nuclei in Col-0 (+/- Lin) and *gun1-102* (+/- Lin) cotyledons. (**A**) Immunoblot analyses of GLK1 transcription factor and UBQ11. Nitrocellulose filters carrying nuclear fractions treated with 100 μM MG-132 (isolated from seedling's cotyledons after a 5 hours-long pretreatment with 50 μM MG-132) were probed with antibodies directed against GLK1 and UBQ11. (**B**) Immunoblot analysis of total protein fraction from Col-0 +/- Lin and *gun1-102* +/- Lin cotyledons filter was probed with HY5 specific antibody. To control for proteins loading, a replica SDS-PAGE was stained with Coomassie Brilliant Blue (C.B.B.).

3.13 Inhibition of Plastid Gene Expression (PGE) leads to upregulation of transcription factor and plastid chaperone transcripts in *gun1-102* mutant background

To further investigate the effect of *gun1* mutation on the nuclear gene expression, quantitative real time PCR (qRT-PCR) analyses were performed on 6 DAS Col-0 and *gun1-102* seedlings, grown in absence and presence of lincomycin (Fig. 3.14). Interestingly, the gene coding for HsfA2, a transcription factor involved in response to different stresses such as heat and osmotic shocks, high salt concentration and high light regimes (Liu et al., 2011), was found highly up-regulated in lincomycin-treated *gun1-102* seedlings (~23 times more than lincomycin-treated Col-0 samples).

An even more larger effect was shown by the plastid chaperone Hsp21, (that is under the transcriptional control of HsfA2) (Schramm et al., 2006) involved in defence against stress-induced protein aggregation together with Hsp100 and cpHsc70 chaperones (Lee & Vierling, 2000; Wang et al., 2004): its transcripts accumulate ~300 times more in lincomycin-treated *gun1-102* samples than the Col-0 treated with lincomycin.

Furthermore, *CPHSC70-1* and *CPHSC70-2* transcripts accumulated twice as much in *gun1-102* mutant seedlings grown in the presence of lincomycin with respect to the Col-0 grown in the same conditions. cpHsc70-1 and cpHsc70-2 are plastid chaperons, induced when chloroplasts are under heat stress (Su & Li, 2008). Overall, these observations confirmed the hypersensitivity of *gun1-102* seedlings to lincomycin, supporting further the key role played by GUN1 in plastid gene expression and protein homeostasis.

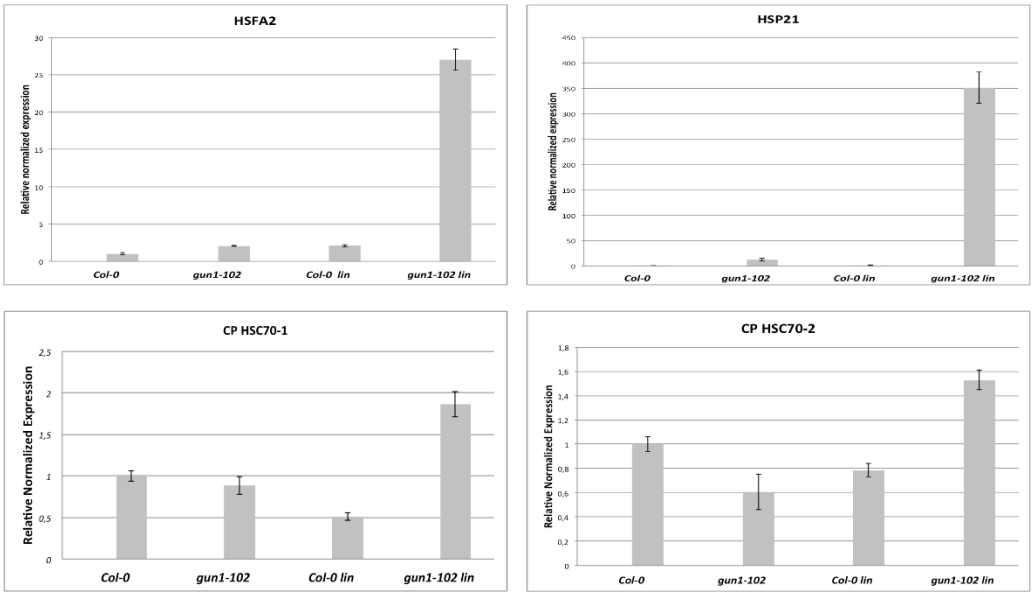

Figure 3.14. Expression of genes involved in response to environmental stresses in Col-0 and *gun1-102* seedlings grown with and without lincomycin (for technical details see paragraph 2.1, Materials and methods). The qRT-PCR analyses were performed to monitor the expression of *HSFA2*, *HSP21*, *CPHSC70-1*, *CPHSC70-2* genes. Values are the average of three biological and 9 technical replicates. Lines indicate the Standard deviation (SD). The *PP2A* and *ACT8* expression levels were used as internal standards.

4. Discussion

The main goal of this study was to investigate the role of GUN1 protein during early stages of chloroplast biogenesis in Arabidopsis cotyledons. A major difficulty in the elucidation of the molecular mechanism, as well as of the precise role of GUN1 in retrograde signaling, is due to the fact that *gun1* mutants are indistinguishable from wild type under optimal growth conditions, with the only difference represented by a small (about 9%) percentage of *gun1* mutants developing chlorophyll-deficient cotyledons (Ruckle et al., 2007). However, *gun1* specific phenotypes can be observed under chemically- or genetically-induced stress conditions, generating a wide range of visible effects. For instance, it was found that GUN1 helps to integrate chloroplast biogenesis with photo-morphogenesis since it can affect cotyledon opening and expansion and hypocotyl elongation upon treatments with lincomycin and different fluence rates of blue light (Ruckle et al., 2007, Ruckle and Larkin, 2009). Seedlings of *gun1-1* grown on either lincomycin or norflurazon containing medium, supplemented with 2% sucrose, have also revealed a role of GUN1 in anthocyanin biosynthesis (Cottage et al., 2008; Cottage et al., 2010; Ruckle and Larkin 2009). In addition, seedlings lacking GUN1 present a hypersensitive phenotype to low concentration of both norflurazon (20 nM) and lincomycin (8.8 μg/mL) as displayed by a visible pale yellow or white and smaller cotyledon phenotype compared to wild type seedlings that retain fully developed green cotyledons under the same growth conditions (Zhao et al., 2018). Accordingly, when the *gun1* mutant was combined with mutations that impair plastid protein synthesis, such as *prps17-1*, *prpl11-1* and *prpl24-1*, the corresponding double mutants were seedling lethal (Tadini et al., 2016). A similar phenotype was also observed in double mutants defective in both GUN1

and Clp protease activity, supporting the notion that the GUN1 protein is essential for protein homeostasis in the chloroplast (Llamas et al., 2017). Our data further support these evidences as shown by the seedling lethal phenotype of *gun1-9 ftsh2-23* and the enhanced variegated phenotype of *gun1-102 ftsh5-3* and *gun1-102 cphsc70-1* cotyledons. Interestingly, the introgression of either *fug1-3* or *prps21-1* mutation into *gun1-102 ftsh5-3* seedlings was able to suppress the leaf- but not the cotyledon-variegated phenotype of the double mutant, implying a specific role of GUN1 in chloroplast biogenesis in cotyledons, distinct from the maintenance of protein homeostasis in thylakoid membranes played by the FtsH protease complex. This notion is, indeed, supported by the differences in chloroplast ultrastructure associated with either FtsH depletion alone or together with GUN1 protein as in *gun1-102 ftsh5-3* and *gun1-9 ftsh2-23* seedlings. Indeed, *ftsh2-22*, *+/ftsh1-1 ftsh5-3* and *ftsh2-22 ftsh5-3* cotyledons showed swollen chloroplasts, characterized by scattered grana and vacuolated membrane structures of various sizes, resembling chloroplasts exposed to stress conditions (Hasan et al., 2018; Islam et al., 2016; Shao et al., 2016). This is in line with the multiple functions of FtsH protease in chloroplasts, including D1 protein degradation, biosynthesis of PSI complex and degradation of cytochrome b_6f complex and LHCI (Wang et al., 2014; Järvi et al., 2016). Furthermore, multiple lines of evidence demonstrated that reduction in protein biosynthesis in plastids suppresses such altered phenotypes. Apparently, the balance between protein biosynthesis and FtsH function during leaf development is crucial for chloroplast differentiation. By contrast, no fully differentiated chloroplasts could be observed in large portions of *gun1-9 ftsh2-23* seedlings and *gun1-102 ftsh5-3* cotyledon cells, which contained either fully developed wild type-like chloroplasts or chloroplasts severely damaged, characterized by large vesicles instead of thylakoids, disrupted outer envelope membranes and the presence of plastoglobules, suggesting a cytosolic response

that coordinates the development/degradation of chloroplasts. Thus, a chloroplast degradation pathway appears to be active in *gun1-9 ftsh2-23* and *gun1-102 ftsh5-3* cotyledon cells, possibly involving an ubiquitin-mediated quality control pathway aimed to remove damaged and/or not properly developed chloroplasts, as can be deduced by the partial rescued phenotype of *pub4-7 gun1-102 ftsh5-3* cotyledons, that show increased chlorophyll content, improved photosynthesis performance and chloroplast ultrastructure.

Overall, it appears that GUN1 and the thylakoid FtsH protease complex act on two independent pathways that act synergistically to promote chloroplast biogenesis and plastid protein homeostasis in cotyledons. Those pathways seem to include specific processes that take place into the chloroplast and that, at the same time, give rise to signals for the communication with the nucleus aimed to regulate photosynthesis related gene expression in response to the chloroplast developmental needs. FtsH2, for instance, beside its role in D1 protein degradation of damaged PSII, promotes $^1O_2$-triggered signaling through the proteolysis of EXECUTER1 (EX1) protein associated with PSII in grana margin (Dogra et al., 2017). A similar dual role can be also envisaged for GUN1 protein.

i. GUN1 plays a key role in the Δ-rpo regulatory process

Based on the observations described above, together with the evidences that GUN1 i) is a chloroplast PPR protein with a C-terminal Small MutS-related (SMR) domain that confers DNA binding capacity; ii) physically interacts with nucleoid subunits and PEP-associated proteins (pTAC6); iii) highly accumulates at very early stages of chloroplast biogenesis; iv) is found accumulated at higher levels upon lincomycin inhibition of plastid translation; v) functionally interacts with proteins involved in chloroplast protein homeostasis; vi) shows similar behaviors of DEAD-box RNA helicase mutant

rh50, when combined with mutants altered in plastid translation, we decided to explore the role of GUN1 protein in plastid transcript accumulation, upon plastid protein homeostasis alteration in Arabidopsis cotyledons. Six-days old seedlings grown on MS medium containing 550 μM lincomycin or with defects in plastid protein degradation, *ftsh5-3*, plastid protein synthesis, *prps21-1* and *prpl11-1*, and plastid protein import and folding, *cphsc70-1*, were selected for our purposes. In all mutants grown on MS medium except for *gun1-102*, the RNA levels of PEP-transcribed genes such as *psaA* and *psbA* were markedly reduced, if compared to Col-0, whereas NEP-dependent transcript accumulation increased. This phenomenon was particularly prominent in mutants with defects in plastid protein synthesis, but could also be observed in *cphsc70-1* cotyledons and, although less pronounced, in *ftsh5-3* seedlings. In agreement with these observations, the addition of lincomycin to the growth medium abolished the PEP-dependent transcript accumulation and dramatically increased the accumulation of NEP-dependent mRNAs both in Col-0 and mutant cotyledons. Strikingly, the lack of GUN1 protein in *gun1-102* and in the corresponding double mutants, or in presence of lincomycin, led to a dramatic reduction of the over-accumulation of NEP-dependent transcripts upon partial or total inhibition of PEP activity, promoting GUN1 to the role of master regulator of NEP-dependent transcript accumulation.

Expression profiles similar to the ones observed in this thesis have been reported in numerous publications. In Arabidopsis, for instance, the lack of the Fe Superoxide dismutase 2 (FSD2) and FSD3 that form a heterotrimeric protein complex in the chloroplast nucleoids, essential for chloroplast development, induces an increased accumulation of NEP-dependent transcripts, whereas the mRNAs of PEP-transcribed genes accumulate to lower levels than the control plants (Myouga et al., 2008). Similarly, T-DNA tagged mutants of three components of the plastid transcriptionally active chromosomes (pTACs),

ptac2, *ptac6* and *ptac12* (Pfalz et al., 2006), showed downregulation of PEP-dependent genes and increased accumulation of NEP-dependent transcripts relative to wild type control. Other Arabidopsis mutants with impaired PEP activity and increased accumulation of NEP-dependent transcripts include *chloroplast biogenesis 19* (*clb19*), lacking a PPR protein required for the editing of two distinct chloroplast transcripts, *rpoA* and *ClpP* (Ramos-Vega et al., 2015) , and *yellow seedlings 1* (ys1), where a nuclear-encoded chloroplast-localized pentatricopeptide repeat protein is required for editing of site 25992 in *rpoB* (Zhou et al., 2009). This characteristic NEP- and PEP-dependent transcript accumulation pattern was originally described in transplastomic tobacco lines in which the plastid *rpo* genes were inactivated by insertion of a gene cassette (Allison et al.,1996; Hajdukiewicz et al., 1997; De Santis-Maciossek et al., 1999) and indicated as Δ-*rpo* phenotype. The molecular details responsible of Δ-*rpo* expression pattern are largely unknown, however PLASTID REDOX INSENSITIVE2 (PRIN2), a redox-regulated protein, has been proposed, recently, as the link between photosynthetic electron transport and activation of PEP-dependent photosynthetic gene expression (Díaz et al., 2018). Taken these observations together, it can be argued that GUN1 and PRIN2 are two main components of the regulatory mechanism that control the shift in the usage of the primary RNA polymerase from NEP to PEP during early stages of chloroplast biogenesis, thus optimizing the switch to photoautotrophic growth, depending on available lipid reserves, light conditions, and chloroplast development. In particular, the relatively high abundance of GUN1 protein during early stages of chloroplast biogenesis could favor the NEP activity, whereas its decrease at later stages together with the photosynthesis-mediated monomerization of PRIN2 would promote PEP activity and the photoautotrophic transition. The interaction of GUN1 with pTAC6, observed through coimmunoprecipitation studies (Tadini et al., 2016),

could be one of the key elements at the basis of this regulatory mechanism. pTAC6, indeed, has been reported to be part of the transcription subdomain of the transcriptionally active chromosomes and essential for the accumulation of PEP-dependent transcripts. Furthermore, the GUN1-dependent Δ-*rpo* regulatory mechanism appears to be present in cotyledons but not in mature leaves, although it cannot be excluded that its activity is restricted to the basal part of developing leaves where the proplastid-to-chloroplast transition takes place. This is also in agreement with recent reports where a post-transcriptional regulatory role of GUN1 has been proposed in mature rosette leaves (Tadini et al., 2016). Interestingly, GUN1, PRIN2, pTAC6 are absent from the genomes of green algae and cyanobacteria, indicating that these proteins appeared during evolution of the plant lineage concomitantly with the appearance of the nucleus-encoded plastid RNA polymerase, NEP.

ii. Regulation of the translocon machinery is a crucial step for plastid protein homeostasis

The effects of plastid protein homeostasis alteration are not only limited to chloroplast transcript accumulation and thylakoid membrane ultrastructure but also affect the accumulation and post-translation modifications of several nucleus-encoded proteins either located in the cytosol or targeted to the chloroplast and involved in different plastid activities. As expected, subunits of the four major thylakoid protein complexes were largely reduced in both *gun1-9 ftsh2-23* and *gun1-102 ftsh5-3* cotyledons grown under optimal conditions and as well in seedlings grown in presence of lincomycin, that abolished, as well, the accumulation of RbcS and RbcL subunits of RUBISCO, together with the antenna proteins of PSI and PSII in Col-0 and *gun-102* cotyledons. By contrast, an almost double amount of the stromal chaperon protein ClpB3 was detected in *ftsh* and *gun1 ftsh* mutants. ClpB3 is the only ClpB-type HSP100 chaperone

targeted to Arabidopsis plastids shown to disaggregate protein clumps and promote protein solubilization either alone or in synergy with cpHsc70 chaperons (Llamas et al., 2017). ClpB3 ability to release protein folding stress has been, recently, reported to be at the center of the chloroplast Unfolded Protein Response (cpUPR). Indeed, ClpB3 together with ClpC2 and cpHsc70-1 chaperons accumulated in Col-0 and *gun1-102* seedlings "transiently exposed to lincomycin", i.e. in conditions of dramatic reduction of stromal and thylakoid protein amounts, at levels identical to the ones of Col-0 untreated control, supporting the notion that stromal chaperone accumulation is triggered through the interference of chloroplast protein homeostasis (Llamas et al., 2017). Because the vast majority of the chloroplast proteins are encoded by the nuclear genome, are synthetized in the cytoplasm, and are imported in an unfolded state into the organelle via specialized translocases, alteration of the stromal proteins folding environment is expected to have a marked impact on the availability of the stromal chaperons and ATP required for protein import and the refolding of the mature proteins upon translocation. Based on that, major changes in protein accumulation and post-translation modification could also be expected at the envelope and in particular with respect to subunits of the translocon machinery. In general, the lack of GUN1 destabilizes the entire TOC complex in Arabidopsis cotyledons, as shown by the reduced accumulation of the GTP-dependent receptor protein, Toc159, and the protein conducting channel Toc75. Furthermore, the other receptor protein Toc34 resulted to be ubiquitinated in *gun1-102* cotyledons and in the *ftsh* single and double mutants, supporting previous findings where ubiquitination of TOC components was reported to adjust the plastid proteome to developmental and physiological needs (Ling et al., 2012; Svozil et al., 2014). Similarly, the reduced accumulation of Tic100 and Tic20-1 indicate that GUN1 protein is important for the accumulation of the 1 MDa TIC complex. Noteworthy, the presence of either lincomycin in the

growth medium or the introgression of *gun1-102* mutation into the *ftsh* mutants further exacerbated the effects on the translocon machinery in terms of protein accumulation and Toc34 ubiquitination. For instance, the Tic20 accumulation was prevented by lincomycin, in agreement with previous reports (Bölter et Soll, 2016; Kohler et al., 2016), and reduced the accumulation of Tic100 and Tic56 dramatically, highlighting the existence of a potential regulatory mechanism aimed to coordinate chloroplast protein synthesis with chloroplast protein import. That could also explain why the *Tic214* (*Ycf1*) gene has been retained in the plastid genome of different plant species. By contrast, the levels of Tic110 and Tic40 increased in *gun1-102* cotyledons and a relatively high accumulation was even maintained in the presence of lincomycin, similarly to what has been observed in Arabidopsis *Clp* mutants and in agreement with the fact that Tic110 has been reported to be a target of the Clp protease in Chlamydomonas (Ramundo et al., 2014).

iii. Retrograde signaling and the ubiquitin-proteasome system

In line with the findings reported above, the chloroplast protein import capacity was found to be altered in *gun1-102* and even more in *gun1-102* seedlings grown in presence of lincomycin. In particular, a combination of different approaches, including immunoblot analysis using FtsH specific antibodies, transgenic lines carrying FtsH chimera in the corresponding *gun1-102 ftsh* mutant backgrounds, and mass-spectrometry analysis demonstrated the accumulation of FtsH precursor proteins in the cytosol of *gun1-102* cotyledon cells, thus giving a possible explanation for the exacerbated phenotypes of *gun1-9 ftsh2-23* and *gun-102 ftsh5-3* seedlings. Furthermore, mass-spectrometry analysis of protein soluble fractions obtained from total proteins extracted form Col-0 and *gun1-102* cotyledons grown in either the presence or

absence of lincomycin allowed the identification of 37 chloroplast precursor proteins, particularly abundant in *gun1-102* seedlings grown on MS medium with lincomycin. As such precursor proteins are thought to be unfolded, their accumulation in the cytosol might cause aggregation, which would be toxic for the cells, thus it is reasonable to hypothesize that only a very limited subfraction of precursors, the one not yet degraded by the 26 proteasome, has been identified in our analysis. Nevertheless, this finding supports further the involvement of GUN1 protein in chloroplast protein import, albeit its role appears to be indirect due to the nucleoid localization of GUN1 protein. The accumulation of precursor proteins is also in agreement with the large accumulation of AtHsp90 and AtHsc70 chaperones and the marked increase of ubiquitinated proteins observed in *gun1-102* cotyledons in presence of lincomycin. Interestingly, the cytosolic heat shock cognate, Hsc70-4, and its interacting E3-ubiquitin ligase, CHIP (Lee et al., 2009), mediate the degradation of unimported chloroplast precursor proteins through the ubiquitin-proteasome system, indicating that under conditions in which chloroplast downstream processes are compromised, cytoplasmic protein degradation is enhanced. As such, the degradation of unimported proteins via the ubiquitin-proteasome system plays a key role in determining the chloroplast proteome in response to intracellular or environmental signals. At least two other mechanisms involving the ubiquitin-proteasome pathway have been shown to have a role in retrograde signaling (Jarvis and López-Juez, 2013; Woodson et al., 2016). One of them is based on the direct regulation of protein translocation machinery. In this mechanism, a RING-type ubiquitin ligase of the chloroplast outer membrane, SP1, directly regulates the context of the TOC complex (Ling et al., 2012). As a matter of fact, the Toc34 subunit is highly ubiquitinated in *gun-102*, *ftsh* and the corresponding double mutant seedlings. In addition, the ubiquitin-proteasome dependent post-translational regulation has been also

shown to play a key role in the accumulation of GOLDEN2-LIKE 1 (GLK1) transcription factor, known to positively regulate the expression of photosynthesis-related genes during chloroplast biogenesis. In particular, the level of GLK1 protein was decreased by treatments with norflurazon and lincomycin that induce plastid damage, regardless of level of *GLK1* mRNA (Tokumaru et al., 2017). Interestingly, the same reduced accumulation of GLK1 protein was observed in the Arabidopsis *ppi2-2* mutant, which lacks the protein import receptor Toc159, implying that defects in plastid protein import regulate the accumulation of GLK1 at post-transcriptional level with the aim to optimize the expression of nuclear genes encoding photosynthesis-related proteins when plastid protein import is compromised (Kakizaki et al., 2009). To this regard, immunoblots performed on nuclear protein fraction revealed that in the *gun1-102* mutant background, in condition of perturbed chloroplast protein homeostasis, the level of the ubiquitinated nuclear proteins rises and the HY5 transcription factor is very poorly accumulated in this mutant background compared to Col-0 seedlings grown in the same condition. Lee et al. (2007) mapped genome-wide and *in vivo,* HY5 binding sites, and produced a list of genes positively and negatively regulated by this transcription factor. Interestingly, they found that, in the list of genes negatively regulated by HY5 there is the Heat shock transcription factor 2 (HSTF2, also called HsfA1e), normally accumulated at very high level in seed (Liu et al., 2011) and here involved in conferring thermotolerance (Liu et al., 2011). This transcription factor, together with HsfA1a, HsfA1b, HsfA1d, is active in the expression of genes coding for the heat shock proteins and heat shock transcription factors, among the others, the ones coding for the cytosolic Hsp70, Hsp90, the chloroplastic cpHsc70-1, Hsp21 and the transcription factor HsfA2 (see Figure 4.1) (Liu et al., 2011; Yoshida et al., 2011). As a matter of fact, *HSFA2* gene was found greatly expressed in *gun1-102* mutant background grown in presence

of lincomycin and the accumulation of this TF also leads to a very high expression of the gene coding for the chloroplastic heat shock protein Hsp21, that, located in the nucleoids, interacts with pTAC5 and has an important role in maintenance of the PEP activity in condition of heat stress (Zhong et al., 2013). Also the genes coding for stromatic heat shock proteins cpHsc70-1 and cpHsc70-2 were found doubly transcribed in *gun1-102* mutant background grown in presence of lincomycin. Llamas and colleagues (Llamas et al., 2018) observed this effect (for *HSP21*, *CPHSC70-2* and *HSFA2* genes) in Col-0 and *gun1* mutant seedlings when transiently exposed to lincomycin (the named before, chloroplast Unfolded Protein Response), interestingly, we found a different effect in *gun1-102* mutant and in Col-0 seedlings when stably grown in presence of lincomycin. More in detail, we found that in *gun1-102* mutant seedlings grown in presence of lincomycin were maintained high levels of transcripts of heat shock proteins and transcription factors (*HSP21*, *CPHSC70-1*, *CPHSC70-2, HSFA2*) and also at protein level, of chaperones like the cytosolic Hsp90 and Hsc70-4 while, in the Col-0 seedlings grown in the same condition, the levels of these analyzed transcripts and proteins are kept at more stable levels. Moreover, HY5 transcription factor is involved in anthocyanin biosynthesis during cold stress (Perea-Resa et al., 2017) and *gun1-102* mutant seedlings grown in presence of lincomycin accumulate less anthocyanins compared to the Col-0 seedlings grown in the same stressfull condition (Cottage et al., 2010). Taken together, all these results suggest a “short circuit” in the response to the chloroplast protein homeostasis perturbation, caused by the absence of GUN1 protein which impacts on the abundance of main transcription factors like HY5, possibly linked with the general high level of ubiquitinated proteins and 26S proteasome hyperactivity.

Finally, it is tempting to speculate that the PUB4 E3 ligase is recruited to damaged chloroplasts and is able to mark them for degradation via

ubiquitination. Afterwards, the cytoplasmic degradation machinery that recognizes ubiquitin conjugates would be targeted to the appropriate altered chloroplasts. Such mechanism could explain, for instance, the ability of *pub4-7* mutation to partially rescue the *gun1-102 ftsh5-3* cotyledon phenotype. Thus, our results together with previous reports indicate that ubiquitination, the 26S proteasome, and the cellular degradation machinery are integral parts of retrograde signaling pathways, together with the reprogramming of nuclear transcription, all aimed to maintain healthy chloroplasts inside plant cells.

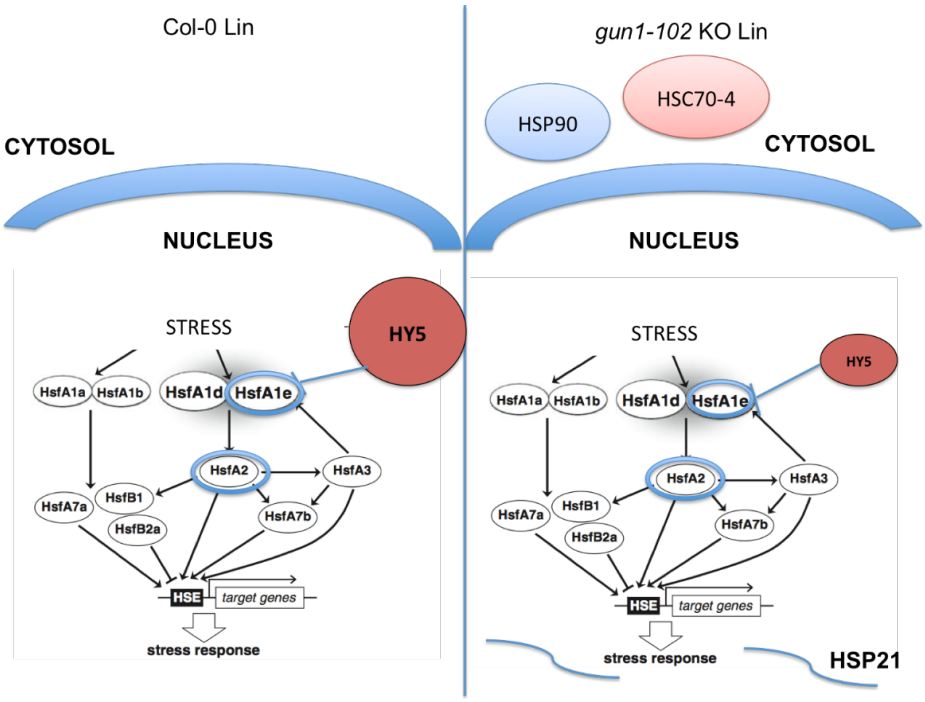

Figure 4.1. Schematic model of the HY5 role in controlling the expression of heat shock-related genes. On the left, the Col-0 situation: in seedlings grown in presence of lincomycin there is an accumulation of the HY5 transcription factor that negatively regulates the expression of *HSFA1E* gene. On the right, in *gun1-102* mutant seedlings grown in presence of lincomycin there is less accumulation of HY5 and a consequent, enhanced expression of genes coding for HsfA2, Hsp21, cpHsc70-2, cpHsc70-1. Moreover, Hsp90 and Hsc70-4 are highly accumulated in the cytosol. (Adapted from Nishizawa-Yokoi et al., 2011)

5. Conclusions and future perspectives

Since the discovery of the *gun1* mutant in 1993 (Susek et al., 1993) and the subsequent isolation of several *gun1* mutant alleles, it was clear that a GUN1-dependent signaling pathway exists and that is part of chloroplast-to-nucleus retrograde communication aimed to adjust nuclear gene expression in response to chloroplast dysfunctions (Koussevitzky et al., 2007). During the last 25 years, we learned that the *GUN1* gene encodes a chloroplast-localized pentatricopeptide-repeat protein, particularly important during early stages of chloroplast biogenesis in Arabidopsis cotyledons (Ruckle et al., 2007; Ruckle and Larkin, 2009; Tadini et al., 2016), however its exact biochemical mechanism, as well as its precise role in retrograde signaling, has remained enigmatic. In this thesis, we believe to have identified the primary function of GUN1 as a positive regulator of NEP-dependent transcript accumulation. In Figure 5.1, we summarize a possible mechanism by which GUN1 is mainly involved in regulating the switch between NEP- and PEP-dependent transcription of plastid genes (indicated with 1 in Fig. 5.1). This model is consistent with: i) the delay in greening observed in *gun1* cotyledons, ii) the localization of GUN1 protein in plastid nucleoids, where transcription takes place; iii) its putative ability to bind DNA due to the presence of the C-terminal SMR domain, as previously reported. The disruption of this process triggers a cascade of events that leads to: ii) altered organization of thylakoid membranes (2 in Fig. 5.1), iii) readjustment of the translocon machinery (3), vi) accumulation of chloroplast precursor proteins in the cytosol (4), v) consequent increased accumulation of cytosolic chaperons, (5), vi) high level of ubiquitinated proteins in the nucleus and changes in the accumulation of main transcription factors like HY5 and HsfA2, (6), vii) PUB4-mediated degradation

of damaged chloroplasts (7). Nucleic acid immunoprecipitation followed by chip hybridization, together with transcriptomic and proteomics analyses to be performed on seedlings showing an active Δ-*rpo* regulatory process, i.e. Col-0 seedling grown in the presence of lincomycin or Arabidopsis mutants with defects in chloroplast protein synthesis, are likely to provide further important insights into the molecular mechanism of GUN1 function and the network of the retrograde signaling pathway. This should lead to novel hints into the complex regulation mechanisms that determine how plants build up their chloroplasts and provide potentially helpful targets for important future challenges such as crop yield improvement and bioenergy production.

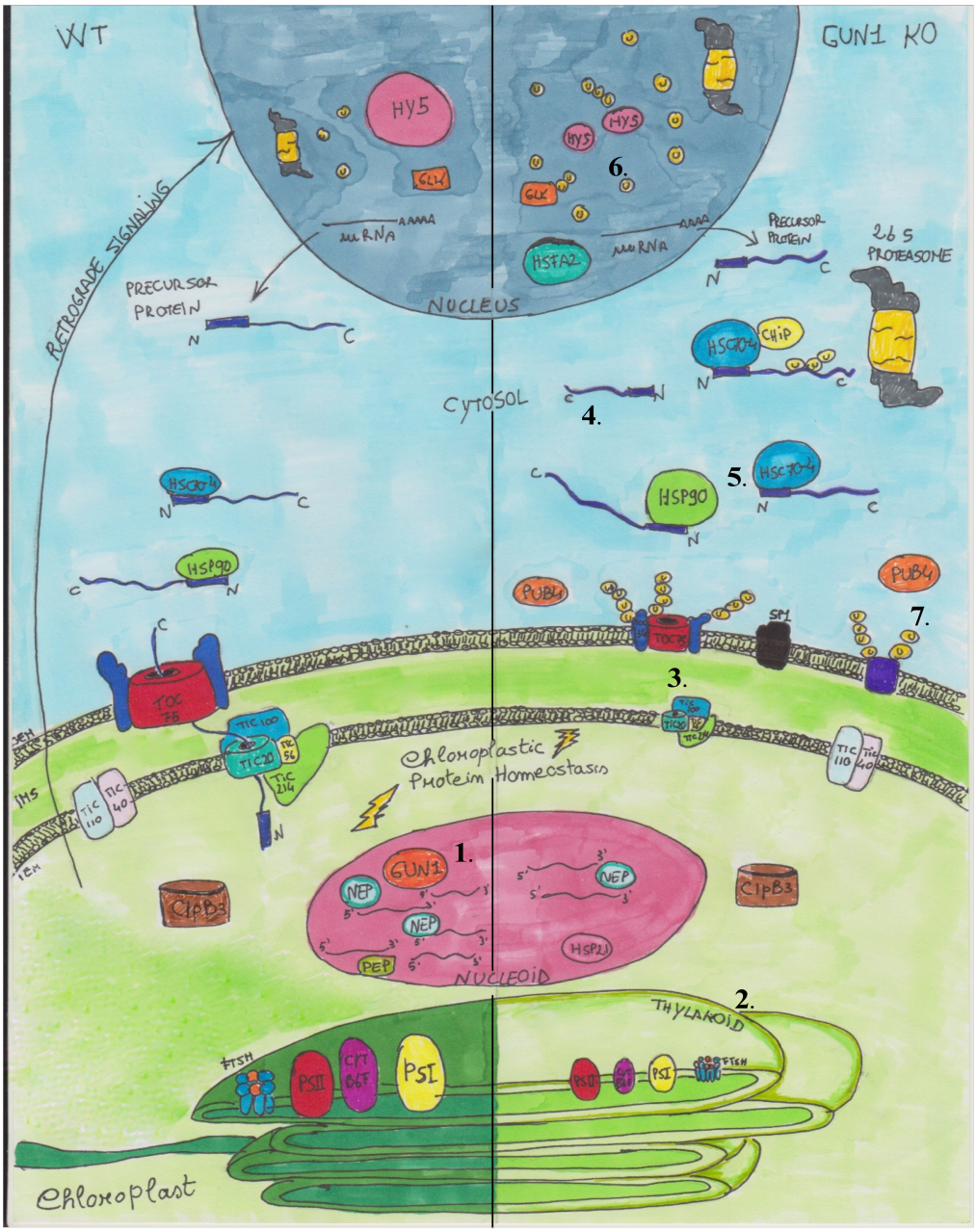

Figure 5.1. Schematic conclusive model of all the obtained results: on the left, the wild type scenario, on the right the *gun1* mutant background scenario both in condition of perturbed chloroplastic protein homeostasis. For the details see the text. OEM, outer envelope membrane, IEM, inner envelope membrane, IMS, intermembrane space, U, ubiquitin (drawing of Carlotta Peracchio)

6. References

Adam, Z., Rudella, A., & van Wijk, K. J. (2006). Recent advances in the study of Clp, FtsH and other proteases located in chloroplasts. *Current Opinion in Plant Biology*, *9*(3), 234–240. https://doi.org/10.1016/j.pbi.2006.03.010

Allison, L. A., Simon, L. D., & Maliga, P. (1996). Deletion of rpoB reveals a second distinct transcription system in plastids of higher plants. *The EMBO Journal*, *15*(11), 2802–2809. https://doi.org/10.1002/j.1460-2075.1996.tb00640.x

Allorent, G., Courtois, F., & Lerbs-mache, F. C. S. (2013). Plastid gene expression during chloroplast differentiation and dedifferentiation into non-photosynthetic plastids during seed formation, 59–70. https://doi.org/10.1007/s11103-013-0037-0

Asakura, Y., Galarneau, E., Watkins, K. P., Barkan, A., & van Wijk, K. J. (2012). Chloroplast RH3 DEAD Box RNA Helicases in Maize and Arabidopsis Function in Splicing of Specific Group II Introns and Affect Chloroplast Ribosome Biogenesis. *Plant Physiology*, *159*(3), 961–974. https://doi.org/10.1104/pp.112.197525

Bölter, B., & Soll, J. (2016). Once upon a Time – Chloroplast Protein Import Research from Infancy to Future Challenges. *Molecular Plant*, *9*(6), 798–812. https://doi.org/10.1016/j.molp.2016.04.014

Börner, T., Yu, A., Zubo, Y. O., & Kusnetsov, V. V. (2015). Biochimica et Biophysica Acta Chloroplast RNA polymerases : Role in chloroplast biogenesis ☆. *BBA - Bioenergetics*, *1847*(9), 761–769. https://doi.org/10.1016/j.bbabio.2015.02.004

Boston R.S., Viitanen P.V., Vierling E. (1996) Molecular chaperones and protein folding in plants. In: Filipowicz W., Hohn T. (eds) Post-Transcriptional Control of Gene Expression in Plants. Springer, Dordrecht

Bräutigam K., Dietzel L., Pfannschmidt T. (2007) Plastid-nucleus communication: anterograde and retrograde signalling in the development and function of plastids. In: Bock R. (eds) Cell and Molecular Biology of Plastids. Topics in Current Genetics, vol 19. Springer, Berlin, Heidelberg

Carrión, C. A., Costa, M. L., Martínez, D. E., Mohr, C., Humbeck, K., & Guiamet, J. J. (2013). In vivo inhibition of cysteine proteases provides evidence for the involvement of "senescence-associated vacuoles" in chloroplast protein degradation during dark-induced senescence of tobacco leaves. *Journal of Experimental Botany*, *64*(16), 4967–4980. https://doi.org/10.1093/jxb/ert285

Chen, M., Choi, Y., Voytas, D. F., & Rodermel, S. (2000). Mutations in the

Arabidopsis VAR2 locus cause leaf variegation due to the loss of a chloroplast FtsH protease. *Plant Journal*, *22*(4), 303–313. https://doi.org/10.1046/j.1365-313X.2000.00738.x

Colombo, M., Tadini, L., Peracchio, C., Ferrari, R., & Pesaresi, P. (2016). GUN1, a Jack-Of-All-Trades in Chloroplast Protein Homeostasis and Signaling. *Frontiers in Plant Science*, *7*(September). https://doi.org/10.3389/fpls.2016.01427

Cottage, A., Mott, E. K., Kempster, J. A., & Gray, J. C. (2010). The Arabidopsis plastid-signalling mutant gun1 (genomes uncoupled1) shows altered sensitivity to sucrose and abscisic acid and alterations in early seedling development. *Journal of Experimental Botany*, *61*(13), 3773–3786. https://doi.org/10.1093/jxb/erq186

Cottage A.J. et al. (2008) *GUN1 (GENOMES UNCOUPLED1)* Encodes a Pentatricopeptide Repeat (PPR) Protein Involved in Plastid Protein Synthesis-Responsive Retrograde Signaling to the Nucleus. In: Allen J.F., Gantt E., Golbeck J.H., Osmond B. (eds) Photosynthesis. Energy from the Sun. Springer, Dordrecht

Cushing, D. A., Forsthoefel, N. R., Gestaut, D. R., & Vernon, D. M. (2005). Arabidopsis emb175 and other ppr knockout mutants reveal essential roles for pentatricopeptide repeat (PPR) proteins in plant embryogenesis. *Planta*, *221*(3), 424–436. https://doi.org/10.1007/s00425-004-1452-x

De Santis-Maciossek, G., Kofer, W., Bock, A., Schoch, S., Maier, R. M., Wanner, G., … Herrmann, R. G. (1999). Targeted disruption of the plastid RNA polymerase genes *rpoA, B* and *C1*: Molecular biology, biochemistry and ultrastructure. *Plant Journal*, *18*(5), 477–489. https://doi.org/10.1046/j.1365-313X.1999.00473.x

Demarsy, E., Courtois, F., Azevedo, J., Buhot, L., & Lerbs-mache, S. (2006). Building Up of the Plastid Transcriptional Machinery during Germination and Early Plant Development 1, *142*(November), 993–1003. https://doi.org/10.1104/pp.106.085043

Demarsy, E., Lakshmanan, A. M., & Kessler, F. (2014). Border control: selectivity of chloroplast protein import and regulation at the TOC-complex. *Frontiers in Plant Science*, *5*(September), 1–10. https://doi.org/10.3389/fpls.2014.00483

Díaz, M. G., Hernández-Verdeja, T., Kremnev, D., Crawford, T., Dubreuil, C., & Strand, Å. (2018). Redox regulation of PEP activity during seedling establishment in Arabidopsis thaliana. *Nature Communications*, *9*(1). https://doi.org/10.1038/s41467-017-02468-2

Dogra, V., Duan, J., Lee, K. P., Lv, S., Liu, R., & Kim, C. (2017). FtsH2-Dependent Proteolysis of EXECUTER1 Is Essential in Mediating Singlet Oxygen-Triggered Retrograde Signaling in Arabidopsis thaliana. *Frontiers in Plant Science*, *8*(June), 1–7. https://doi.org/10.3389/fpls.2017.01145

Drescher, A., Stephanie, R., Calsa, T., Carrer, H., & Bock, R. (2000). The two largest chloroplast genome-encoded open reading frames of higher plants are essential genes. *Plant Journal*, *22*(2), 97–104. https://doi.org/10.1046/j.1365-313X.2000.00722.x

Endow, J. K., Singhal, R., Fernandez, D. E., & Inoue, K. (2015). Chaperone-assisted post-translational transport of plastidic type i signal peptidase 1. *Journal of Biological Chemistry*, *290*(48), 28778–28791. https://doi.org/10.1074/jbc.M115.684829

Fauser, F., Schiml, S., & Puchta, H. (2014). Both CRISPR/Cas-based nucleases and nickases can be used efficiently for genome engineering in Arabidopsis thaliana. *Plant Journal*, *79*(2), 348–359. https://doi.org/10.1111/tpj.12554

Flores-Pérez, Ú., Bédard, J., Tanabe, N., Lymperopoulos, P., Clarke, A. K., & Jarvis, P. (2016). Functional Analysis of the Hsp93/ClpC Chaperone at the Chloroplast Envelope. *Plant Physiology*, *170*(1), 147–162. https://doi.org/10.1104/pp.15.01538

Flores-Pérez, Ú., & Jarvis, P. (2013). Molecular chaperone involvement in chloroplast protein import. *Biochimica et Biophysica Acta - Molecular Cell Research*, *1833*(2), 332–340. https://doi.org/10.1016/j.bbamcr.2012.03.019

Gao, Z.-P., Yu, Q.-B., Zhao, T.-T., Ma, Q., Chen, G.-X., & Yang, Z.-N. (2011). A Functional Component of the Transcriptionally Active Chromosome Complex, Arabidopsis pTAC14, Interacts with pTAC12/HEMERA and Regulates Plastid Gene Expression. *Plant Physiology*, *157*(4), 1733–1745. https://doi.org/10.1104/pp.111.184762

Gray, J.C., Sornarajah, R., Zabron, A.A., Duckett, C.M., and Khan, M.S. (1995). Chloroplast control of nuclear gene expres- sion. In Photosynthesis: From Light to Biosphere, Vol. 3, P. Mathis, ed (Dordrecht, The Netherlands: Kluwer Academic Pub- lishers), pp. 543–550.

Hajdukiewicz, P. T. J., Allison, L. A., & Maliga, P. (1997). The two RNA polymerases encoded by the nuclear and the plastid compartments transcribe distinct groups of genes in tobacco plastids. *EMBO Journal*, *16*(13), 4041–4048. https://doi.org/10.1093/emboj/16.13.4041

Hasan, M., Ma, F., Prodhan, Z., Li, F., Shen, H., Chen, Y., & Wang, X. (2018). Molecular and Physio-Biochemical Characterization of Cotton Species for Assessing Drought Stress Tolerance. *International Journal of Molecular Sciences*, *19*(9), 2636. https://doi.org/10.3390/ijms19092636

Hedtke, B., Legen, J., Weihe, A., Herrmann, R. G., & Börner, T. (2002). Six active phage-type RNA polymerase genes in Nicotiana tabacum. *Plant Journal*, *30*(6), 625–637. https://doi.org/10.1046/j.1365-313X.2002.01318.x

Huang, P.-K., Chan, P.-T., Su, P.-H., Chen, L.-J., & Li, H. (2016). Chloroplast

Hsp93 Directly Binds to Transit Peptides at an Early Stage of the Preprotein Import Process. *Plant Physiology*, *170*(2), 857–866. https://doi.org/10.1104/pp.15.01830

Inoue, H., Li, M., & Schnell, D. J. (2013). An essential role for chloroplast heat shock protein 90 (Hsp90C) in protein import into chloroplasts. *Proceedings of the National Academy of Sciences*, *110*(8), 3173–3178. https://doi.org/10.1073/pnas.1219229110

Ishida, H., Izumi, M., Wada, S., & Makino, A. (2014). Roles of autophagy in chloroplast recycling. *Biochimica et Biophysica Acta - Bioenergetics*, *1837*(4), 512–521. https://doi.org/10.1016/j.bbabio.2013.11.009

Ishizaki, Y., Tsunoyama, Y., Hatano, K., Ando, K., Kato, K., Shinmyo, A., … Takeba, G. (2005). A nuclear-encoded sigma factor , Arabidopsis SIG6 , recognizes sigma-70 type chloroplast promoters and regulates early chloroplast development in cotyledons, 133–144. https://doi.org/10.1111/j.1365-313X.2005.02362.x

Islam, F., Ali, B., Wang, J., Farooq, M. A., Gill, R. A., Ali, S., … Zhou, W. (2016). Combined herbicide and saline stress differentially modulates hormonal regulation and antioxidant defense system in Oryza sativa cultivars. *Plant Physiology and Biochemistry*, *107*, 82–95. https://doi.org/10.1016/j.plaphy.2016.05.027

Izumi, M., Ishida, H., Nakamura, S., & Hidema, J. (2017). Entire Photodamaged Chloroplasts Are Transported to the Central Vacuole by Autophagy. *The Plant Cell*, *29*(2), 377–394. https://doi.org/10.1105/tpc.16.00637

Izumi, M., & Nakamura, S. (2018). Chloroplast protein turnover: The influence of extraplastidic processes, including autophagy. *International Journal of Molecular Sciences*, *19*(3). https://doi.org/10.3390/ijms19030828

Izumi, M., Wada, S., Makino, A., & Ishida, H. (2010). The Autophagic Degradation of Chloroplasts via Rubisco-Containing Bodies Is Specifically Linked to Leaf Carbon Status But Not Nitrogen Status in Arabidopsis. *Plant Physiology*, *154*(3), 1196–1209. https://doi.org/10.1104/pp.110.158519

Jackson-Constan, D., & Keegstra, K. (2001). Arabidopsis genes encoding components of the chloroplastic protein import apparatus. *Plant Physiology*, *125*(4), 1567–1576. https://doi.org/10.1104/pp.125.4.1567

Järvi, S., Suorsa, M., Paakkarinen, V., & Aro, E.-M. (2011). Optimized native gel systems for separation of thylakoid protein complexes: novel super- and mega-complexes. *Biochemical Journal*, *439*(2), 207–214. https://doi.org/10.1042/BJ20102155

Järvi, S., Suorsa, M., Tadini, L., Ivanauskaite, A., Rantala, S., Allahverdiyeva, Y., … Aro, E.-M. (2016). FtsH facilitates proper biosynthesis of photosystem I in Arabidopsis thaliana. *Plant Physiology*, *171*(June),

pp.00200.2016. https://doi.org/10.1104/pp.16.00200
Jarvis, P., & López-Juez, E. (2013). Biogenesis and homeostasis of chloroplasts and other plastids. *Nature Reviews Molecular Cell Biology*, *14*(12), 787–802. https://doi.org/10.1038/nrm3702
Jensen, P. E., & Leister, D. (2014). Chloroplast evolution, structure and functions. *F1000Prime Reports*, *6*(June), 1–14. https://doi.org/10.12703/P6-40
Kakizaki, T., Matsumura, H., Nakayama, K., Che, F.-S., Terauchi, R., & Inaba, T. (2009). Coordination of Plastid Protein Import and Nuclear Gene Expression by Plastid-to-Nucleus Retrograde Signaling. *Plant Physiology*, *151*(3), 1339–1353. https://doi.org/10.1104/pp.109.145987
Kangasjärvi, S., Lepistö, A., Hännikäinen, K., Piippo, M., Luomala, E.-M., Aro, E.-M., & Rintamäki, E. (2008). Diverse roles for chloroplast stromal and thylakoid-bound ascorbate peroxidases in plant stress responses. *Biochemical Journal*, *412*(2), 275–285. https://doi.org/10.1042/BJ20080030
Kato, Y., Miura, E., Ido, K., Ifuku, K., & Sakamoto, W. (2009). The Variegated Mutants Lacking Chloroplastic FtsHs Are Defective in D1 Degradation and Accumulate Reactive Oxygen Species. *Plant Physiology*, *151*(4), 1790–1801. https://doi.org/10.1104/pp.109.146589
Kato, Y., & Sakamoto, W. (2018). FtsH Protease in the Thylakoid Membrane: Physiological Functions and the Regulation of Protease Activity. *Frontiers in Plant Science*, *9*(June), 1–8. https://doi.org/10.3389/fpls.2018.00855
Kikuchi, S., Bédard, J., Hirano, M., Hirabayashi, Y., Oishi, M., Imai, M., … Nakai, M. (2013). Uncovering the protein translocon at the chloroplast inner envelope membrane. *Science*, *339*(6119), 571–574. https://doi.org/10.1126/science.1229262
Kikuchi, S., Hirohashi, T., & Nakai, M. (2006). Characterization of the preprotein translocon at the outer envelope membrane of chloroplasts by blue native PAGE. *Plant and Cell Physiology*, *47*(3), 363–371. https://doi.org/10.1093/pcp/pcj002
Kikuchi, S., Oishi, M., Hirabayashi, Y., Lee, D. W., Hwang, I., & Nakai, M. (2009). A 1-Megadalton Translocation Complex Containing Tic20 and Tic21 Mediates Chloroplast Protein Import at the Inner Envelope Membrane. *The Plant Cell Online*, *21*(6), 1781–1797. https://doi.org/10.1105/tpc.108.063552
Kleine, T., Maier, U. G., & Leister, D. (2009). DNA Transfer from Organelles to the Nucleus: The Idiosyncratic Genetics of Endosymbiosis. *Annual Review of Plant Biology*, *60*(1), 115–138. https://doi.org/10.1146/annurev.arplant.043008.092119
Köhler, D., Helm, S., Agne, B., & Baginsky, S. (2016). Importance of Translocon Subunit Tic56 for rRNA Processing and Chloroplast Ribosome

Assembly. *Plant Physiology*, *172*(4), 2429–2444. https://doi.org/10.1104/pp.16.01393
Koussevitzky, S., Nott, A., Mockler, T. C., Hong, F., Sachetto-martins, G., Surpin, M., … Chory, J. (2007). Multiple Signals from Damaged Chloroplasts Converge on a Common Pathway to Regulate Nuclear Gene Expression. *Plant Biology*, (March), 1–3. https://doi.org/10.1126/science.
Kunst, L. (1998). Preparation of physiologically active chloroplasts from Arabidopsis. *Methods in Molecular Biology (Clifton, N.J.)*, *82*, 43–48.
Larkin, R. M., Alonso, J. M., Ecker, J. R., & Chory, J. (2003). GUN4, a regulator of chlorophyll synthesis and intracellular signaling. *Science*, *299*(5608), 902–906. https://doi.org/10.1126/science.1079978
Lee, D. W., Lee, J., & Hwang, I. (2017). Sorting of nuclear-encoded chloroplast membrane proteins. *Current Opinion in Plant Biology*, *40*, 1–7. https://doi.org/10.1016/j.pbi.2017.06.011
Lee, G. J., & Vierling, E. (2000). A Small Heat Shock Protein Cooperates with Heat Shock Protein 70 Systems to Reactivate a Heat-Denatured Protein. *Plant Physiology*, *122*(1), 189–198. https://doi.org/10.1104/pp.122.1.189
Lee, J., He, K., Stolc, V., Lee, H., Figueroa, P., Gao, Y., … Deng, X. W. (2007). Analysis of Transcription Factor HY5 Genomic Binding Sites Revealed Its Hierarchical Role in Light Regulation of Development. *The Plant Cell Online*, *19*(3), 731–749. https://doi.org/10.1105/tpc.106.047688
Lee, S., Lee, D. W., Lee, Y., Mayer, U., Stierhof, Y.-D., Lee, S., … Hwang, I. (2009). Heat Shock Protein Cognate 70-4 and an E3 Ubiquitin Ligase, CHIP, Mediate Plastid-Destined Precursor Degradation through the Ubiquitin-26S Proteasome System in Arabidopsis. *The Plant Cell*, *21*(12), 3984–4001. https://doi.org/10.1105/tpc.109.071548
Liere, K., Weihe, A., & Börner, T. (2011). The transcription machineries of plant mitochondria and chloroplasts : Composition , function , and regulation. *Journal of Plant Physiology*, *168*(12), 1345–1360. https://doi.org/10.1016/j.jplph.2011.01.005
Lindahl, M., Tabak, S., Cseke, L., Pichersky, E., Andersson, B., & Adam, Z. (1996). Indentification, characterization, and molecular cloning of a homologue of the bacterial FtsH protease in chloroplast of higher plants. *Journal of Biological Chemistry*, *271*(46), 229334–293329.
Ling, Q., Huang, W., Baldwin, A., & Jarvis, P. (2012). Chloroplast biogenesis is regulated by direct action of the ubiquitin-proteasome system. *Science*, *338*(6107), 655–659. https://doi.org/10.1126/science.1225053
Ling, Q., & Jarvis, P. (2015). Regulation of chloroplast protein import by the ubiquitin E3 ligase SP1 is important for stress tolerance in plants. *Current Biology*, *25*(19), 2527–2534. https://doi.org/10.1016/j.cub.2015.08.015
Liu, H. C., Liao, H. T., & Charng, Y. Y. (2011). The role of class A1 heat shock factors (HSFA1s) in response to heat and other stresses in Arabidopsis.

Plant, Cell and Environment, *34*(5), 738–751. https://doi.org/10.1111/j.1365-3040.2011.02278.x

Llamas, E., Pulido, P., & Rodriguez-Concepcion, M. (2017). Interference with plastome gene expression and Clp protease activity in Arabidopsis triggers a chloroplast unfolded protein response to restore protein homeostasis. *PLoS Genetics*, *13*(9), 1–27. https://doi.org/10.1371/journal.pgen.1007022

Madueno, F. (1993). Newly Imported Rieske Iron-Sulfur Protein Associates with Both Cpn60 and Hsp70 in the Chloroplast Stroma. *The Plant Cell Online*, *5*(12), 1865–1876. https://doi.org/10.1105/tpc.5.12.1865

Marsoni, M., Bracale, M., Espen, L., Prinsi, B., Negri, A. S., & Vannini, C. (2008). Proteomic analysis of somatic embryogenesis in Vitis vinifera. *Plant Cell Reports*, *27*(2), 347–356. https://doi.org/10.1007/s00299-007-0438-0

Martínez-García, J. F., Monte, E., & Quail, P. H. (1999). A simple, rapid and quantitative method for preparing Arabidopsis protein extracts for immunoblot analysis. *Plant Journal*, *20*(2), 251–257. https://doi.org/10.1046/j.1365-313X.1999.00579.x

Melonek, J., Oetke, S., & Krupinska, K. (2016). Multifunctionality of plastid nucleoids as revealed by proteome analyses. *Biochimica et Biophysica Acta - Proteins and Proteomics*, *1864*(8), 1016–1038. https://doi.org/10.1016/j.bbapap.2016.03.009

Meurer, J., Lezhneva, L., Amann, K., Godel, M., Bezhani, S., Sherameti, I., & Oelmuller, R. (2002). A peptide chain release factor 2 affects the stability of UGA-containing transcripts in Arabidopsis chloroplasts. *Plant Cell*, *14*(12), 3255–3269. https://doi.org/10.1105/tpc.006809

Michaeli, S., Honig, A., Levanony, H., Peled-Zehavi, H., & Galili, G. (2014). Arabidopsis ATG8-INTERACTING PROTEIN1 Is Involved in Autophagy-Dependent Vesicular Trafficking of Plastid Proteins to the Vacuole. *The Plant Cell*, *26*(10), 4084–4101. https://doi.org/10.1105/tpc.114.129999

Miura, E., Kato, Y., Matsushima, R., Albrecht, V., Laalami, S., & Sakamoto, W. (2007). The Balance between Protein Synthesis and Degradation in Chloroplasts Determines Leaf Variegation in Arabidopsis yellow variegated Mutants. *The Plant Cell Online*, *19*(4), 1313–1328. https://doi.org/10.1105/tpc.106.049270

Mochizuki, N., Brusslan, J. A., Larkin, R., Nagatani, A., & Chory, J. (2001). Arabidopsis genomes uncoupled 5 (GUN5) mutant reveals the involvement of Mg-chelatase H subunit in plastid-to-nucleus signal transduction. *Proceedings of the National Academy of Sciences*, *98*(4), 2053–2058. https://doi.org/10.1073/pnas.98.4.2053

Moreira, D., & Philippe, H. (1999). Smr: A bacterial and eukaryotic homologue of the C-terminal region of the MutS2 family. *Trends in Biochemical*

Sciences, *24*(8), 298–300. https://doi.org/10.1016/S0968-0004(99)01419-X

Murashige, T., & Skoog, F. (1962). A Revised Medium for Rapid Growth and Bio Assays with Tobacco Tissue Cultures. *Physiologia Plantarum*, *15*(3), 473–497. https://doi.org/10.1111/j.1399-3054.1962.tb08052.x

Myouga, F., Hosoda, C., Umezawa, T., Iizumi, H., Kuromori, T., Motohashi, R., … Shinozaki, K. (2008). A Heterocomplex of Iron Superoxide Dismutases Defends Chloroplast Nucleoids against Oxidative Stress and Is Essential for Chloroplast Development in Arabidopsis. *The Plant Cell Online*, *20*(11), 3148–3162. https://doi.org/10.1105/tpc.108.061341

Nakai, M. (2015a). The TIC complex uncovered: The alternative view on the molecular mechanism of protein translocation across the inner envelope membrane of chloroplasts. *Biochimica et Biophysica Acta*, *1847*(9), 957–967. https://doi.org/10.1016/j.bbabio.2015.02.011

Nakai, M. (2015b). YCF1: A Green TIC: Response to the de Vries et al. Commentary: Figure 1. *The Plant Cell*, *27*(7), 1834–1838. https://doi.org/10.1105/tpc.15.00363

Nakai, M. (2018). New perspectives on chloroplast protein import. *Plant and Cell Physiology*, *59*(6), 1111–1119. https://doi.org/10.1093/pcp/pcy083

Nakatogawa, H., Suzuki, K., Kamada, Y., & Ohsumi, Y. (2009). Dynamics and diversity in autophagy mechanisms: Lessons from yeast. *Nature Reviews Molecular Cell Biology*, *10*(7), 458–467. https://doi.org/10.1038/nrm2708

Nishizawa-Yokoi, A., Nosaka, R., Hayashi, H., Tainaka, H., Maruta, T., Tamoi, M., … Shigeoka, S. (2011). HsfA1d and HsfA1e involved in the transcriptional regulation of hsfa2 function as key regulators for the hsf signaling network in response to environmental stress. *Plant and Cell Physiology*, *52*(5), 933–945. https://doi.org/10.1093/pcp/pcr045

Nott, A., Jung, H.-S., Koussevitzky, S., & Chory, J. (2006). Plastid-To-Nucleus Retrograde Signaling. *Annual Review of Plant Biology*, *57*(1), 739–759. https://doi.org/10.1146/annurev.arplant.57.032905.105310

Oelmüller, R., Levitan, I., Bergfeld, R., Rajasekhar, V. K., & Mohr, H. (1986). Expression of nuclear genes as affected by treatments acting on the plastids. *Planta*, *168*(4), 482–492. https://doi.org/10.1007/BF00392267

Olinares, P. D. B., Ponnala, L., & van Wijk, K. J. (2010). Megadalton Complexes in the Chloroplast Stroma of *Arabidopsis thaliana* Characterized by Size Exclusion Chromatography, Mass Spectrometry, and Hierarchical Clustering. *Molecular & Cellular Proteomics*, *9*(7), 1594–1615. https://doi.org/10.1074/mcp.M000038-MCP201

Paieri, F., Tadini, L., Manavski, N., Kleine, T., Ferrari, R., Morandini, P. A., … Leister, D. (2017). The DEAD-box RNA helicase RH50 is a 23S-4.5S rRNA maturation factor that functionally overlaps with the plastid signaling factor GUN1. *Plant Physiology*, pp.01545.2017.

https://doi.org/10.1104/pp.17.01545
Paila, Y. D., Richardson, L. G. L., & Schnell, D. J. (2015). New insights into the mechanism of chloroplast protein import and its integration with protein quality control, organelle biogenesis and development. *Journal of Molecular Biology*, *427*(5), 1038–1060. https://doi.org/10.1016/j.jmb.2014.08.016
Peng, L., & Shikanai, T. (2011). Supercomplex Formation with Photosystem I Is Required for the Stabilization of the Chloroplast NADH Dehydrogenase-Like Complex in Arabidopsis. *Plant Physiology*, *155*(4), 1629–1639. https://doi.org/10.1104/pp.110.171264
Perea-Resa, C., Rodríguez-Milla, M. A., Iniesto, E., Rubio, V., & Salinas, J. (2017). Prefoldins Negatively Regulate Cold Acclimation in Arabidopsis thaliana by Promoting Nuclear Proteasome-Mediated HY5 Degradation. *Molecular Plant*, *10*(6), 791–804. https://doi.org/10.1016/j.molp.2017.03.012
Pesaresi, P., Hertle, A., Pribil, M., Kleine, T., Wagner, R., Strissel, H., … Leister, D. (2009). Arabidopsis STN7 Kinase Provides a Link between Short- and Long-Term Photosynthetic Acclimation. *The Plant Cell Online*, *21*(8), 2402–2423. https://doi.org/10.1105/tpc.108.064964
Pesaresi, P., Varotto, C., Meurer, J., Jahns, P., Salamini, F., & Leister, D. (2001). Knock-out of the plastid ribosomal protein L11 in Arabidopsis: Effects on mRNA translation and photosynthesis. *Plant Journal*, *27*(3), 179–189. https://doi.org/10.1046/j.1365-313X.2001.01076.x
Pfalz, J. (2006). pTAC2, -6, and -12 Are Components of the Transcriptionally Active Plastid Chromosome That Are Required for Plastid Gene Expression. *The Plant Cell Online*, *18*(1), 176–197. https://doi.org/10.1105/tpc.105.036392
Pogson, B. J., Woo, N. S., Förster, B., & Small, I. D. (2008). Plastid signalling to the nucleus and beyond. *Trends in Plant Science*, *13*(11), 602–609. https://doi.org/10.1016/j.tplants.2008.08.008
Ramos-Vega, M., Guevara-García, A., Llamas, E., Sánchez-León, N., Olmedo-Monfil, V., Vielle-Calzada, J. P., & León, P. (2015). Functional analysis of the Arabidopsis thaliana CHLOROPLAST BIOGENESIS 19 pentatricopeptide repeat editing protein. *New Phytologist*, *208*(2), 430–441. https://doi.org/10.1111/nph.13468
Ramundo, S., Casero, D., Muhlhaus, T., Hemme, D., Sommer, F., Crevecoeur, M., … Rochaix, J. D. (2014). Conditional Depletion of the Chlamydomonas Chloroplast ClpP Protease Activates Nuclear Genes Involved in Autophagy and Plastid Protein Quality Control. *The Plant Cell*, *26*(5), 2201–2222. https://doi.org/10.1105/tpc.114.124842
Ramundo, S., Rahire, M., Schaad, O., & Rochaix, J.-D. (2013). Repression of Essential Chloroplast Genes Reveals New Signaling Pathways and

Regulatory Feedback Loops in *Chlamydomonas*. *The Plant Cell*, *25*(1), 167–186. https://doi.org/10.1105/tpc.112.103051

Robles, P., Micol, J. L., & Quesada, V. (2012). Arabidopsis MDA1, a nuclear-encoded protein, functions in chloroplast development and abiotic stress responses. *PLoS ONE*, *7*(8). https://doi.org/10.1371/journal.pone.0042924

Romani, I., Tadini, L., Rossi, F., Masiero, S., Pribil, M., Jahns, P., … Pesaresi, P. (2012). Versatile roles of Arabidopsis plastid ribosomal proteins in plant growth and development. *Plant Journal*, *72*(6), 922–934. https://doi.org/10.1111/tpj.12000

Ruckle, M. E., DeMarco, S. M., & Larkin, R. M. (2007). Plastid Signals Remodel Light Signaling Networks and Are Essential for Efficient Chloroplast Biogenesis in Arabidopsis. *The Plant Cell Online*, *19*(12), 3944–3960. https://doi.org/10.1105/tpc.107.054312

Sakamoto, W. (2003). Coordinated Regulation and Complex Formation of YELLOW VARIEGATED1 and YELLOW VARIEGATED2, Chloroplastic FtsH Metalloproteases Involved in the Repair Cycle of Photosystem II in Arabidopsis Thylakoid Membranes. *The Plant Cell Online*, *15*(12), 2843–2855. https://doi.org/10.1105/tpc.017319

Sakamoto, W., Tamura, T., Hanba-Tomita, Y., Sodmergen, & Murata, M. (2002). The VAR1 locus of Arabidopis encodes a choloroplastic FtsH and is responsible for leaf variegation in the mutant alleles. *Genes to Cells*, *7*(8), 769–780. https://doi.org/10.1046/j.1365-2443.2002.00558.x

Sakamoto, W., Uno, Y., Zhang, Q., Miura, E., Kato, Y., & Sodmergen. (2009). Arrested differentiation of proplastids into chloroplasts in variegated leaves characterized by plastid ultrastructure and nucleoid morphology. *Plant and Cell Physiology*, *50*(12), 2069–2083. https://doi.org/10.1093/pcp/pcp127

Sato, S., Nakamura, Y., Kaneko, T., Asamizu, E., & Tabata, S. (1999). Complete Structure of the Chloroplast Genome of thaliana. *DNA Research*, *290*, 283–290. https://doi.org/10.1093/dnares/6.5.283

Schägger, C., & von Jagow, G. (1987). Tricine-sodium dodecyl sulfate-polyacrylamide gel electrophoresis for the separation of proteins in the range from 1 to 100 kDa. *Analytical Biochemistry*, *166*(2), 368–379. https://doi.org/10.1016/0003-2697(87)90587-2

Schägger, H., & von Jagow, G. (1991). Blue native electrophoresis for isolation of membrane protein complexes in enzymatically active form. *Analytical Biochemistry*, *199*(2), 223–231. https://doi.org/10.1016/0003-2697(91)90094-A

Schramm, F., Ganguli, A., Kiehlmann, E., Englich, G., Walch, D., & Von Koskull-Döring, P. (2006). The heat stress transcription factor HsfA2 serves as a regulatory amplifier of a subset of genes in the heat stress response in Arabidopsis. *Plant Molecular Biology*, *60*(5), 759–772.

https://doi.org/10.1007/s11103-005-5750-x
Schuhmann, H., & Adamska, I. (2012). Deg proteases and their role in protein quality control and processing in different subcellular compartments of the plant cell. *Physiologia Plantarum*, *145*(1), 224–234. https://doi.org/10.1111/j.1399-3054.2011.01533.x
Shao, R. X., Xin, L. F., Zheng, H. F., Li, L. L., Ran, W. L., Mao, J., & Yang, Q. H. (2016). Changes in chloroplast ultrastructure in leaves of drought-stressed maize inbred lines. *Photosynthetica*, *54*(1), 74–80. https://doi.org/10.1007/s11099-015-0158-6
Srivastava, A. K., Senapati, D., Srivastava, A. K., Chakraborty, M., Gangappa, S. N., & Chattopadhyay, S. (2015). SHW1 Interacts with HY5 and COP1, and Promotes COP1-mediated Degradation of HY5 During Arabidopsis Seedling Development. *Plant Physiology*, pp.01184.2015. https://doi.org/10.1104/pp.15.01184
Su, P.-H., & Li, H. -m. (2008). Arabidopsis Stromal 70-kD Heat Shock Proteins Are Essential for Plant Development and Important for Thermotolerance of Germinating Seeds. *Plant Physiology*, *146*(3), 1231–1241. https://doi.org/10.1104/pp.107.114496
Su, P.-H., & Li, H. -m. (2010). Stromal Hsp70 Is Important for Protein Translocation into Pea and Arabidopsis Chloroplasts. *The Plant Cell Online*, *22*(5), 1516–1531. https://doi.org/10.1105/tpc.109.071415
Susek, R. E., Ausubel, F. M., & Chory, J. (1993). Signal transduction mutants of arabidopsis uncouple nuclear CAB and RBCS gene expression from chloroplast development. *Cell*, *74*(5), 787–799. https://doi.org/10.1016/0092-8674(93)90459-4
Suzuki, K., Nakanishi, H., Bower, J., Yoder, D. W., Osteryoung, K. W., & Miyagishima, S. Y. (2009). Plastid chaperonin proteins Cpn60?? and Cpn60 are required for plastid division in Arabidopsis thaliana. *BMC Plant Biology*, *9*. https://doi.org/10.1186/1471-2229-9-38
Svozil, J., Hirsch-Hoffmann, M., Dudler, R., Gruissem, W., & Baerenfaller, K. (2014). Protein Abundance Changes and Ubiquitylation Targets Identified after Inhibition of the Proteasome with Syringolin A. *Molecular & Cellular Proteomics*, *13*(6), 1523–1536. https://doi.org/10.1074/mcp.M113.036269
Tadini, L., Pesaresi, P., Kleine, T., Rossi, F., Guljamow, A., Sommer, F., … Leister, D. (2016). GUN1 Controls Accumulation of the Plastid Ribosomal Protein S1 at the Protein Level and Interacts with Proteins Involved in Plastid Protein Homeostasis. *Plant Physiology*, *170*(3), 1817–1830. https://doi.org/10.1104/pp.15.02033
Tokumaru, M., Adachi, F., Toda, M., Ito-Inaba, Y., Yazu, F., Hirosawa, Y., … Inaba, T. (2017). Ubiquitin-Proteasome Dependent Regulation of the GOLDEN2-LIKE 1 Transcription Factor in Response to Plastid Signals.

Plant Physiology, *173*(1), 524–535. https://doi.org/10.1104/pp.16.01546
Trotta, A., Suorsa, M., Rantala, M., Lundin, B., & Aro, E. M. (2016). Serine and threonine residues of plant STN7 kinase are differentially phosphorylated upon changing light conditions and specifically influence the activity and stability of the kinase. *The Plant Journal : For Cell and Molecular Biology*, *87*(5), 484–494. https://doi.org/10.1111/tpj.13213
Tsugeki, R., & Nishimura, M. (1993). Interaction of homologues of Hsp70 and Cpn60 with ferredoxin-NADP+ reductase upon its import into chloroplasts. *FEBS Letters*, *320*(3), 198–202. https://doi.org/10.1016/0014-5793(93)80585-I
Wada, S., Ishida, H., Izumi, M., Yoshimoto, K., Ohsumi, Y., Mae, T., & Makino, A. (2008). Autophagy Plays a Role in Chloroplast Degradation during Senescence in Individually Darkened Leaves. *Plant Physiology*, *149*(2), 885–893. https://doi.org/10.1104/pp.108.130013
Wagner, R., Aigner, H., & Funk, C. (2012). FtsH proteases located in the plant chloroplast. *Physiologia Plantarum*, *145*(1), 203–214. https://doi.org/10.1111/j.1399-3054.2011.01548.x
Wang, F., Girard-bascou, J., & Vitry, C. De. (2014). Thylakoid FtsH Protease Contributes to Photosystem II and Cytochrome b 6 f Remodeling in Chlamydomonas reinhardtii under Stress Conditions, 1–19. https://doi.org/10.1105/tpc.113.120113
Wang, H., Lu, Y., Jiang, T., Berg, H., Li, C., & Xia, Y. (2013). The Arabidopsis U-box/ARM repeat E3 ligase AtPUB4 influences growth and degeneration of tapetal cells, and its mutation leads to conditional male sterility. *Plant Journal*, *74*(3), 511–523. https://doi.org/10.1111/tpj.12146
Wang, L., Kim, C., Xu, X., Piskurewicz, U., Dogra, V., Singh, S., … Apel, K. (2016). Singlet oxygen- and EXECUTER1-mediated signaling is initiated in grana margins and depends on the protease FtsH2. *Proceedings of the National Academy of Sciences*, *113*(26), E3792–E3800. https://doi.org/10.1073/pnas.1603562113
Wang, S., & Blumwald, E. (2014). Stress-Induced Chloroplast Degradation in *Arabidopsis* Is Regulated via a Process Independent of Autophagy and Senescence-Associated Vacuoles. *The Plant Cell Online*, *26*(12), 4875–4888. https://doi.org/10.1105/tpc.114.133116
Wang, W., Vinocur, B., Shoseyov, O., & Altman, A. (2004). Role of plant heat-shock proteins and molecular chaperones in the abiotic stress response. *Trends in Plant Science*, *9*(5), 244–252. https://doi.org/10.1016/j.tplants.2004.03.006
Woodson, J. D. (2016). Chloroplast quality control - balancing energy production and stress. *The New Phytologist*, *212*(1), 36–41. https://doi.org/10.1111/nph.14134
Woodson, J. D., & Chory, J. (2008). Coordination of gene expression between

organellar and nuclear genomes. *Nature Reviews Genetics*, *9*(5), 383–395. https://doi.org/10.1038/nrg2348

Woodson, J. D., Joens, M. S., Sinson, A. B., Gilkerson, J., Salomé, P. A., Weigel, D., … Chory, J. (2015). Ubiquitin facilitates a quality-control pathway that removes damaged chloroplasts. *Science*, *350*(6259), 450–454. https://doi.org/10.1126/science.aac7444

Woodson, J. D., Perez-ruiz, J. M., & Chory, J. (2011). Supplemental Information Heme Synthesis by Plastid Ferrochelatase I Regulates Nuclear Gene Expression in Plants. *Current Biology*, *21*(10), 897–903. https://doi.org/10.1016/j.cub.2011.04.004.Woodson

Woodson, J. D., Perez-Ruiz, J. M., Schmitz, R. J., Ecker, J. R., & Chory, J. (2013). Sigma factor-mediated plastid retrograde signals control nuclear gene expression. *Plant Journal*, *73*(1), 1–13. https://doi.org/10.1111/tpj.12011

Wu, G.-Z., Chalvin, C., Hoelscher, M. P., Meyer, E. H., Wu, X. N., & Bock, R. (2018). Control of Retrograde Signaling by Rapid Turnover of GENOMES UNCOUPLED 1. *Plant Physiology*, pp.00009.2018. https://doi.org/10.1104/pp.18.00009

Xing, H. L., Dong, L., Wang, Z. P., Zhang, H. Y., Han, C. Y., Liu, B., … Chen, Q. J. (2014). A CRISPR/Cas9 toolkit for multiplex genome editing in plants. *BMC Plant Biology*, *14*(1), 1–12. https://doi.org/10.1186/s12870-014-0327-y

Yoshida, T., Ohama, N., Nakajima, J., Kidokoro, S., Mizoi, J., Nakashima, K., … Yamaguchi-Shinozaki, K. (2011). Arabidopsis HsfA1 transcription factors function as the main positive regulators in heat shock-responsive gene expression. *Molecular Genetics and Genomics*, *286*(5–6), 321–332. https://doi.org/10.1007/s00438-011-0647-7

Yoshimoto, K. (2004). Processing of ATG8s, Ubiquitin-Like Proteins, and Their Deconjugation by ATG4s Are Essential for Plant Autophagy. *The Plant Cell Online*, *16*(11), 2967–2983. https://doi.org/10.1105/tpc.104.025395

Yu, F., Park, S., & Rodermel, S. R. (2004). The Arabidopsis FtsH metalloprotease gene family: Interchangeability of subunits in chloroplast oligomeric complexes. *Plant Journal*, *37*(6), 864–876. https://doi.org/10.1111/j.1365-313X.2003.02014.x

Yu, F., Park, S., & Rodermel, S. R. (2005). Functional redundancy of AtFtsH metalloproteases in thylakoid membrane complexes. *Plant Physiology*, *138*(4), 1957–1966. https://doi.org/10.1104/pp.105.061234

Zaltsman, A. (2005). Two Types of FtsH Protease Subunits Are Required for Chloroplast Biogenesis and Photosystem II Repair in Arabidopsis. *The Plant Cell Online*, *17*(10), 2782–2790. https://doi.org/10.1105/tpc.105.035071

Zhao, X., Huang, J., & Chory, J. (2018). Genome uncoupled 1 mutants are hypersensitive to norflurazon and lincomycin. *Plant Physiology*, pp.00772.2018. https://doi.org/10.1104/pp.18.00772

Zhong, L., Zhou, W., Wang, H., Ding, S., Lu, Q., Wen, X., … Lu, C. (2013). Chloroplast Small Heat Shock Protein HSP21 Interacts with Plastid Nucleoid Protein pTAC5 and Is Essential for Chloroplast Development in Arabidopsis under Heat Stress. *The Plant Cell*, *25*(8), 2925–2943. https://doi.org/10.1105/tpc.113.111229

7. Acknowledgments

Many thanks to my supervisor Prof. Paolo Pesaresi, for giving me the opportunity to work in his research group and on this fascinating project of broad views

To the members of my Ph.D. commission: Prof. Eva Mari Aro, Prof. Martin Kater, Prof. Roberto Barbato; for all the suggestions and useful tips, they helped me grow as a scientist

To my Tutor and Post-doc, Dr. Luca Tadini, for working with me shoulder to shoulder on this project

To my colleagues Dr. Monica Colombo, Dr. Roberto Ferrari

To the Master student Ilaria Mancini

To all the collaborators: Prof. Franco Faoro, Prof Alex Costa, Prof. Bracale Marcella, Prof. Simona Masiero, Post-doc Andrea Trotta, Ph.D. student Azfar Ali Bajwa

Last but not least, thanks to all the members of the Lab (3^{th} and 5^{th} floors, Department of Biosciences) for the help and the friendship.

8. Appendices

The manuscript

In order to gave my contribute for writing this review:

Colombo M., Tadini L., Peracchio C., Ferrari R., Pesaresi P. (2016) GUN1, a jack-of-all-trades in chloroplast protein homeostasis and signaling. *Front. Plant Sci.* **7**:1427. doi:10.3389/fpls.2016.01427

i used the following steps:

Firstly , I took part in academic debate in order to glean valuable insights as to how best organise and present the findings and put them across as clearly as possible

Secondly, I helped in the design of tables and figures

Finally, I carried out the necessary corrections and concluded by adding my comments

frontiers in Plant Science

REVIEW
published: 22 September 2016
doi: 10.3389/fpls.2016.01427

GUN1, a Jack-Of-All-Trades in Chloroplast Protein Homeostasis and Signaling

Monica Colombo[1], *Luca Tadini*[2], *Carlotta Peracchio*[2], *Roberto Ferrari*[2] *and Paolo Pesaresi*[2]*

[1] Centro Ricerca e Innovazione, Fondazione Edmund Mach, San Michele all'Adige, Italy, [2] Dipartimento di Bioscienze, Università degli Studi di Milano, Milan, Italy

The *GENOMES UNCOUPLED 1 (GUN1)* gene has been reported to encode a chloroplast-localized pentatricopeptide-repeat protein, which acts to integrate multiple indicators of plastid developmental stage and altered plastid function, as part of chloroplast-to-nucleus retrograde communication. However, the molecular mechanisms underlying signal integration by GUN1 have remained elusive, up until the recent identification of a set of GUN1-interacting proteins, by co-immunoprecipitation and mass-spectrometric analyses, as well as protein–protein interaction assays. Here, we review the molecular functions of the different GUN1 partners and propose a major role for GUN1 as coordinator of chloroplast translation, protein import, and protein degradation. This regulatory role is implemented through proteins that, in most cases, are part of multimeric protein complexes and whose precise functions vary depending on their association states. Within this framework, GUN1 may act as a platform to promote specific functions by bringing the interacting enzymes into close proximity with their substrates, or may inhibit processes by sequestering particular pools of specific interactors. Furthermore, the interactions of GUN1 with enzymes of the tetrapyrrole biosynthesis (TPB) pathway support the involvement of tetrapyrroles as signaling molecules in retrograde communication.

Keywords: nucleoid, GUN1, protein homeostasis, retrograde signaling, biogenic control

OPEN ACCESS

Edited by:
Fiammetta Alagna, Research Council for Agriculture and Agricultural Economy, Italy

Reviewed by:
Lynn Richardson, Michigan State University, USA
Silvia Ramundo, University of California, San Francisco & Carnegie Institution for Science & Howard Hughes Medical Institute, USA

***Correspondence:**
Paolo Pesaresi
paolo.pesaresi@unimi.it

Specialty section:
This article was submitted to Plant Cell Biology, a section of the journal Frontiers in Plant Science

Received: *21 July 2016*
Accepted: *07 September 2016*
Published: *22 September 2016*

Citation:
Colombo M, Tadini L, Peracchio C, Ferrari R and Pesaresi P (2016) GUN1, a Jack-Of-All-Trades in Chloroplast Protein Homeostasis and Signaling. Front. Plant Sci. 7:1427. doi: 10.3389/fpls.2016.01427

INTRODUCTION

Upon illumination, proplastids differentiate into functional chloroplasts in developing photosynthetic tissues of cotyledons, leaves, and stems (Jarvis and López-Juez, 2013). Chloroplast biogenesis also occurs during the growth of young green tissues, as cells expand and mature chloroplasts undergo division by binary fission (Okazaki et al., 2010). This process is characterized macroscopically by rapid greening of the young chloroplast and microscopically by the concomitant formation of thylakoid membranes and the reorganization of nucleoids, i.e., DNA-containing structures without defined boundaries, which differ in number, size, and distribution within plastids at different developmental stages, and harbor the plastid gene expression (PGE) machinery (Pfalz and Pfannschmidt, 2013; Melonek et al., 2016).

At the molecular level, this rather complex biogenic transition is achieved by cytosolic synthesis of chloroplast-targeted proteins, followed by import, assembly, folding, and degradation of unfolded/misfolded proteins (Jarvis and López-Juez, 2013). Indeed, the plastid genome itself (the

plastome) comprises fewer than 100 protein-coding genes, and the vast majority of the 2000–3000 proteins that make up the chloroplast proteome are encoded in the nucleus (Richly and Leister, 2004). In particular, precursor proteins carrying N-terminal transit peptides initially interact with two multiprotein complexes termed Translocon at the outer envelope membrane of chloroplasts (TOC) and Translocon at the inner envelope membrane of chloroplasts (TIC), which facilitate their active transport through the chloroplast envelope, powered by an ATP import motor, consisting of the stromal heat-shock protein 93 (Hsp93), heat-shock protein 70 (Hsp70), and heat-shock protein 90 (Hsp90; Flores-Perez and Jarvis, 2013; Inoue et al., 2013; Shi and Theg, 2013a,b). Upon translocation, proteins are exposed to different proteolytic systems of prokaryotic origin, which are responsible for protein maturation, control of protein abundance, and removal of either misfolded or damaged components. Among these, the stromal protease Clp is a multimeric complex made of chaperones and serine protease subunits, which serve general housekeeping functions. In contrast, the thylakoid-associated FtsH (Filamentous temperature sensitive H) proteases are zinc-containing metalloendopeptidases that have both chaperone and proteolytic functions, and participate in the Photosystem II repair cycle, together with the DEG serine proteases (Kato and Sakamoto, 2010; Van Wijk, 2015).

Besides translation and post-translational processes, chloroplast biogenesis also requires transcriptional coordination of thousands of nuclear genes with the expression of the comparatively few plastid genes in order to meet the needs of the developing chloroplast (Chan et al., 2016; Kleine and Leister, 2016). This is achieved through extensive exchange of information between plastids and the nucleus, for instance, via biogenic retrograde signaling—a system in which developmentally relevant stimuli in plastids induce the accumulation of specific signaling molecules that relay information to the nucleus, and in turn adjust the expression of nuclear genes to the needs of the plastids (Pogson et al., 2008; Woodson and Chory, 2008; Chan et al., 2016).

During the last 30 years, experiments with the carotenoid biosynthesis inhibitor norfluorazon (NF) and the inhibitor of plastid translation lincomycin (LIN), each of which arrests chloroplast development at the proplastid stage and represses the expression of photosynthesis-associated nuclear genes (PhANGs), have provided insights into the plastid's biogenic retrograde pathways (Oelmüller and Mohr, 1986; Oelmüller et al., 1986).

Six *genome uncoupled* (*gun*) mutants have been characterized in *Arabidopsis thaliana* that fail to repress transcription of the nuclear gene *Lhcb1.2* after NF treatment, and are thus impaired in retrograde signaling (Susek et al., 1993; Mochizuki et al., 2001; Larkin et al., 2003; Koussevitzky et al., 2007; Adhikari et al., 2011; Woodson et al., 2011). Five of these genes, *GUN2-6*, were found to be involved in tetrapyrrole biosynthesis (TPB), whereas *GUN1*, which encodes a nucleoid-localized pentatricopeptide repeat protein (PPR), has been shown to have a role in PGE, and to act as an integrator of multiple retrograde signals, since *gun1* mutants are unique in exhibiting a *gun* phenotype in response to both norfluorazon and lincomycin (Gray et al., 2003; Koussevitzky et al., 2007). However, the exact molecular role of GUN1 remained enigmatic until the new insights provided by the recent identification of a set of GUN1-interacting proteins (Tadini et al., 2016; **Table 1**).

Based on the functions of these partners, GUN1 appears to take part in multiple processes essential for chloroplast biogenesis and maintenance of the chloroplast proteome. GUN1-mediated control of plastid ribosomal protein S1 (PRPS1) accumulation, together with co-immunoprecipitation (CoIP) of proteins involved in different steps of plastid translation, support the involvement of GUN1 in the regulation of plastid protein synthesis. Furthermore, the presence of several chaperones in the CoIP mixture suggests a role for GUN1 in the coordination of chloroplast protein import and protein degradation.

Intriguingly, several GUN1 interactors appear to accumulate to higher levels upon induction of the unfolded protein response (UPR) in *Chlamydomonas reinhardtii* chloroplasts, which is triggered upon conditional repression of the catalytic subunit of Clp protease (ClpP1; Ramundo et al., 2013; Ramundo and Rochaix, 2014; Rochaix and Ramundo, 2015). This finding suggests the possible involvement of GUN1 in the UPR signaling pathway.

In this review, we describe the functional roles of the different GUN1 protein partners and propose some testable hypotheses that should clarify the molecular role of GUN1 in chloroplast biogenesis and chloroplast protein homeostasis.

GUN1 IS FOUND IN PLASTID NUCLEOIDS AND INTERACTS WITH THE TRANSCRIPTIONAL MACHINERY

GUN1 encodes a member of PPR-containing protein family, which has a small MutS-related (SMR) domain at the C-terminal end and a plastid targeting signal sequence at its N terminus. PPR motifs have been shown to mediate interactions with nucleic acids, and the SMR domain is found in proteins that act in DNA repair and recombination. However, *in vivo* RNA and DNA immunoprecipitation on chip (NIP-chip), as well as one-hybrid assays, have failed to detect any stable interaction of GUN1 with nucleic acids (Tadini et al., 2016), in contrast to a previous report, in which a GUN1 fragment containing both the PPR and SMR domains was shown to bind DNA *in vitro* (Koussevitzky et al., 2007). Nevertheless, GUN1 appears to be associated with nucleoids in the chloroplast, and more specifically with the domain of active plastid transcription, as shown by the relatively large and distinct foci of a fluorescent GUN1-YFP (Yellow Fluorescence Protein) chimera that co-localize with a Plastid Transcriptionally Active Chromosome 2-Cyan Fluorescence Protein (pTAC2-CFP) fusion in chloroplasts of mesophyll cells (Koussevitzky et al., 2007). However, although the repertoire of nucleoid-associated proteins so far identified is quite extensive, the GUN1 protein is not listed in any of the chloroplast or nucleoid/pTAC proteomes published to date (for a review see Melonek et al., 2016), most probably because it accumulates in very small amounts at specific developmental stages or under

TABLE 1 | GUN1 interactors together with their functions and impacts on plant development.

Designation	AGI code	Mutant phenotype[a]	Molecular function/Defect	Nucleoid subunit[b]	Identification assay[c]	References
TRANSCRIPTION AND RNA METABOLISM						
pTAC6/PAP8	AT1G21600	Albino	Low PEP activity	+	CoIP-MS	Pfalz et al., 2006; Steiner et al., 2011; Pfalz and Pfannschmidt, 2013
RH3/EMB1138	AT5G26742	Embryo lethal	RNA splicing of group II introns, assembly of the 50S ribosomal particle	+	CoIP-MS	Asakura et al., 2012; Majeran et al., 2012
AtPPR_3g49240/ EMB1796	AT3G49240	Embryo lethal	n.d.	+	CoIP-MS	Cushing et al., 2005; Majeran et al., 2012
TRANSLATION						
rpl2	ATCG00830	n.d.	Promotes translation initiation	+	CoIP-MS	Manuell et al., 2007; Melonek et al., 2016
rps3	ATCG00800	Essential for cell survival in tobacco	Promotes translation initiation	+	CoIP-MS	Manuell et al., 2007; Fleischmann et al., 2011; Melonek et al., 2016
rps4	ATCG00380	Essential for cell survival in tobacco	Involved in the assembly of the 30S ribosomal particle; binds to16S rRNA	+	CoIP-MS	Rogalski et al., 2008; Shoji et al., 2011; Melonek et al., 2016
PRPL10/ EMB3136	AT5G13510	Embryo lethal	Part of the L12 stalk and required for translation, since it recruits auxiliary translation factors such as cpIF2	–	CoIP-MS	Baba et al., 2006; Bryant et al., 2011; Shoji et al., 2011; Pfalz and Pfannschmidt, 2013
PRPS1	AT5G30510	n.d.	Promotes translation initiation	–	Y2H; BiFC	Manuell et al., 2007; Shoji et al., 2011; Tadini et al., 2016
cpIF2/FUG1	AT1G17220	Embryo lethal	Promotes translation initiation; leaky mutant alleles suppress leaf variegation in *var* mutants	–	CoIP-MS	Miura et al., 2007
PROTEIN IMPORT, PROTEIN FOLDING, AND PROTEIN UNFOLDING/DEGRADATION						
Hsp93-III/ClpC2	AT3G48870	Single mutant identical to WT; *hsp93-III hsp93-V* double mutant is embryo lethal	Cooperates with Tic110 and Tic40 in chloroplast protein import; chaperone in the Clp protease complex	–	CoIP-MS	Inaba et al., 2003; Kovacheva et al., 2005; Chou et al., 2006; Sakamoto, 2006; Kovacheva et al., 2007; Van Wijk, 2015
Hsp93-V/ClpC1	At5g50920	Single mutant exhibits a chlorotic phenotype; *hsp93-III hsp93-V* double mutant is embryo lethal	Cooperates with Tic110 and Tic40 in chloroplast protein import; chaperone in the Clp protease complex	+	CoIP-MS	Inaba et al., 2003; Kovacheva et al., 2005; Chou et al., 2006; Sakamoto, 2006; Kovacheva et al., 2007; Van Wijk, 2015; Melonek et al., 2016
Hsp70-1	AT4G24280	Single mutant exhibits variegated cotyledons, malformed leaves, growth retardation and impaired root growth; *hsp70-1 hsp70-2* double mutant is lethal	Involved in chloroplast protein import, folding and onward guidance of newly imported polypeptide chains	+	CoIP-MS	Su and Li, 2008; Shi and Theg, 2010; Su and Li, 2010; Liu et al., 2014; Melonek et al., 2016
Hsp70-2	AT5G49910	Single mutant identical to WT; *hsp70-1 hsp70-2* double mutant is lethal	Involved in chloroplast protein import, folding and onward guidance of newly imported polypeptide chains	–	CoIP-MS	Su and Li, 2008; Shi and Theg, 2010; Liu et al., 2014; Su and Li, 2010
ptCpn60α1	AT2G28000	Albino	Involved in folding and onward guidance of newly imported polypeptide chains; essential for plastid division in *A. thaliana*; involved in Rubisco and NdhH assembly	+	CoIP-MS	Gutteridge and Gatenby, 1995; Apuya et al., 2001; Suzuki et al., 2009; Peng et al., 2011; Flores-Perez and Jarvis, 2013; Melonek et al., 2016

(Continued)

TABLE 1 | Continued

Designation	AGI code	Mutant phenotype[a]	Molecular function/Defect	Nucleoid subunit[b]	Identification assay[c]	References
ptCpn60β1	AT1G55490	Leaves of the *len1* mutant have wrinkled and irregular surfaces and display lesions due to spontaneous cell death	Involved in folding and onward guidance of newly imported polypeptide chains; essential for plastid division in *A. thaliana*; involved in Rubisco and NdhH assembly	–	CoIP-MS	Gutteridge and Gatenby, 1995; Boston et al., 1996; Kessler and Blobel, 1996; Jackson-Constan et al., 2001; Ishikawa et al., 2003; Ishikawa, 2005; Suzuki et al., 2009; Flores-Perez and Jarvis, 2013
TPB ENZYMES						
CHLD	AT1G08520	Albino	Encodes the D subunit of the Mg-chelatase enzyme, involved in chlorophyll biosynthesis	–	Y2H; BiFC	Strand et al., 2003; Tanaka et al., 2011
PBGD	AT5G08280	n.d.	Porphobilinogen deaminase activity. Enzyme in the tetrapyrrole biosynthesis pathway	–	Y2H; BiFC	Tanaka et al., 2011
UROD2	AT2G40490	n.d.	Uroporphyrinogen decarboxylase activity; Enzyme in the tetrapyrrole biosynthesis pathway	–	Y2H; BiFC	Tanaka et al., 2011
FC1	AT5G26030	No visible phenotype; overexpression of the *FC1* gene is responsible for the *gun6* phenotype	Encodes ferrochelatase I, involved in heme biosynthesis	–	Y2H; BiFC	Tanaka et al., 2011; Woodson et al., 2011
DIVERSE FUNCTIONS						
rbcL	ATCG00490	Essential for photoautotrophy	Large subunit of Rubisco	+	CoIP-MS	Phinney and Thelen, 2005; Majeran et al., 2012; Huang et al., 2013
ATP-synthase β subunit	ATCG00480	Essential for photoautotrophy	Beta subunit of the thylakoid ATP synthase complex	+	CoIP-MS	Phinney and Thelen, 2005; Pfalz et al., 2006; Majeran et al., 2012; Melonek et al., 2012; Huang et al., 2013
RER4	AT5G12470	Mutant exhibits stunted growth, weak leaf reticulation and smaller mesophyll cells	Integral component of chloroplast outer and inner envelope membranes; possibly involved in retrograde signaling, supply of metabolites, control of ROS	–	CoIP-MS	Perez-Perez et al., 2013
2-Cys PrxA	AT3G11630	Mutant exhibits increased tolerance to photo-oxidative stress	Involved in peroxide detoxification in the chloroplast; functions as a redox sensor and chaperone; controls the conversion of Mg-protoporphyrin monomethyl ester into protochlorophyllide	–	CoIP-MS	Stenbaek et al., 2008; Rey et al., 2007; Pulido et al., 2010; König et al., 2013; Dietz, 2016

Note that proteins Q9SIP7 (AT2G31610) and Q42112 (AT3G09200) reported to be identified in coimmunoprecipitates of GUN1-GFP (Tadini et al., 2016) are not listed in this Table, since they have been described as subunits of cytosolic ribosomes. Furthermore, the protein Q9C5C2 (AT5G25980) has not been included, since it localizes to the tonoplast (Agee et al., 2010).

n.d., not determined.

[a]Phenotype of knock-out mutants is described.

[b]Protein already identified as part of chloroplast nucleoid by proteomic approaches.

[c]Assays used to identify the corresponding protein as a GUN1 interactor: coimmunoprecipitation followed by mass spectrometry (CoIP-MS), yeast two-hybrid (Y2H) analysis, and Bimolecular Fluorescence Complementation (BiFC).

particular physiological conditions. This inference is supported by CoIP experiments with a Green Fluorescence Protein (GUN1-GFP) fusion and subsequent mass spectrometry (MS), which identified several nucleoid subunits as interactors with GUN1 (Tadini et al., 2016; **Table 1**).

pTAC6 is among the GUN1 interactors, and it has been reported to interact directly with the plastid-encoded RNA polymerase (PEP), building together with pTAC2 and other polymerase-associated proteins (PAPs) the soluble RNA polymerase (sRNPase) complex (Pfalz et al., 2006), a central

component of nucleoids (Steiner et al., 2011; **Figure 1**). Intriguingly, pTAC6 (also known as PAP8) contains no known domain and exhibits no homologies that could provide hints as to its function in PGE (Steiner et al., 2011). However, functional genomics analyses have indicated that homozygous *pap* knockout lines develop white cotyledons, fail to accumulate chlorophyll even under low light intensities, and do not produce primary leaves unless they are cultivated on MS medium supplemented with sucrose (for a review, see Pfalz and Pfannschmidt, 2013). Furthermore, analyses of PGE in *pap* mutants revealed strong repression of the accumulation of PEP-dependent transcripts, whereas levels of nucleus-encoded RNA polymerase (NEP)-dependent transcripts were not depleted, while some were enhanced, indicating that pTAC6/PAP8 and the other PAP proteins are essential for the activity of PEP (see **Table 1**).

GUN1 CONTROLS PLASTID TRANSLATION AND RIBOSOME BIOGENESIS

GUN1 also interacts with several ribosomal subunits, such as the plastid-encoded ribosomal proteins L2, S3, and S4 (rpl2, rps3, and rps4) and the nucleus-encoded plastid ribosomal protein L10 (PRPL10; **Figure 1**). Furthermore, yeast two-hybrid and Bimolecular Fluorescence Complementation (BiFC) assays revealed a physical interaction between GUN1 and PRPS1 (Tadini et al., 2016). Ribosomal proteins have been reproducibly detected in nucleoid and pTAC proteomes (Melonek et al., 2016), further supporting the existence of a translational subdomain within the nucleoids, as proposed by Pfalz and Pfannschmidt (2013). The homologs of PRPL10, rpl2, PRPS1, rps3, and rps4 are essential components of the protein biosynthetic machinery in *Escherichia coli* (Baba et al., 2006; Shoji et al., 2011) and the indispensability of rps3 and rps4 has been also proven in tobacco plastids (Rogalski et al., 2008; Fleischmann et al., 2011). Furthermore, PRPL10 is annotated as EMBryo defective 3136 (EMB3136) in the SeedGenes Project database (http://www.seedgenes.org/), and in its absence Arabidopsis embryo development arrests at the globular stage (Bryant et al., 2011). Mutants devoid of PRPS1 have not been described. However, given the conservation of PRPS1 function in prokaryotes and chloroplasts, it can be confidently assumed that complete lack of PRPS1 is lethal in Arabidopsis.

Taking into consideration the function of these ribosomal proteins, it can be argued that their interaction with GUN1 has a dual purpose. On the one hand, GUN1 modulates protein synthesis by controlling the abundance of PRPS1, which, together with rps3 and rps2, has been reported to form the domain responsible for the interaction of the 30S ribosomal subunit with mRNA, promoting translation initiation (Manuell et al., 2007; Tadini et al., 2016). This role is supported further by the stable interaction of GUN1 with the chloroplast translation initiation

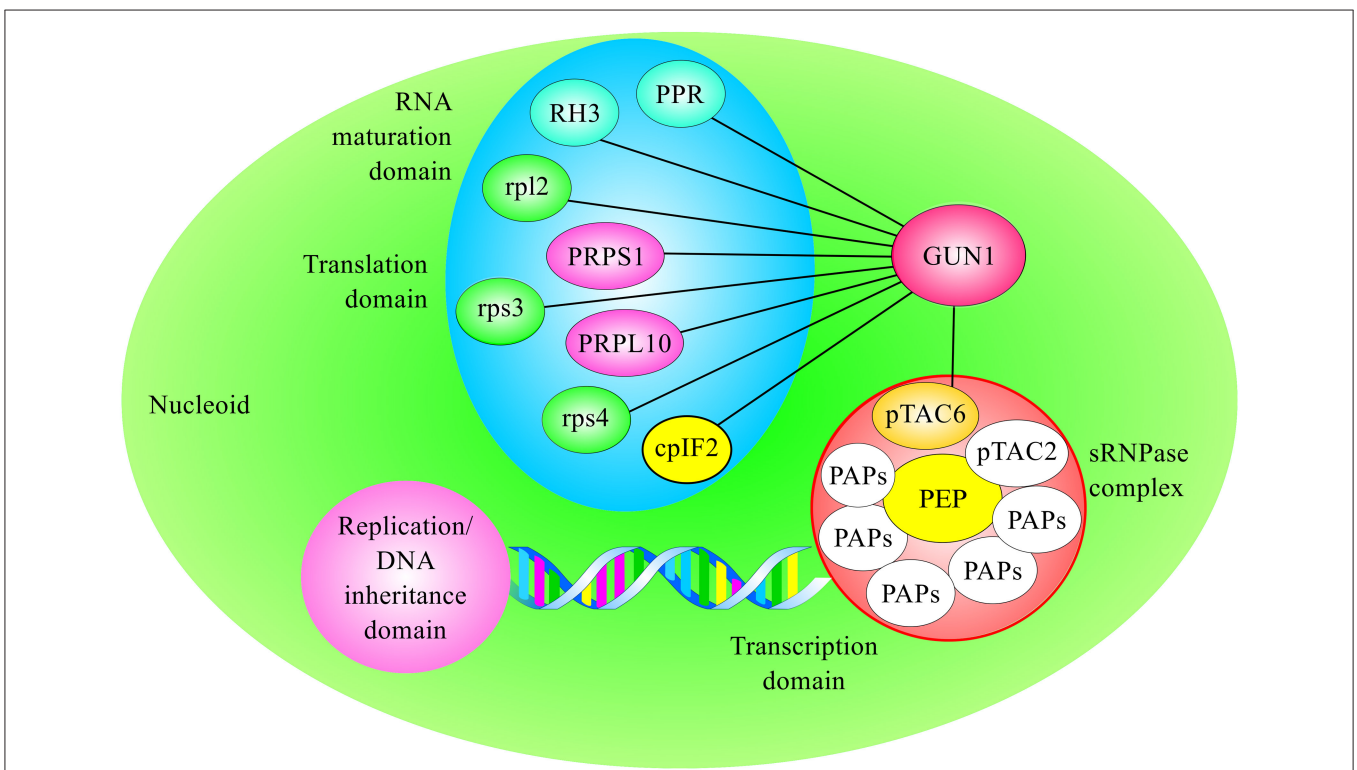

FIGURE 1 | Schematic overview of GUN1 protein interactors involved in gene transcription, ribosome biogenesis and plastid translation. The scheme takes into account the partition of nucleoids into functional subdomains proposed by Pfalz and Pfannschmidt (2013). PPR refers to AtPPR_3g49240, also known as EMB1796, as reported in **Table 1**.

factor 2 (cpIF2; Tadini et al., 2016), also known as FUG1, and reported to be essential for chloroplast biogenesis (Miura et al., 2007).

On the other hand, GUN1 seems to be involved in the process of ribosome biogenesis too, since nucleoid-associated ribosomes are thought to be in various stages of assembly, with several rRNA maturation steps occurring in a co-transcriptional and assembly-assisted manner, as in prokaryotic systems (Bohne, 2014). For instance, the DEAD-box-containing, ATP-dependent RNA helicase 3 (RH3), which has been functionally linked to the chloroplast nucleoid (Majeran et al., 2012), is among the proteins that interact with GUN1 (Tadini et al., 2016; see also **Figure 1** and **Table 1**). RH3 is directly involved in the splicing of group II introns in the *rpl2*, *trnA*, *trnI*, and *rps12* transcripts and could be coimmunoprecipitated with immature and mature 23S rRNA (Asakura et al., 2012). Furthermore, the PPR protein At3g49240 also known as AtPPR_3g49240, according to the PPR protein database (http://www.plantenergy.uwa.edu.au/applications/ppr/ppr.php), is also part of GUN1's interactors, and its maize ortholog, GRMZM2G074599_P01, has been identified in the chloroplast nucleoid (Majeran et al., 2012). The gene is annotated as embryo defective 1796 (EMB1796) in the SeedGenes database, since the complete lack of AtPPR_3g49240 leads to the arrest of embryonic development at the globular stage (Cushing et al., 2005), further supporting the essential role of GUN1 interactors in chloroplast biogenesis.

GUN1 AND THE IMPORT OF CHLOROPLAST PROTEINS

Almost a quarter of the GUN1 interactors identified by CoIP-MS are chaperones (see **Table 1**), a relatively high proportion when compared with the extensive repertoire of protein functions found within the nucleoid (Melonek et al., 2016). The stromal Hsp93 and Hsp70 chaperones mediate different steps in protein import into the chloroplast stroma, whereas the 60 KD chaperonin Cpn60 is thought to be involved in the folding of newly imported mature proteins and to function downstream of Hsp93 and Hsp70 (Kessler and Blobel, 1996; Jackson-Constan et al., 2001; Flores-Perez and Jarvis, 2013). Furthermore, the two genes most highly co-regulated with *GUN1* encode the proteins TIC110 and TOC159 (Tadini et al., 2016), which are part of the outer and inner chloroplast translocons, respectively, suggesting a role of GUN1 in chloroplast protein import (**Figure 2**).

The Hsp93 Chaperones

In Arabidopsis, there are two nearly identical isoforms of Hsp93, termed Hsp93-V and Hsp93-III (or ClpC1 and ClpC2, respectively) and both interact with GUN1. The two proteins are highly homologous, but Hsp93-V is expressed at much higher levels than Hsp93-III (Kovacheva et al., 2005, 2007), and only Hsp93-V has been reported as a component of the nucleoid proteome (Phinney and Thelen, 2005; Majeran et al., 2012; Melonek et al., 2012; Huang et al., 2013). Furthermore, both *hsp93* single mutants are viable whereas *hsp93-III hsp93-V* double mutant is embryo-lethal, indicating that the two proteins have redundant functions in Arabidopsis chloroplasts (Constan et al., 2004; Sjögren et al., 2004; Kovacheva et al., 2007).

The current model for chloroplast protein import assumes that the preprotein transit peptide interacts with the TOC, and is subsequently transported through the TIC in an energy-dependent process (Shi and Theg, 2013b). In particular, the Tic110–Tic40 interaction is proposed to trigger the release of the transit peptide from Tic110 and enable the association of the preprotein with Hsp93 (Inaba et al., 2003). Tic40 then stimulates ATP hydrolysis by Hsp93, which harnesses the energy released to draw the preprotein into the stroma (Chou et al., 2006).

The Hsp70 Chaperones

Recent work has also demonstrated the involvement of Hsp70 in protein translocation into chloroplasts, as part of the translocon energy-dependent engine together with Hsp93 and Hsp90 (Inoue et al., 2013; Liu et al., 2014). Like Hsp93, Hsp70 proteins occur in two isoforms, Hsp70-1 and Hsp70-2, in the chloroplasts of Arabidopsis (Su and Li, 2008) and only Hsp70-1 was found in the proteomes of pTAC and crude nucleoids (for a review see Melonek et al., 2016). However, both Hsp70 proteins have been identified as GUN1 interactors (Tadini et al., 2016). Protein import assays using chloroplasts isolated from the Arabidopsis Hsp70 knockout mutants *hsp70-1* and *hsp70-2* showed that stromal Hsp70s are important for the import of both photosynthetic and non-photosynthetic precursor proteins, especially in early developmental stages (Su and Li, 2010). Furthermore, no *hsp70-1 hsp70-2* double mutant has ever been isolated. Thus, the two Hsp70s are likely to have redundant functions that are essential for plant development and chloroplast biogenesis.

The Cpn60 Chaperonins

After preproteins delivered to the stroma have been processed, they may require accessory factors to enable them to fold into their functional conformation, or to reach their final intra-organellar destination. The stromal molecular chaperones Hsp70, Cpn60, and Cpn10 are all believed to mediate the folding or onward guidance of newly imported polypeptide chains (Boston et al., 1996; Jackson-Constan et al., 2001). In particular, immunoprecipitation experiments have revealed that Cpn60 operates in close proximity with Tic110 (Kessler and Blobel, 1996), while import experiments have shown a transient association of mature, newly imported proteins with the Cpn60-Tic110 complex, suggesting that Tic110 can recruit Cpn60 in an ATP-dependent manner for the folding of proteins upon their arrival in the stroma. It has also been suggested that stromal Hsp70 and Cpn60 act sequentially to facilitate the maturation of imported proteins, particularly those destined for the thylakoid membranes (Madueno et al., 1993; Tsugeki and Nishimura, 1993; Peng et al., 2011). The Arabidopsis genome encodes two members of the Cpn60α family, denoted ptCpn60α1 and ptCpn60α2, and four members of Cpn60β, known as ptCpn60β1–β4 (Suzuki et al., 2009). Two of them, ptCpn60α1 and ptCpn60β2, have been linked to the nucleoid proteome (Melonek et al., 2016), and ptCpn60α1 and ptCpn60β1 are among the GUN1 interactors identified via the CoIP-MS strategy (see **Table 1**). The complete loss of ptCpn60α1, in the

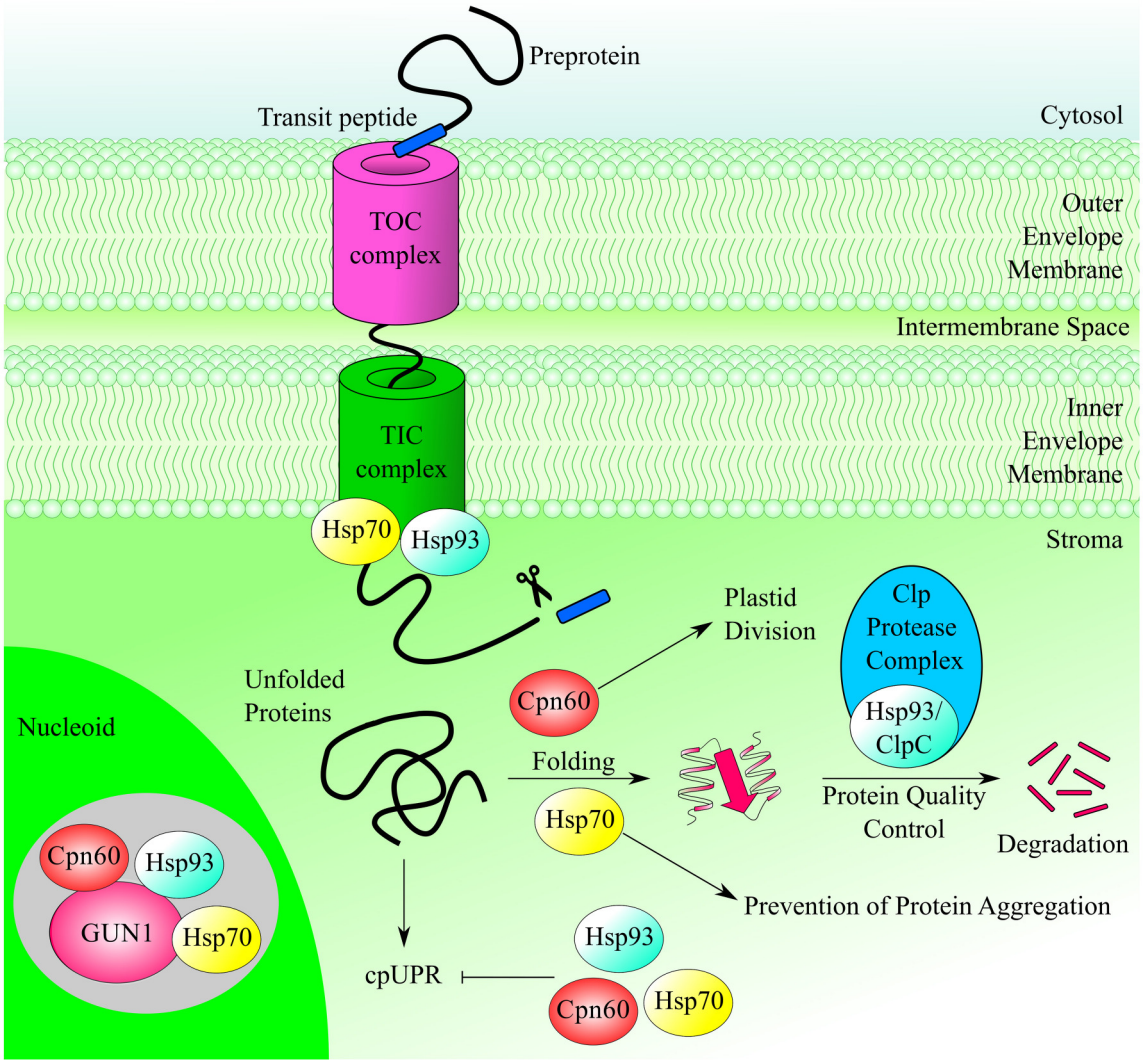

FIGURE 2 | GUN1 interacts with different plastid chaperones. The chaperones Hsp93, Hsp70, and Cpn60 participate in different processes within the chloroplast, such as protein import, protein folding/unfolding, prevention of protein aggregation, and regulation of plastid division, and they might play a key role in the chloroplast Unfolded Protein Response (cpUPR). CoIP-MS analysis has shown that they are also part of GUN1-containing protein complexes.

mutant termed *schlepperless* (*slp*), causes retardation of embryo development before the heart stage and an albino seedling phenotype, indicating that ptCpn60α1 is essential for chloroplast biogenesis (Apuya et al., 2001). Conversely, plants devoid of ptCpn60β1, also known as *lesion initiation 1* (*len1*), have leaves with wrinkled and irregular surfaces and undergo localized, spontaneous cell death in the absence of pathogen attack, i.e., lesion formation, under short-day conditions (Ishikawa et al., 2003).

OTHER FUNCTIONS OF PLASTID CHAPERONES

Besides their roles in plastid protein import, all GUN1-interacting chaperones are present in the stroma at significant amounts relative to their association with the chloroplast import apparatus and perform various other functions together with different protein complexes (**Figure 2**). For instance Hsp93, also termed ClpC, acts as a regulatory chaperone in the Clp protease complex, the most abundant stromal protease with general household functions (Sakamoto, 2006; Van Wijk, 2015). Clp substrates are selected through various signals intrinsic to amino acid sequences and the ATP-dependent ClpC chaperone activity helps to progressively unfold selected substrates that are delivered to the ClpPR core for degradation into small peptides (~8–10 amino acids long; Olinares et al., 2011).

Similarly, Cpn60 forms a large oligomeric protein complex (>600 KDa) that promotes the assembly of Rubisco (Gutteridge and Gatenby, 1995). In particular, it has been observed that the large subunit of Rubisco (RbcL) is specifically associated with

Cpn60 before assembly into the holoenzyme and that the Cpn60-RbcL complex is an obligatory intermediate. Furthermore, Cpn60 proteins have been shown to be essential for plastid division in *A. thaliana* (Suzuki et al., 2009). Thus, mesophyll cells in *ptcpn60α1-1* (a missense mutant) and *ptcpn60β1-1* (a protein null) plants, contain fewer and larger chloroplasts, indicating that normal levels of plastid Cpn60 are required for the correct folding of the stromal plastid division proteins and/or regulation of FtsZ (Filamentous temperature-sensitive Z) polymer dynamics (Suzuki et al., 2009).

The same holds true for the Hsp70 proteins, which are also involved in modulation of protein activity, regulation of protein degradation and prevention of irreversible protein aggregation when they are free in the stroma (Su and Li, 2008). Potentially GUN1 can be involved in a multitude of activities, besides plastid protein import, thus further investigations are needed to clarify the functional significance of GUN1–chaperone interactions.

GUN1 AND THE CHLOROPLAST UNFOLDED PROTEIN RESPONSE (cpUPR)

Chaperones, together with enzymes that process and degrade proteins, are also necessary to maintain protein folding homeostasis in the various compartments of eukaryotic cells. Distinct signal transduction pathways, known as unfolded protein responses (UPRs), have evolved to couple the unfolded/misfolded protein load to the expression of specific chaperones and enzymes that promote folding and the disposal of misfolded proteins in each compartment.

The unfolded protein response was first discovered in the endoplasmic reticulum (ER) in yeast, where inhibition of protein folding leads to the transcriptional up-regulation of several chaperones (Cox et al., 1993), and subsequently in mitochondria, where accumulation of unfolded proteins in the mitochondrial matrix stimulates the expression of nuclear gene transcripts coding for mitochondrial chaperones (Aldridge et al., 2007; Lin and Haynes, 2016). Compared to yeast and metazoans, studies of plant UPRs are less advanced, and molecular details are known mainly for the ER-dependent UPR, which shows certain similarities with the process in multicellular eukaryotes, as well as plant-specific features (Ruberti et al., 2015). Recently, the possible existence of a chloroplast UPR (cpUPR) has been investigated in the green alga *Chlamydomonas reinhardtii*. Taking advantage of a repressible chloroplast gene expression system (Rochaix et al., 2014), Ramundo et al. (2014) induced the selective gradual depletion of the essential stromal Clp protease, in order to follow the early and late events caused by the decrease in its abundance. Temporal profiles of gene expression and protein accumulation revealed a marked increase in levels of chaperones, including Hsp70B, upon Clp depletion. Similar data have also been reported for Arabidopsis, where up-regulation of chloroplast chaperones and protein-sorting components occurred upon constitutive repression of Clp (Rudella et al., 2006; Zybailov et al., 2009). In particular, characterization of total leaf proteomes of WT and *clpr2-1* highlighted differential expression of 768 proteins. The largest functional category quantified (with 205 proteins) comprised proteins involved in translation, folding and degradation. Strikingly, all the chaperones interacting with GUN1, including Hsp93, Hsp70, Cpn60, as well as the DEAD box RNA helicase RH3, are among those up-regulated (by between 1.6- and 8.5-fold) in *clpr2-1* leaves, whereas no significant change in the chloroplast ribosomal protein population was observed (Zybailov et al., 2009).

Taken together, these findings suggest that disruption of protein homeostasis in organelles can be sensed and transduced to the nucleus to induce the expression of a specific set of factors responsible for promoting folding and monitoring protein quality control (Ramundo and Rochaix, 2014; Rochaix and Ramundo, 2015). After entering the higher plant chloroplast, these factors are able to interact with the nucleoid-associated GUN1 protein (**Figure 2**), which might therefore play a role in the cpUPR process.

GUN1 AND CHLOROPLAST METABOLISM

The large subunit of ribulose bisphosphate carboxylase (RbcL) and the β subunit of the ATP synthase are also among the interactors of GUN1 identified by CoIP-MS analysis (Tadini et al., 2016). Because of their relatively high abundance in the chloroplast proteome, it is tempting to assume that these proteins are simply contaminants. However, RbcL and subunits of the ATP synthase have been repeatedly identified in the pTAC/nucleoid proteomes, even though different procedures were employed for isolation of crude nucleoid fractions and highly purified pTAC complexes (for a review see Melonek et al., 2016), thus suggesting these proteins might have a dual localization to the chloroplast stroma and nucleoids. The nucleoid association of RbcL and ATP synthase, i.e., of proteins that are not directly involved in core nucleoid functions, might also indicate that nucleoids also monitor photosynthesis and energy metabolism and respond appropriately to any perturbations (**Figure 3**).

Unlike RbcL and the ATP synthase β subunit, RETICULATA-RELATED 4 (RER4), an integral component of the chloroplast envelope membranes with three transmembrane α-helices, has never been identified in the pTAC/nucleoid proteome, although it appears to be an interactor of GUN1 (**Table 1**). The mutant *rer4-1* exhibits leaf reticulation, having green veins that stand out against paler intervein tissue, with fewer and smaller mesophyll cells than those of the wild type leaves (Perez-Perez et al., 2013). The molecular function of RER4 remains to be established. However, some hints as to its role in the chloroplast can be derived from features of the *rer4-1* mutant phenotype. A possible involvement of RER4 in retrograde signaling is suggested by the altered growth and development of mesophyll cells. Alternatively, the absence of RER4 might deplete the supply of essential metabolites during early stages of leaf development, which could explain the aberrant mesophyll structure. Furthermore, RER4 has been suggested to be involved in the control of reactive oxygen species (ROS), since the reticulated pigmentation of the *rer4-1* mutant grown under long-day conditions can be rescued

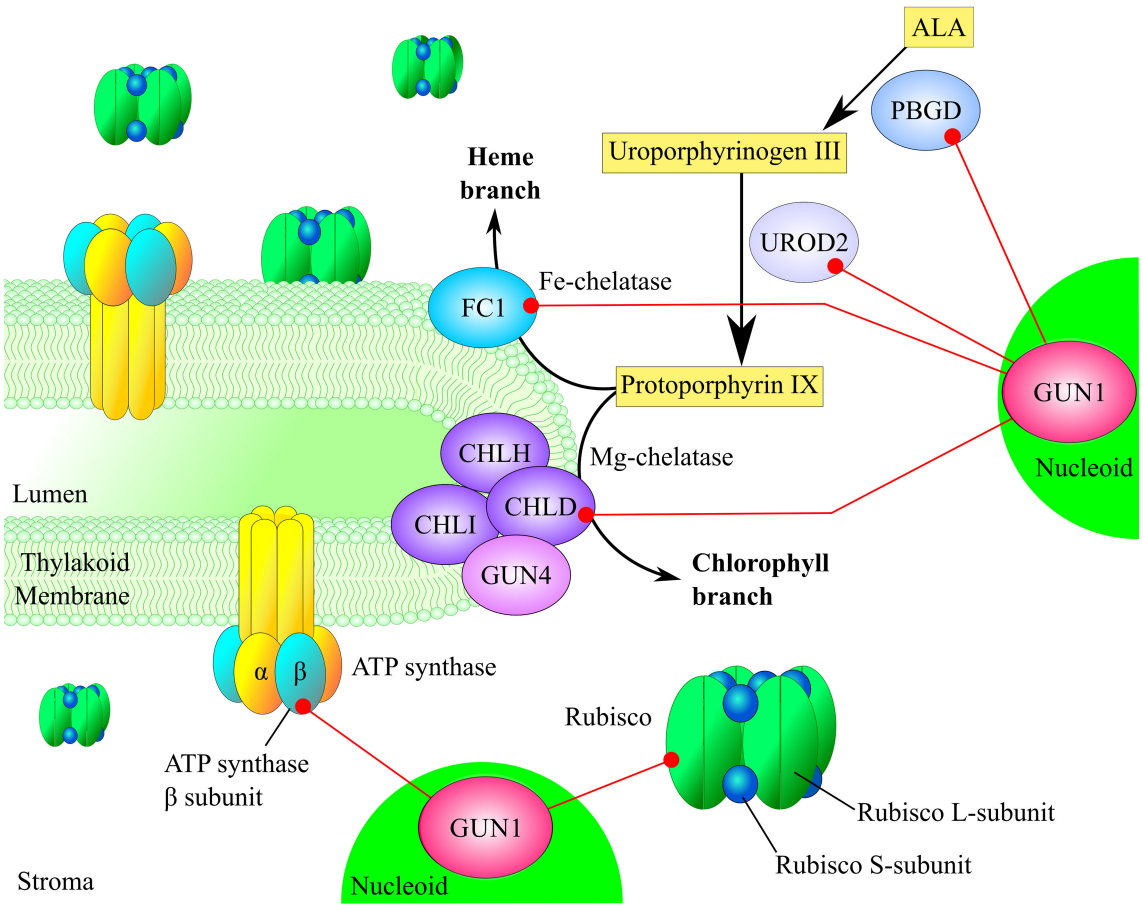

FIGURE 3 | GUN1 is involved in photosynthesis and tetrapyrrole biosynthesis. The large subunit of Rubisco and the β-subunit of the thylakoid ATP synthase have been coimmunoprecipitated with GUN1, supporting a role for GUN1 in coordinating nucleoid activities with chloroplast metabolism. GUN1 also interacts with four enzymes of the tetrapyrrole biosynthesis pathway, i.e., the D subunit of Mg chelatase (CHLD), porphobilinogen deaminase (PBGD), uroporphyrinogen III decarboxylase (UROD2), and ferrochelatase I (FC1), as shown by yeast two-hybrid and Bimolecular Fluorescence Complementation. Note that the proteins RER4 and 2-Cys PrxA have not been included in this scheme for reasons of clarity.

by a short-day photoperiod, which markedly dampens ROS accumulation.

The 2-Cys peroxiredoxin A (2-Cys Prx A; see also **Table 1**), another interactor with GUN1, appears also to have a role in ROS scavenging (Rey et al., 2007; Pulido et al., 2010; Dietz, 2016) and, like RER4, it has never been reported to be part of the pTAC/nucleoid proteome (Pfalz et al., 2006; Majeran et al., 2012; Huang et al., 2013). 2-Cys Prx A and the highly homologous 2-Cys Prx B function as redox sensors and chaperones, thanks to the flexibility of their protein structure (König et al., 2013), and they have been shown to control the conversion of Mg-protoporphyrin monomethyl ester into protochlorophyllide (Stenbaek et al., 2008).

The involvement of GUN1 in TPB is further supported by its interaction with four TPB enzymes, namely subunit D of Mg chelatase (CHLD), porphobilinogen deaminase (PBGD), uroporphyrinogen III decarboxylase (UROD2), and ferrochelatase I (FC1), as demonstrated by both yeast two-hybrid and BiFC assays (Tadini et al., 2016; **Figure 3**). Interestingly, mutants defective in three of these GUN1 interactors—CHLD, PBGD, and FC1—have themselves been described as *gun* mutants (Strand et al., 2003; Huang and Li, 2009; Woodson et al., 2011), but have never been identified in crude nucleoid preparations, unlike subunit I of Mg chelatase (CHLI; Melonek et al., 2012; Huang et al., 2013).

GUN1 AND PLASTID PROTEIN HOMEOSTASIS: SOME TESTABLE HYPOTHESES

The recent identification of the GUN1 protein's partners in chloroplasts of Arabidopsis by means of CoIP-MS studies as well as in yeast two-hybrid and BiFC assays (Tadini et al., 2016) strongly suggests a major role for GUN1 in plastid protein homeostasis (**Figure 4**). This regulatory role involves proteins that are, in most cases, members of multimeric protein complexes and whose functions are often context-dependent. Furthermore, most GUN1 interactors appear to participate in four major processes:

Chloroplast Protein Synthesis

A wealth of evidence accumulated during the last two decades supports the primacy of plastid protein synthesis in the control of chloroplast gene expression (Choquet and Wollman, 2002; Manuell et al., 2007; Tiller and Bock, 2014; Sun and Zerges, 2015). In this context, GUN1 has been suggested to regulate translation in plastids by modulating the abundance and binding affinity of PRPS1 (Tadini et al., 2016). In particular, PRPS1 is the only ribosomal protein that shuttles between ribosome-bound and ribosome-free forms (Merendino et al., 2003; Delvillani et al., 2011), the latter being more abundant in plants that lack GUN1. Based on observations in *E. coli*, where the unbound form is thought to inhibit translation by competing with ribosomes for mRNAs (Delvillani et al., 2011), it can be argued that the GUN1-dependent equilibrium between the two PRPS1 states has an important role in controlling polysome assembly and protein synthesis in chloroplasts (**Figure 4A**). However, further investigations are needed to clarify this issue. For instance, lines characterized by the ectopic expression of *PRPS1* or carrying *PRPS1* constructs under the control of inducible promoters, coupled with assays aimed to measure the translation rate in plastids, should allow us to verify the role of PRPS1 in modulating protein synthesis. Furthermore, GUN1 controls the abundance of PRPS1 at the post-transcriptional level. This suggests the involvement of an as yet unidentified plastid protease in this aspect of GUN1 function. In addition, the significance of the interaction of GUN1 with other ribosomal proteins, factors involved in ribosome biogenesis and regulators of plastid protein synthesis remains to be elucidated.

Chloroplast Protein Import and Degradation

Based on the observations reported above, it appears that GUN1 may well control the interactions of a sub-set of chaperones, promoting plastid protein import when their association with the TIC complex is favored, and stimulating protein degradation, folding/unfolding when they interact with proteases or other protein complexes in the stroma or in the thylakoid membranes (**Figure 4B**). Such a regulatory mechanism would enable GUN1 to coordinate protein translocation across the chloroplast envelope with protein degradation in the stroma,

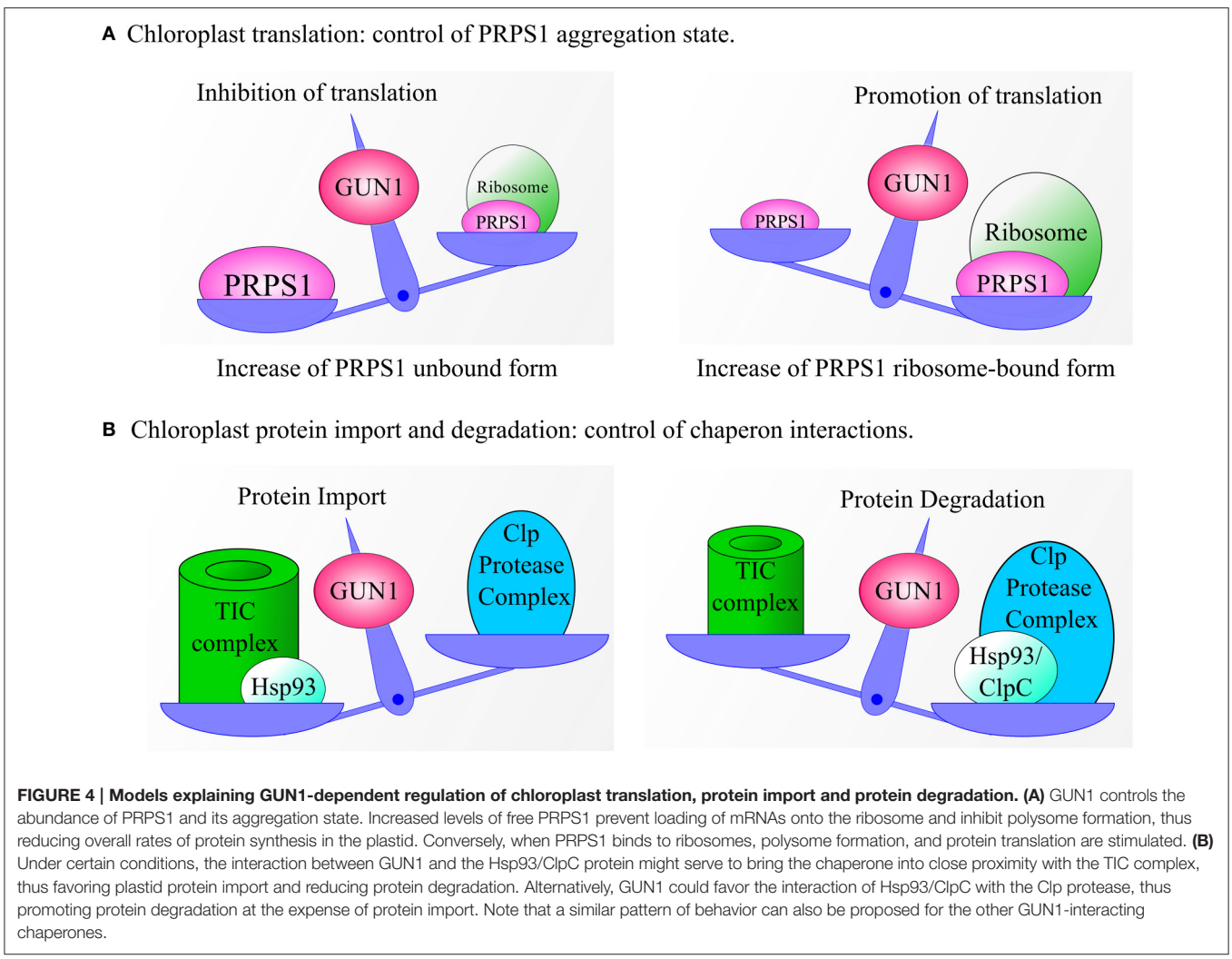

FIGURE 4 | Models explaining GUN1-dependent regulation of chloroplast translation, protein import and protein degradation. (A) GUN1 controls the abundance of PRPS1 and its aggregation state. Increased levels of free PRPS1 prevent loading of mRNAs onto the ribosome and inhibit polysome formation, thus reducing overall rates of protein synthesis in the plastid. Conversely, when PRPS1 binds to ribosomes, polysome formation, and protein translation are stimulated. **(B)** Under certain conditions, the interaction between GUN1 and the Hsp93/ClpC protein might serve to bring the chaperone into close proximity with the TIC complex, thus favoring plastid protein import and reducing protein degradation. Alternatively, GUN1 could favor the interaction of Hsp93/ClpC with the Clp protease, thus promoting protein degradation at the expense of protein import. Note that a similar pattern of behavior can also be proposed for the other GUN1-interacting chaperones.

as well as with plastid division, thus modulating the protein content of the chloroplast in accordance with physiological requirements.

Relatively simple biochemical analyses can be used to verify the importance of GUN1 in influencing the interactions of the stromal chaperones, such as protein complex fractionation via sucrose-gradient ultracentrifugation and/or Blue-Native PAGE coupled with two-dimensional (2D) SDS-PAGE, and immunoblot analyses. Furthermore, the interactions of GUN1 with chaperones should be shown to occur at the plastid envelope and protein import efficiency should be tested in chloroplasts isolated from *gun1* and WT seedlings in order to implicate GUN1 in regulating plastid protein import.

Retrograde Signal Induction

GUN1 may well be a master regulator of plastid-to-nucleus communication in *A. thaliana*, as it appears to integrate signals derived from perturbations in PGE, TPB, and redox state, in order to modulate nuclear gene expression. Indeed, components of all three pathways have been shown to interact with GUN1, suggesting that signal integration might take place through physical interaction.

Due to the limited abundance of GUN1, as indicated by the fact that the protein has yet to be detected in plastid proteome studies, it is tempting to disregard the idea that its physical interaction with PGE-, TPB-, and redox-related proteins could lead to protein sequestration and directly to differences in protein translation, TPB, and redox balance (Koussevitzky et al., 2007; Pogson et al., 2008; Woodson and Chory, 2008; Kleine and Leister, 2016). Nevertheless, a direct association with GUN1 could control protein abundance through post-transcriptional mechanisms, as in the case of PRPS1 and CHLD (Tadini et al., 2016). Thus, control of CHLD and possibly of FC1 levels could alter the tetrapyrrole flux and influence the abundance of the tetrapyrrole intermediate Mg-protoporphyrin IX (Mg-ProtoIX), or the tetrapyrrole product Fe-protoporphyrin IX (heme), which have been reported to act as negative and positive retrograde signals, respectively (for a review, see Chan et al., 2016). Alternatively, the interaction of GUN1 with the near-identical paralogs ClpC1 and ClpC2 could contribute to the coordination of plastid protein content with tetrapyrrole biosynthesis. Indeed, the activity of the stromal Clp protease has been shown to modulate tetrapyrrole flux by controlling (i) the accumulation of chlorophyll a oxygenase, which converts chlorophyll a into chlorophyll b (Nakagawara et al., 2007), and (ii) the level of glutamyl-tRNA reductase (GluTR), thus regulating the rate-limiting reaction in tetrapyrrole synthesis—the conversion of glutamate-1-semialdehyde into 5-aminolevulinic acid (Apitz et al., 2016).

Therefore, accurate determination of tetrapyrrole intermediates should be performed in *gun1* mutant and WT backgrounds. The analyses should be restricted to young seedlings or even to different developmental stages of the chloroplast, in line with the roles of tetrapyrrole and GUN1-mediated signaling in chloroplast development.

CONCLUDING REMARKS

In the past decade, substantial progress has been made in elucidating retrograde signaling, with the identification of multiple retrograde pathways and more than 40 components involved at different levels in chloroplast-to-nucleus communication. Nevertheless, the molecular function of GUN1 has remained unclear until the recent identification of the GUN1 protein's partners. Based on the functional roles of GUN1 interactors and the embryo lethal or albino phenotypes of most of the corresponding knock-out mutants, we have learned that GUN1 plays a role in chloroplast biogenesis, possibly by controlling protein turnover and protein import, and through the coordination of plastid and nuclear gene expression. Furthermore, GUN1 could have a role in the cpUPR process. Nonetheless, the involvement of GUN1 in plastid biogenesis and protein homeostasis is only just beginning to be understood. For instance, other approaches will be needed to validate the GUN1's protein partners identified by CoIP-MS. The use of a GUN1-GFP protein chimera, expressed under the control of a strong constitutive promoter such as the Cauliflower Mosaic Virus 35S (35S-CaMV), is indeed prone to the identification of false interactors. CoIP-MS studies using a GUN1 specific antibody appears to be the ideal strategy to identify protein partners. Alternatively, the use of GUN1 chimeras under the control of GUN1 native promoter is also practicable. Moreover, we do not know whether all these activities take place within one GUN1-containing nucleoid or if there are different nucleoids/locations for each GUN1-dependent function. The developmental stages of the chloroplast itself may even show distinct patterns of compartmentalization of the different functions. In addition, GUN1's interactions with its diverse partners might have quite different functional consequences: (i) promote specific functions, by bringing enzymes into close proximity with their own substrates and, ultimately, controlling the enzyme abundance, (ii) inhibit processes by sequestering sub-pools of specific proteins and, also in this case, controlling their abundance.

We are confident that future work, based on the exciting breakthroughs discussed in this Review, will shed new light on the molecular functions of GUN1 and its involvement in chloroplast biogenesis and protein homeostasis.

AUTHOR CONTRIBUTIONS

MC, LT, CP, RF, and PP participated to the organization of the manuscript. MC and PP designed and conceived the pictures. PP wrote the manuscript.

ACKNOWLEDGMENTS

This work was supported by ERA-NET Cofund FACCE SURPLUS (BarPLUS grant id. 93). We thank Paul Hardy for critical reading of the manuscript. The authors wish to acknowledge the reviewers for the detailed and helpful comments to the manuscript.

REFERENCES

Adhikari, N. D., Froehlich, J. E., Strand, D. D., Buck, S. M., Kramer, D. M., and Larkin, R. M. (2011). GUN4-porphyrin complexes bind the ChlH/GUN5 subunit of Mg-Chelatase and promote chlorophyll biosynthesis in Arabidopsis. *Plant Cell* 23, 1449–1467. doi: 10.1105/tpc.110.082503

Agee, A. E., Surpin, M., Sohn, E. J., Girke, T., Rosado, A., Kram, B. W., et al. (2010). MODIFIED VACUOLE PHENOTYPE1 is an Arabidopsis myrosinase-associated protein involved in endomembrane protein trafficking. *Plant Physiol.* 152, 120–132. doi: 10.1104/pp.109.145078

Aldridge, J. E., Horibe, T., and Hoogenraad, N. J. (2007). Discovery of genes activated by the mitochondrial unfolded protein response (mtUPR) and cognate promoter elements. *PLoS ONE* 2:e874. doi: 10.1371/journal.pone.0000874

Apitz, J., Nishimura, K., Schmied, J., Wolf, A., Hedtke, B., Van Wijk, K. J., et al. (2016). Posttranslational control of ALA synthesis includes GluTR degradation by Clp protease and stabilization by GluTR-binding protein. *Plant Physiol.* 170, 2040–2051. doi: 10.1104/pp.15.01945

Apuya, N. R., Yadegari, R., Fischer, R. L., Harada, J. J., Zimmerman, J. L., and Goldberg, R. B. (2001). The Arabidopsis embryo mutant schlepperless has a defect in the chaperonin-60alpha gene. *Plant Physiol.* 126, 717–730. doi: 10.1104/pp.126.2.717

Asakura, Y., Galarneau, E., Watkins, K. P., Barkan, A., and Van Wijk, K. J. (2012). Chloroplast RH3 DEAD box RNA helicases in maize and Arabidopsis function in splicing of specific group II introns and affect chloroplast ribosome biogenesis. *Plant Physiol.* 159, 961–974. doi: 10.1104/pp.112.197525

Baba, T., Ara, T., Hasegawa, M., Takai, Y., Okumura, Y., Baba, M., et al. (2006). Construction of *Escherichia coli* K-12 in-frame, single-gene knockout mutants: the Keio collection. *Mol. Syst. Biol.* 2, 2006.0008. doi: 10.1038/msb4100050

Bohne, A. V. (2014). The nucleoid as a site of rRNA processing and ribosome assembly. *Front. Plant Sci.* 5:257. doi: 10.3389/fpls.2014.00257

Boston, R. S., Viitanen, P. V., and Vierling, E. (1996). Molecular chaperones and protein folding in plants. *Plant Mol. Biol.* 32, 191–222. doi: 10.1007/BF00039383

Bryant, N., Lloyd, J., Sweeney, C., Myouga, F., and Meinke, D. (2011). Identification of nuclear genes encoding chloroplast-localized proteins required for embryo development in Arabidopsis. *Plant Physiol.* 155, 1678–1689. doi: 10.1104/pp.110.168120

Chan, K. X., Phua, S. Y., Crisp, P., McQuinn, R., and Pogson, B. J. (2016). Learning the languages of the chloroplast: retrograde signaling and beyond. *Annu. Rev. Plant Biol.* 67, 25–53. doi: 10.1146/annurev-arplant-043015-111854

Choquet, Y., and Wollman, F. A. (2002). Translational regulations as specific traits of chloroplast gene expression. *FEBS Lett.* 529, 39–42. doi: 10.1016/S0014-5793(02)03260-X

Chou, M. L., Chu, C. C., Chen, L. J., Akita, M., and Li, H. M. (2006). Stimulation of transit-peptide release and ATP hydrolysis by a cochaperone during protein import into chloroplasts. *J. Cell Biol.* 175, 893–900. doi: 10.1083/jcb.200609172

Constan, D., Froehlich, J. E., Rangarajan, S., and Keegstra, K. (2004). A stromal Hsp100 protein is required for normal chloroplast development and function in Arabidopsis. *Plant Physiol.* 136, 3605–3615. doi: 10.1104/pp.104.052928

Cox, J. S., Shamu, C. E., and Walter, P. (1993). Transcriptional induction of genes encoding endoplasmic reticulum resident proteins requires a transmembrane protein kinase. *Cell* 73, 1197–1206. doi: 10.1016/0092-8674(93)90648-A

Cushing, D. A., Forsthoefel, N. R., Gestaut, D. R., and Vernon, D. M. (2005). Arabidopsis emb175 and other ppr knockout mutants reveal essential roles for pentatricopeptide repeat (PPR) proteins in plant embryogenesis. *Planta* 221, 424–436. doi: 10.1007/s00425-004-1452-x

Delvillani, F., Papiani, G., Dehò, G., and Briani, F. (2011). S1 ribosomal protein and the interplay between translation and mRNA decay. *Nucleic Acids Res.* 39, 7702–7715. doi: 10.1093/nar/gkr417

Dietz, K. J. (2016). Thiol-based peroxidases and ascorbate peroxidases: why plants rely on multiple peroxidase systems in the photosynthesizing chloroplast? *Mol. Cells* 39, 20–25. doi: 10.14348/molcells.2016.2324

Fleischmann, T. T., Scharff, L. B., Alkatib, S., Hasdorf, S., Schöttler, M. A., and Bock, R. (2011). Nonessential plastid-encoded ribosomal proteins in tobacco: a developmental role for plastid translation and implications for reductive genome evolution. *Plant Cell* 23, 3137–3155. doi: 10.1105/tpc.111.088906

Flores-Pérez, U., and Jarvis, P. (2013). Molecular chaperone involvement in chloroplast protein import. *Biochim. Biophys. Acta* 1833, 332–340. doi: 10.1016/j.bbamcr.2012.03.019

Gray, J. C., Sullivan, J. A., Wang, J. H., Jerome, C. A., and Maclean, D. (2003). Coordination of plastid and nuclear gene expression. *Philos. Trans. R. Soc. Lond. B Biol. Sci.* 358, 135–144. discussion 144–145. doi: 10.1098/rstb.2002.1180

Gutteridge, S., and Gatenby, A. A. (1995). Rubisco synthesis, assembly, mechanism, and regulation. *Plant Cell* 7, 809–819. doi: 10.1105/tpc.7.7.809

Huang, M., Friso, G., Nishimura, K., Qu, X., Olinares, P. D., Majeran, W., et al. (2013). Construction of plastid reference proteomes for maize and Arabidopsis and evaluation of their orthologous relationships; the concept of orthoproteomics. *J. Proteome Res.* 12, 491–504. doi: 10.1021/pr300952g

Huang, Y. S., and Li, H. M. (2009). Arabidopsis CHLI2 can substitute for CHLI1. *Plant Physiol.* 150, 636–645. doi: 10.1104/pp.109.135368

Inaba, T., Li, M., Alvarez-Huerta, M., Kessler, F., and Schnell, D. J. (2003). atTic110 functions as a scaffold for coordinating the stromal events of protein import into chloroplasts. *J. Biol. Chem.* 278, 38617–38627. doi: 10.1074/jbc.M306367200

Inoue, H., Li, M., and Schnell, D. J. (2013). An essential role for chloroplast heat shock protein 90 (Hsp90C) in protein import into chloroplasts. *Proc. Natl. Acad. Sci. U.S.A.* 110, 3173–3178. doi: 10.1073/pnas.1219229110

Ishikawa, A. (2005). Tetrapyrrole metabolism is involved in lesion formation, cell death, in the Arabidopsis lesion initiation 1 mutant. *Biosci. Biotechnol. Biochem.* 69, 1929–1934. doi: 10.1271/bbb.69.1929

Ishikawa, A., Tanaka, H., Nakai, M., and Asahi, T. (2003). Deletion of a chaperonin 60 beta gene leads to cell death in the Arabidopsis lesion initiation 1 mutant. *Plant Cell Physiol.* 44, 255–261. doi: 10.1093/pcp/pcg031

Jackson-Constan, D., Akita, M., and Keegstra, K. (2001). Molecular chaperones involved in chloroplast protein import. *Biochim. Biophys. Acta* 1541, 102–113. doi: 10.1016/S0167-4889(01)00148-3

Jarvis, P., and López-Juez, E. (2013). Biogenesis and homeostasis of chloroplasts and other plastids. *Nat. Rev. Mol. Cell Biol.* 14, 787–802. doi: 10.1038/nrm3702

Kato, Y., and Sakamoto, W. (2010). New insights into the types and function of proteases in plastids. *Int. Rev. Cell Mol. Biol.* 280, 185–218. doi: 10.1016/S1937-6448(10)80004-8

Kessler, F., and Blobel, G. (1996). Interaction of the protein import and folding machineries of the chloroplast. *Proc. Natl. Acad. Sci. U.S.A.* 93, 7684–7689. doi: 10.1073/pnas.93.15.7684

Kleine, T., and Leister, D. (2016). Retrograde signaling: organelles go networking. *Biochim. Biophys. Acta.* 1857, 1313–1325. doi: 10.1016/j.bbabio.2016.03.017

König, J., Galliardt, H., Jütte, P., Schäper, S., Dittmann, L., and Dietz, K. J. (2013). The conformational bases for the two functionalities of 2-cysteine peroxiredoxins as peroxidase and chaperone. *J. Exp. Bot.* 64, 3483–3497. doi: 10.1093/jxb/ert184

Koussevitzky, S., Nott, A., Mockler, T. C., Hong, F., Sachetto-Martins, G., Surpin, M., et al. (2007). Signals from chloroplasts converge to regulate nuclear gene expression. *Science* 316, 715–719. doi: 10.1126/science. 1140516

Kovacheva, S., Bédard, J., Patel, R., Dudley, P., Twell, D., Ríos, G., et al. (2005). *In vivo* studies on the roles of Tic110, Tic40 and Hsp93 during chloroplast protein import. *Plant J.* 41, 412–428. doi: 10.1111/j.1365-313X.2004.02307.x

Kovacheva, S., Bédard, J., Wardle, A., Patel, R., and Jarvis, P. (2007). Further *in vivo* studies on the role of the molecular chaperone, Hsp93, in plastid protein import. *Plant J.* 50, 364–379. doi: 10.1111/j.1365-313X.2007.03060.x

Larkin, R. M., Alonso, J. M., Ecker, J. R., and Chory, J. (2003). GUN4, a regulator of chlorophyll synthesis and intracellular signaling. *Science* 299, 902–906. doi: 10.1126/science.1079978

Lin, Y. F., and Haynes, C. M. (2016). Metabolism and the UPR(mt). *Mol. Cell* 61, 677–682. doi: 10.1016/j.molcel.2016.02.004

Liu, L., McNeilage, R. T., Shi, L. X., and Theg, S. M. (2014). ATP requirement for chloroplast protein import is set by the Km for ATP hydrolysis of stromal Hsp70 in *Physcomitrella patens*. *Plant Cell* 26, 1246–1255. doi: 10.1105/tpc.113.121822

Madueno, F., Napier, J. A., and Gray, J. C. (1993). Newly imported rieske iron-sulfur protein associates with Both Cpn60 and Hsp70 in the chloroplast stroma. *Plant Cell* 5, 1865–1876. doi: 10.1105/tpc.5.12.1865

Majeran, W., Friso, G., Asakura, Y., Qu, X., Huang, M., Ponnala, L., et al. (2012). Nucleoid-enriched proteomes in developing plastids and chloroplasts from maize leaves: a new conceptual framework for nucleoid functions. *Plant Physiol.* 158, 156–189. doi: 10.1104/pp.111.188474

Manuell, A. L., Quispe, J., and Mayfield, S. P. (2007). Structure of the chloroplast ribosome: novel domains for translation regulation. *PLoS Biol.* 5:e209. doi: 10.1371/journal.pbio.0050209

Melonek, J., Matros, A., Trösch, M., Mock, H. P., and Krupinska, K. (2012). The core of chloroplast nucleoids contains architectural SWIB domain proteins. *Plant Cell* 24, 3060–3073. doi: 10.1105/tpc.112.099721

Melonek, J., Oetke, S., and Krupinska, K. (2016). Multifunctionality of plastid nucleoids as revealed by proteome analyses. *Biochim. Biophys. Acta.* 1864, 1016–1038. doi: 10.1016/j.bbapap.2016.03.009

Merendino, L., Falciatore, A., and Rochaix, J. D. (2003). Expression and RNA binding properties of the chloroplast ribosomal protein S1 from *Chlamydomonas reinhardtii*. *Plant Mol. Biol.* 53, 371–382. doi: 10.1023/B:PLAN.0000006941.56233.42

Miura, E., Kato, Y., Matsushima, R., Albrecht, V., Laalami, S., and Sakamoto, W. (2007). The balance between protein synthesis and degradation in chloroplasts determines leaf variegation in Arabidopsis yellow variegated mutants. *Plant Cell* 19, 1313–1328. doi: 10.1105/tpc.106.049270

Mochizuki, N., Brusslan, J. A., Larkin, R., Nagatani, A., and Chory, J. (2001). Arabidopsis genomes uncoupled 5 (GUN5) mutant reveals the involvement of Mg-chelatase H subunit in plastid-to-nucleus signal transduction. *Proc. Natl. Acad. Sci. U.S.A.* 98, 2053–2058. doi: 10.1073/pnas.98.4.2053

Nakagawara, E., Sakuraba, Y., Yamasato, A., Tanaka, R., and Tanaka, A. (2007). Clp protease controls chlorophyll b synthesis by regulating the level of chlorophyllide a oxygenase. *Plant J.* 49, 800–809. doi: 10.1111/j.1365-313X.2006.02996.x

Oelmüller, R., Levitan, I., Bergfeld, R., Rajasekhar, V. K., and Mohr, H. (1986). Expression of nuclear genes as affected by treatments acting on the plastids. *Planta* 168, 482–492. doi: 10.1007/BF00392267

Oelmüller, R., and Mohr, H. (1986). Photooxidative destruction of chloroplasts and its consequences for expression of nuclear genes. *Planta* 167, 106–113. doi: 10.1007/BF00446376

Okazaki, K., Kabeya, Y., and Miyagishima, S. Y. (2010). The evolution of the regulatory mechanism of chloroplast division. *Plant Signal. Behav.* 5, 164–167. doi: 10.4161/psb.5.2.10461

Olinares, P. D., Kim, J., and van Wijk, K. J. (2011). The Clp protease system; a central component of the chloroplast protease network. *Biochim. Biophys. Acta* 1807, 999–1011. doi: 10.1016/j.bbabio.2010.12.003

Peng, L., Fukao, Y., Myouga, F., Motohashi, R., Shinozaki, K., and Shikanai, T. (2011). A chaperonin subunit with unique structures is essential for folding of a specific substrate. *PLoS Biol.* 9:e1001040. doi: 10.1371/journal.pbio.1001040

Pérez-Pérez, J. M., Esteve-Bruna, D., González-Bayón, R., Kangasjarvi, S., Caldana, C., Hannah, M. A., et al. (2013). Functional redundancy and divergence within the Arabidopsis RETICULATA-RELATED gene family. *Plant Physiol.* 162, 589–603. doi: 10.1104/pp.113.217323

Pfalz, J., Liere, K., Kandlbinder, A., Dietz, K. J., and Oelmüller, R. (2006). pTAC2, -6, and -12 are components of the transcriptionally active plastid chromosome that are required for plastid gene expression. *Plant Cell* 18, 176–197. doi: 10.1105/tpc.105.036392

Pfalz, J., and Pfannschmidt, T. (2013). Essential nucleoid proteins in early chloroplast development. *Trends Plant Sci.* 18, 186–194. doi: 10.1016/j.tplants.2012.11.003

Phinney, B. S., and Thelen, J. J. (2005). Proteomic characterization of a triton-insoluble fraction from chloroplasts defines a novel group of proteins associated with macromolecular structures. *J. Proteome Res.* 4, 497–506. doi: 10.1021/pr049791k

Pogson, B. J., Woo, N. S., Förster, B., and Small, I. D. (2008). Plastid signalling to the nucleus and beyond. *Trends Plant Sci.* 13, 602–609. doi: 10.1016/j.tplants.2008.08.008

Pulido, P., Spínola, M. C., Kirchsteiger, K., Guinea, M., Pascual, M. B., Sahrawy, M., et al. (2010). Functional analysis of the pathways for 2-Cys peroxiredoxin reduction in *Arabidopsis thaliana* chloroplasts. *J. Exp. Bot.* 61, 4043–4054. doi: 10.1093/jxb/erq218

Ramundo, S., Casero, D., Mühlhaus, T., Hemme, D., Sommer, F., Crèvecoeur, M., et al. (2014). Conditional depletion of the chlamydomonas chloroplast ClpP protease activates nuclear genes involved in autophagy and plastid protein quality control. *Plant Cell* 26, 2201–2222. doi: 10.1105/tpc.114.124842

Ramundo, S., Rahire, M., Schaad, O., and Rochaix, J. D. (2013). Repression of essential chloroplast genes reveals new signaling pathways and regulatory feedback loops in chlamydomonas. *Plant Cell* 25, 167–186. doi: 10.1105/tpc.112.103051

Ramundo, S., and Rochaix, J. D. (2014). Chloroplast unfolded protein response, a new plastid stress signaling pathway? *Plant Signal. Behav.* 9:e972874. doi: 10.4161/15592316.2014.972874

Rey, P., Becuwe, N., Barrault, M. B., Rumeau, D., Havaux, M., Biteau, B., et al. (2007). The *Arabidopsis thaliana* sulfiredoxin is a plastidic cysteine-sulfinic acid reductase involved in the photooxidative stress response. *Plant J.* 49, 505–514. doi: 10.1111/j.1365-313X.2006.02969.x

Richly, E., and Leister, D. (2004). An improved prediction of chloroplast proteins reveals diversities and commonalities in the chloroplast proteomes of Arabidopsis and rice. *Gene* 329, 11–16. doi: 10.1016/j.gene.2004.01.008

Rochaix, J. D., and Ramundo, S. (2015). Conditional repression of essential chloroplast genes: evidence for new plastid signaling pathways. *Biochim. Biophys. Acta* 1847, 986–992. doi: 10.1016/j.bbabio.2014.11.011

Rochaix, J. D., Surzycki, R., and Ramundo, S. (2014). Tools for regulated gene expression in the chloroplast of Chlamydomonas. *Methods Mol. Biol.* 1132, 413–424. doi: 10.1007/978-1-62703-995-6_28

Rogalski, M., Schöttler, M. A., Thiele, W., Schulze, W. X., and Bock, R. (2008). Rpl33, a nonessential plastid-encoded ribosomal protein in tobacco, is required under cold stress conditions. *Plant Cell* 20, 2221–2237. doi: 10.1105/tpc.108.060392

Ruberti, C., Kim, S. J., Stefano, G., and Brandizzi, F. (2015). Unfolded protein response in plants: one master, many questions. *Curr. Opin. Plant Biol.* 27, 59–66. doi: 10.1016/j.pbi.2015.05.016

Rudella, A., Friso, G., Alonso, J. M., Ecker, J. R., and Van Wijk, K. J. (2006). Downregulation of ClpR2 leads to reduced accumulation of the ClpPRS protease complex and defects in chloroplast biogenesis in Arabidopsis. *Plant Cell* 18, 1704–1721. doi: 10.1105/tpc.106.042861

Sakamoto, W. (2006). Protein degradation machineries in plastids. *Annu. Rev. Plant Biol.* 57, 599–621. doi: 10.1146/annurev.arplant.57.032905.105401

Shi, L. X., and Theg, S. M. (2010). A stromal heat shock protein 70 system functions in protein import into chloroplasts in the moss *Physcomitrella patens*. *Plant Cell* 22, 205–220. doi: 10.1105/tpc.109.071464

Shi, L. X., and Theg, S. M. (2013a). The chloroplast protein import system: from algae to trees. *Biochim. Biophys. Acta* 1833, 314–331. doi: 10.1016/j.bbamcr.2012.10.002

Shi, L. X., and Theg, S. M. (2013b). Energetic cost of protein import across the envelope membranes of chloroplasts. *Proc. Natl. Acad. Sci. U.S.A.* 110, 930–935. doi: 10.1073/pnas.1115886110

Shoji, S., Dambacher, C. M., Shajani, Z., Williamson, J. R., and Schultz, P. G. (2011). Systematic chromosomal deletion of bacterial ribosomal protein genes. *J. Mol. Biol.* 413, 751–761. doi: 10.1016/j.jmb.2011.09.004

Sjögren, L. L., Macdonald, T. M., Sutinen, S., and Clarke, A. K. (2004). Inactivation of the clpC1 gene encoding a chloroplast Hsp100 molecular chaperone causes growth retardation, leaf chlorosis, lower photosynthetic activity, and a specific reduction in photosystem content. *Plant Physiol.* 136, 4114–4126. doi: 10.1104/pp.104.053835

Steiner, S., Schröter, Y., Pfalz, J., and Pfannschmidt, T. (2011). Identification of essential subunits in the plastid-encoded RNA polymerase complex reveals building blocks for proper plastid development. *Plant Physiol.* 157, 1043–1055. doi: 10.1104/pp.111.184515

Stenbaek, A., Hansson, A., Wulff, R. P., Hansson, M., Dietz, K. J., and Jensen, P. E. (2008). NADPH-dependent thioredoxin reductase and 2-Cys peroxiredoxins are needed for the protection of Mg-protoporphyrin monomethyl ester cyclase. *FEBS Lett.* 582, 2773–2778. doi: 10.1016/j.febslet.2008.07.006

Strand, A., Asami, T., Alonso, J., Ecker, J. R., and Chory, J. (2003). Chloroplast to nucleus communication triggered by accumulation of Mg-protoporphyrinIX. *Nature* 421, 79–83. doi: 10.1038/nature01204

Su, P. H., and Li, H. M. (2008). Arabidopsis stromal 70-kD heat shock proteins are essential for plant development and important for thermotolerance of germinating seeds. *Plant Physiol.* 146, 1231–1241. doi: 10.1104/pp.107.114496

Su, P. H., and Li, H. M. (2010). Stromal Hsp70 is important for protein translocation into pea and Arabidopsis chloroplasts. *Plant Cell* 22, 1516–1531. doi: 10.1105/tpc.109.071415

Sun, Y., and Zerges, W. (2015). Translational regulation in chloroplasts for development and homeostasis. *Biochim. Biophys. Acta* 1847, 809–820. doi: 10.1016/j.bbabio.2015.05.008

Susek, R. E., Ausubel, F. M., and Chory, J. (1993). Signal transduction mutants of Arabidopsis uncouple nuclear CAB and RBCS gene expression from chloroplast development. *Cell* 74, 787–799. doi: 10.1016/0092-8674(93)90459-4

Suzuki, K., Nakanishi, H., Bower, J., Yoder, D. W., Osteryoung, K. W., and Miyagishima, S. Y. (2009). Plastid chaperonin proteins Cpn60 alpha and Cpn60 beta are required for plastid division in *Arabidopsis thaliana*. *BMC Plant Biol.* 9:38. doi: 10.1186/1471-2229-9-38

Tadini, L., Pesaresi, P., Kleine, T., Rossi, F., Guljamow, A., Sommer, F., et al. (2016). GUN1 controls accumulation of the plastid ribosomal protein S1 at the protein level and interacts with proteins involved in plastid protein homeostasis. *Plant Physiol.* 170, 1817–1830. doi: 10.1104/pp.15.02033

Tanaka, R., Kobayashi, K., and Masuda, T. (2011). Tetrapyrrole metabolism in *Arabidopsis thaliana*. *Arabidopsis Book* 9:e0145. doi: 10.1199/tab.0145

Tiller, N., and Bock, R. (2014). The translational apparatus of plastids and its role in plant development. *Mol. Plant* 7, 1105–1120. doi: 10.1093/mp/ssu022

Tsugeki, R., and Nishimura, M. (1993). Interaction of homologues of Hsp70 and Cpn60 with ferredoxin-NADP+ reductase upon its import into chloroplasts. *FEBS Lett.* 320, 198–202. doi: 10.1016/0014-5793(93)80585-I

Van Wijk, K. J. (2015). Protein maturation and proteolysis in plant plastids, mitochondria, and peroxisomes. *Annu. Rev. Plant Biol.* 66, 75–111. doi: 10.1146/annurev-arplant-043014-115547

Woodson, J. D., and Chory, J. (2008). Coordination of gene expression between organellar and nuclear genomes. *Nat. Rev. Genet.* 9, 383–395. doi: 10.1038/nrg2348

Woodson, J. D., Perez-Ruiz, J. M., and Chory, J. (2011). Heme synthesis by plastid ferrochelatase I regulates nuclear gene expression in plants. *Curr. Biol.* 21, 897–903. doi: 10.1016/j.cub.2011.04.004

Zybailov, B., Friso, G., Kim, J., Rudella, A., Rodríguez, V. R., Asakura, Y., et al. (2009). Large scale comparative proteomics of a chloroplast Clp protease mutant reveals folding stress, altered protein homeostasis, and feedback regulation of metabolism. *Mol. Cell. Proteomics* 8, 1789–1810. doi: 10.1074/mcp.M900104-MCP200

Conflict of Interest Statement: The authors declare that the research was conducted in the absence of any commercial or financial relationships that could be construed as a potential conflict of interest.